NAVAL POSTGRADUATE SCHOOL

MONTEREY, CALIFORNIA

THESIS

NAVY'S N-LAYER MAGNETIC MODEL WITH APPLICATION TO NAVAL MAGNETIC DEMINING

by

Sam Poteete

September 2010

Thesis Advisor: Peter C. Chu
Second Readers: Ronald Betsch
Roger Meredith

THIS PAGE INTENTIONALLY LEFT BLANK

REPORT DOCUMENTATION PAGE			Form Approved OMB No. 0704-0188
Public reporting burden for this collection of information is estimated to average 1 hour per response, including the time for reviewing instruction, searching existing data sources, gathering and maintaining the data needed, and completing and reviewing the collection of information. Send comments regarding this burden estimate or any other aspect of this collection of information, including suggestions for reducing this burden, to Washington headquarters Services, Directorate for Information Operations and Reports, 1215 Jefferson Davis Highway, Suite 1204, Arlington, VA 22202-4302, and to the Office of Management and Budget, Paperwork Reduction Project (0704-0188) Washington DC 20503.			
1. AGENCY USE ONLY ***(Leave blank)***	**2. REPORT DATE** September 2010	**3. REPORT TYPE AND DATES COVERED** Master's Thesis	
4. TITLE AND SUBTITLE Navy's N-Layer Magnetic Model with Application to Naval Magnetic Demining		**5. FUNDING NUMBERS**	
6. AUTHOR(S) Sam Poteete			
7. PERFORMING ORGANIZATION NAME(S) AND ADDRESS(ES) Naval Postgraduate School Monterey, CA 93943-5000		**8. PERFORMING ORGANIZATION REPORT NUMBER**	
9. SPONSORING /MONITORING AGENCY NAME(S) AND ADDRESS(ES) N/A		**10. SPONSORING/MONITORING AGENCY REPORT NUMBER**	
11. SUPPLEMENTARY NOTES The views expressed in this thesis are those of the author and do not reflect the official policy or position of the Department of Defense or the U.S. Government. IRB Protocol number _____N/A_____.			
12a. DISTRIBUTION / AVAILABILITY STATEMENT Approved for public release; distribution is unlimited		**12b. DISTRIBUTION CODE**	

13. ABSTRACT (maximum 200 words)

The Navy and Marine Corps' Forward . . . From the Sea strategic concept has expanded naval operations from open-ocean, blue-water combat environments to the littoral regions in which naval mines can both be an extremely menacing threat to U.S. forces and an effective force multiplier for the Fleet. The Navy/Marine Corps must have efficient Mine Warfare (MIW) forces to ensure the Fleet can carry out operations in the open ocean and littorals, including maintaining open sea lanes of communication and supporting Ship-to-Objective Maneuver Warfare from the Sea while denying operating areas to the enemy.

Every ship has a magnetic signature, which is caused by its iron and steel components. Additionally, the earth's natural magnetic field induces a magnetization in a ship depending on its latitude, longitude, and heading. Exploitation of surface ship and submarine magnetic field signatures by naval influence mines has occurred throughout time. In order to calculate the swept path width for magnetic minesweeping systems currently in use by the U.S. Mine Warfare (MIW) forces, it is necessary to calculate the vector components of the magnetic field strength which are generated by each of several possible system configurations. The Navy's Magnetic Model addresses this needed capability.

The Navy's N-Layer Magnetic Model (NLMM) is used to predict the expected performance of magnetic minesweeping equipment in a complex environment consisting of N layers, each with arbitrary conductivity and thickness. The model is used to compute the magnetic field strength produced by various U.S. Navy magnetic minesweeping configurations using a random environmental vertical conductivity structure. To better determine which parameters had the greatest effect on the model and which could be simplified or enhanced, a series of tests were run on actual data sets.

14. SUBJECT TERMS Magnetic demining, magnetic field strength, Navy's N-Layer Magnetic Model, magnetic minesweeping equipment, Physical Oceanography,			**15. NUMBER OF PAGES** 122
			16. PRICE CODE
17. SECURITY CLASSIFICATION OF REPORT Unclassified	**18. SECURITY CLASSIFICATION OF THIS PAGE** Unclassified	**19. SECURITY CLASSIFICATION OF ABSTRACT** Unclassified	**20. LIMITATION OF ABSTRACT** UU

NSN 7540-01-280-5500 Standard Form 298 (Rev. 2-89)
Prescribed by ANSI Std. 239-18

THIS PAGE INTENTIONALLY LEFT BLANK

Approved for public release; distribution is unlimited

NAVY'S N-LAYER MAGNETIC MODEL WITH APPLICATION TO NAVAL MAGNETIC DEMINING

Sam Poteete
Lieutenant Commander, United States Navy
B.A., University of Washington 2000

Submitted in partial fulfillment of the
requirements for the degree of

MASTER OF SCIENCE IN METEOROLOGY AND PHYSICAL OCEANOGRAPHY

from the

NAVAL POSTGRADUATE SCHOOL
September 2010

Author: Sam Poteete

Approved by: Peter C.Chu
Thesis Advisor

Ronald Betsch
Second Reader

Roger Meredith
Second Reader

Jeffrey Paduan
Chairman, Department of Oceanography

THIS PAGE INTENTIONALLY LEFT BLANK

ABSTRACT

The Navy and Marine Corps' Forward . . . From the Sea strategic concept has expanded naval operations from open-ocean, blue-water combat environments to the littoral regions in which naval mines can both be an extremely menacing threat to U.S. forces and an effective force multiplier for the Fleet. The Navy/Marine Corps must have efficient Mine Warfare (MIW) forces to ensure the Fleet can carry out operations in the open ocean and littorals, including maintaining open sea lanes of communication and supporting Ship-to-Objective Maneuver Warfare from the Sea while denying operating areas to the enemy.

Every ship has a magnetic signature, which is caused by its iron and steel components. Additionally, the earth's natural magnetic field induces a magnetization in a ship depending on its latitude, longitude, and heading. Exploitation of surface ship and submarine magnetic field signatures by naval influence mines has occurred throughout time. In order to calculate the swept path width for magnetic minesweeping systems currently in use by the U.S. Mine Warfare (MIW) forces, it is necessary to calculate the vector components of the magnetic field strength which are generated by each of several possible system configurations. The Navy's Magnetic Model addresses this needed capability.

The Navy's N-Layer Magnetic Model (NLMM) is used to predict the expected performance of magnetic minesweeping equipment in a complex environment consisting of N layers, each with arbitrary conductivity and thickness. The model is used to compute the magnetic field strength produced by various U.S. Navy magnetic minesweeping configurations using a random environmental vertical conductivity structure. To better determine which parameters had the greatest effect on the model, and which could be simplified or enhanced, a series of tests were run on actual data sets.

THIS PAGE INTENTIONALLY LEFT BLANK

TABLE OF CONTENTS

THIS PAGE INTENTIONALLY LEFT BLANK

LIST OF FIGURES

LIST OF TABLES

THIS PAGE INTENTIONALLY LEFT BLANK

LIST OF ACRONYMS AND ABBREVIATIONS

AOI	Areas of Interest
EOD	Explosive Ordnance Disposal
ILM	Induced Longitudinal Magnetization
ITM	Induced Transverse Magnetization
IVM	Induced Vertical Magnetization
MCM	Mine Countermeasures
MIW	Mine Warfare
NAVO	Naval Oceanographic Office
NLMM	N-layer Magnetic Model
PLM	Permanent Longitudinal Magnetization
PSS-78	Practical Salinity Scale of 1978
PTM	Permanent Transverse Magnetization
PVM	Permanent Vertical Magnetization
S,t,p	Salinity, Temperature, Pressure
VSW	Very Shallow Water

THIS PAGE INTENTIONALLY LEFT BLANK

ACKNOWLEDGMENTS

I would like to thank Professor Peter Chu for his professionalism and adaptability for taking me on with a short time line. Without his flexibility & knowledge, I would not have been able to do this. Many thanks go out to Mr. Roger Meredith at NAVO for being my second reader, as well as his insight during my TAD visit to Stennis and numerous emails answering my questions. Dr Richard Bennett SEAPROBE Inc/University of Southern Mississippi, for opening his library and resources for my research. Thanks to Mr. Chenwu Fan for his assistance running various models on Linux and adapting MatLab programs to view results. I can't go without mentioning Ens. Bill (Jenkins), whose programming experience & availability saved me more time than he knows. To all the professors throughout the program, their teaching and mentoring made my NPS experience memorable.

Thanks first, to God to whom I owe everything. To Family & Friends; my wonderful boyfriend Matt Libby, whose constant support and dedication, along with an occasional kick in the heiney, kept me motivated and invigorated to stay on task. Next, my Dad Gary Neal, my sister Serena, and my daughter Kelly for their long talks and reality checks, Matt's family for their continuous encouragement, my best friends Becky and Patty for care packages and unconditional love, and my Seaside SDA church family, especially Jenny Stevens, for sanity and time to relax. Many thanks to Donna Cuadrez for her assistance and patience these last few weeks making sure my thesis was in good order. Finally, to the Magnificent gentlemen (Shane Stoughton, Dwight Smith, David Lewis, David Colbert, Russ Ingersoll, and Giani Waghelstein) in my class that made it possible, over the last 30 months, for me to complete this curriculum. To all: Have a Great Navy Day!

THIS PAGE INTENTIONALLY LEFT BLANK

I. INTRODUCTION

A. HISTORY AND IMPORTANCE OF MINE WARFARE

The conclusion of the cold war culminated with the Union of Soviet Socialist Republics (USSR) effectively ceasing to exist under international law on December 31, 1991. This historical event caused the U.S. military and specifically the Navy and Marine Corps Team to shift tactical emphasis from blue water, deep ocean doctrine to littoral warfare doctrine. This predicated military responses dealing with a wide range of worldwide regional crises requiring forward sea basing, and expeditionary force landing support. The change from traditional blue water operations to brown water has brought with it a somewhat unfamiliar area for naval operations. That of an increased shallow water mine threat. The challenges that come along with this change in focus include an update to the mine warfare mission.

> ...the very shallow water (VSW) region is a critical point for our offensive forces and can easily, quickly and cheaply be exploited by the enemy. The magnitude of the current deficiency in reconnaissance and neutralization in these regions and the impact on amphibious assault operations were demonstrated during Operation Desert Storm.
>
> Maj. Gen. Edward J. Hanlon Jr. (Rhodes & Holder, 1998)

One of the Navy's objectives has been to conquer the mine warfare threat. As mines and mine warfare techniques evolve and become more sophisticated, so does the ability of the United States to counter the threat. Any military operation that occurs in the littoral regions also occurs in mine country. The increasing pace of shallow-water naval operations (i.e., Persian Gulf, Yellow Sea, and Gulf of Aden) translates into a high probability of encountering mines. Naval mines may be found throughout the water column and on or within the seafloor. Describing a typical naval mine would provide a depiction of the spherical, hertz-horn World War II vintage drifting mine shape commonly seen in Hollywood films. Yet, there are many types of mines in use. The proliferation of inexpensive, bottom type and magnetic mines make shallow water and

very shallow water Mine Countermeasures (MCM) a critical and expensive challenge. The required shift in focus of naval operations from the open ocean to the regional off-shore areas also increases the importance of mine warfare as a navy core competency. In times of conflict, domination of coastal operating areas will largely depend on the ability to remove or neutralize any littoral mine threat and prepare the battle space for follow-on action in a timely fashion. The United States uses several methods for detecting mines. One method to improve the mission of the MCM is utilizing an environmental model in two layers that calculates a magnetic field and the probability of detecting magnetic mines.

The actuation contour for an ideal optimum mine setting, along with those that are considered to be suboptimum in this example, are shown in Figure 1. It can bee seen in this example that mines set too sensitive may detonate when their targets are yet too far away to wreak on them the desired level of damage called for in the minefield plan. Additionally, mines that are too sensitive are easier to sweep. Conversely, if the mine setting is not sensitive enough it may miss targets that it could have damaged or sunk. In both these instances mines incorrectly set can be considered wasted and leave a gap in the minefield. Noting the ability to determine optimum actuation contours, the signature characteristics (amplitude and shape) of naval vessels are closely guarded.

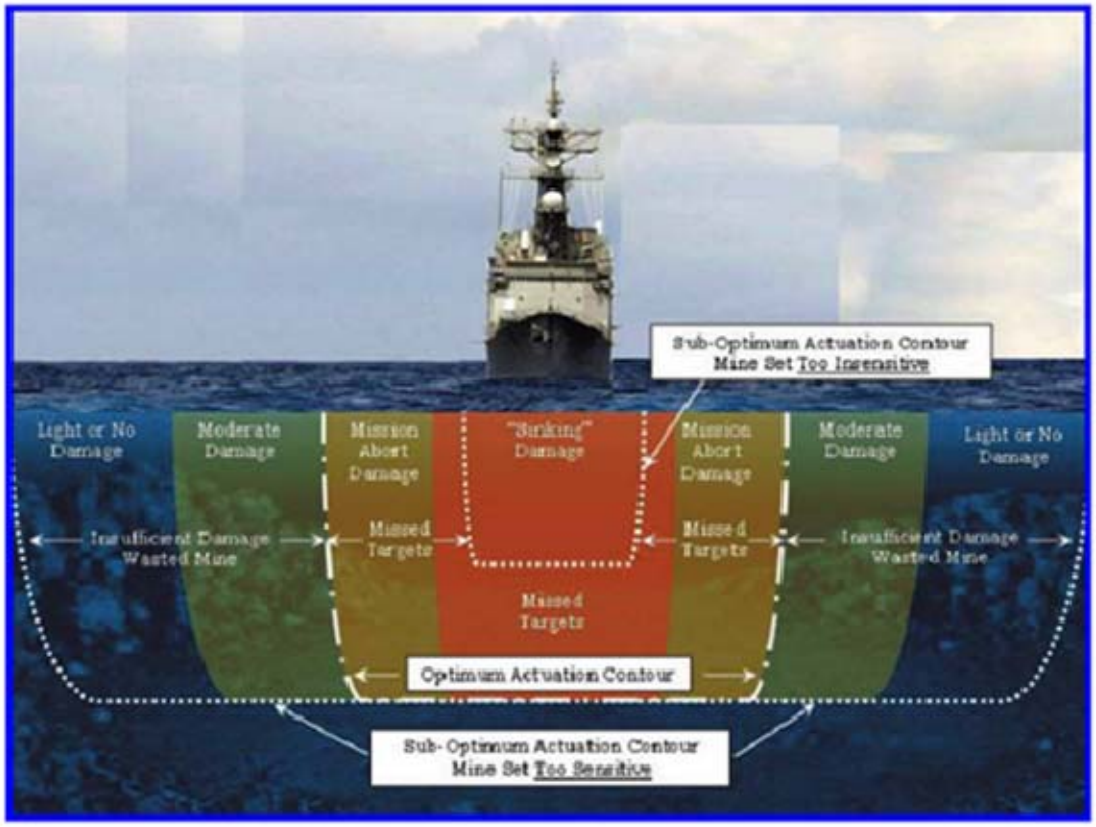

Figure 1. Idealized example of a magnetic mine actuation contour matched to its Mission-abort damage contour, along with two settings that are sub-optimum (From Holmes, 2006)

B. MINE WARFARE MISSION

> Without MCM capability, we simply can't put marines ashore, nor can we safely operate any ships in the mine danger areas. Because of that, full integration of mine warfare into the warfare campaign plan and the force commander's scheme in terms of sequence is vital. Without mine warfare, the campaign stops.
>
> RADM Mike Mullen, USN (former CNO)

Losing a ship to a minefield or inflicting casualties to its crew is unacceptable. However, cost of repairing ships does not solely drive this mission. The sinking of a ship

or infliction of mine damage to even a single naval platform is critical. Yet, the price of getting the correct equipment to and neutralizing the minefield can cost as much or more than the repair.

The Navy's vulnerability to influence mines is dependent on the amount of MCM effort used before the ships transits the path suspected to be mined. Figure 2 shows hypothetical examples of this parabolic relationship for dense, medium-dense, and sparse minefields. The units for MCM effort, platform-days, are equal to the sum of the number of days each MCM platform (ship, helicopter, unmanned underwater and surface vehicle, etc.) is used to hunt, sweep, or otherwise dispose of threat mines (Holmes, 2006). Unfortunately to note, the risk of transiting ships in a dense minefield could be virtually unchanged after only a few days of MCM platform effort. The trends noted in Figure 2 can be applied to any minefield, although the scales of the graph and relative separation between the three curves will vary based on the specific scenario.

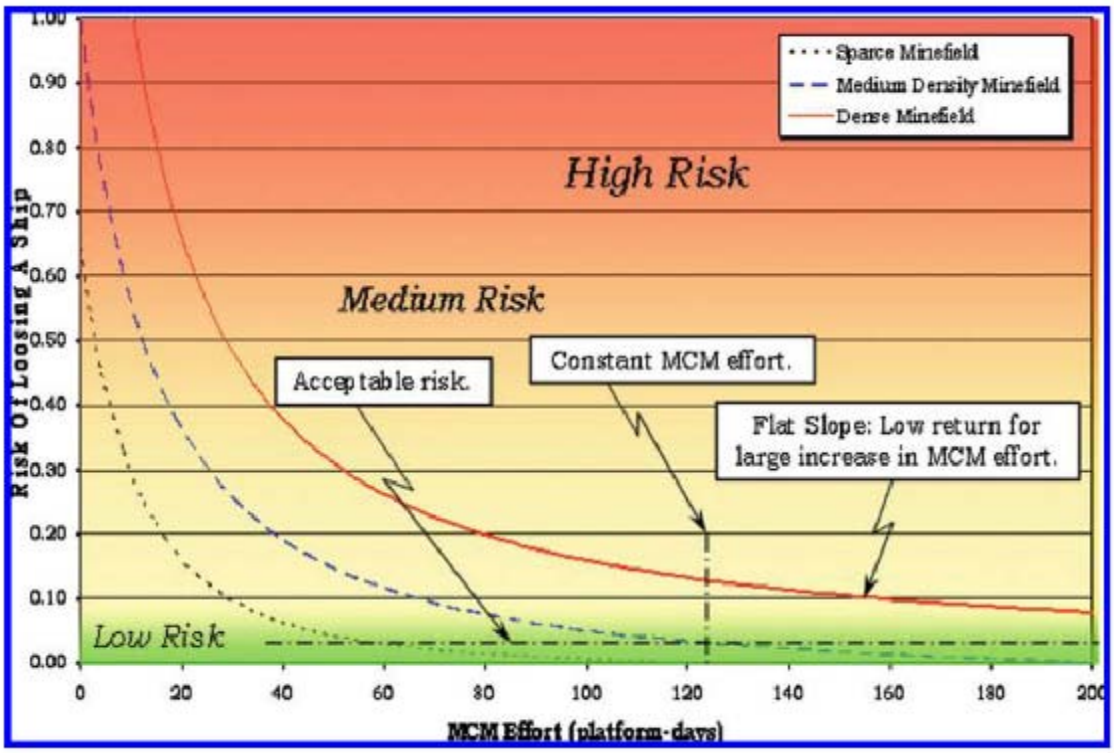

Figure 2. Hypothetical examples of the relationship between mine countermeasure effort and the risk of losing a following ship (From Holmes, 2006)

Risk levels for transiting ships are based on mission critical decision making. It would be expected to have low to very-low risk levels for transiting combatants. The optimal low risk condition would require considerable or even unfeasible amounts of MCM resources and time and still be dependent on density of the minefield.

> Diminishing returns of the MCM effectiveness curves (flattening at higher levels of MCM effort) are caused by the resource-intensive process of removing the last one or two mines from the field; a characteristic of all mine-clearing scenarios. It takes only one missed $10,000 mine to sink a $2,000,000,000 ship.
>
> J.J. Holmes, 2006

Methods for detecting submerged objects such as mines may be categorized as either passive or active systems. Passive systems emit no energy, but instead sense disturbances in the underwater environment created by the presence of a submerged object. Passive countermeasures involve minimizing a ship's acoustic and magnetic signature in order to prevent mines from detecting it. Active systems, on the other hand, rely on the sensing of emitted energy either reflected or radiated by the object to be detected. Although satisfactory for many uses, sonar devices have several inherent limitations. Nearby objects can cause echoes and these may obscure the echo of the object to be detected. A rocky bottom will produce many echoes, thus making efficient detections of objects on the bottom almost impossible. Another type of active system includes systems which set up electric or magnetic fields and measure variations therein. Magnetic objects will cause a variation in the magnetic field due to their being magnetized by the applied magnetic field while non-metallic objects immersed in sea water will cause a variation in the electromagnetic field by creating a "hole" in the conductivity pattern of the sea water. In general, the variation in the applied electromagnetic field created by these objects is small and it has, in the past, been difficult to find sensors that could detect these perturbations. Once found, an object must be identified in order to tell whether or not it is a hostile threat. Additionally, there may

be hundreds of mines within a given region such as a mined surf zone which must be neutralized. Then, after finding a mine either floating or buried, its effectiveness must be destroyed, either by removal or by elimination.

1. Mine Neutralization

The Navy's Mine Countermeasure mission is to prevent or reduce the danger to our surface ships and submarines from waterborne mines. Active and passive countermeasures are used for minimizing the threat of mines. Avoidance of known mines is another technique. Active countermeasures entail minehunting (Figure 3) and minesweeping (Figure 4). Minehunting is the systematic detection and subsequent elimination of mines, whereas minesweeping is the method of clearing a pre-defined area and terminating mines that are detected. Minehunting involves towing sonar arrays and magnetometers. The vessel uses its active sonar as it moves across the water searching for mines. It continues this operation until it finds a mine or determines the area to be safe. If a mine is found it is neutralized by placing explosives on or near it, this has the effect of crippling the mine's detonation sensors.

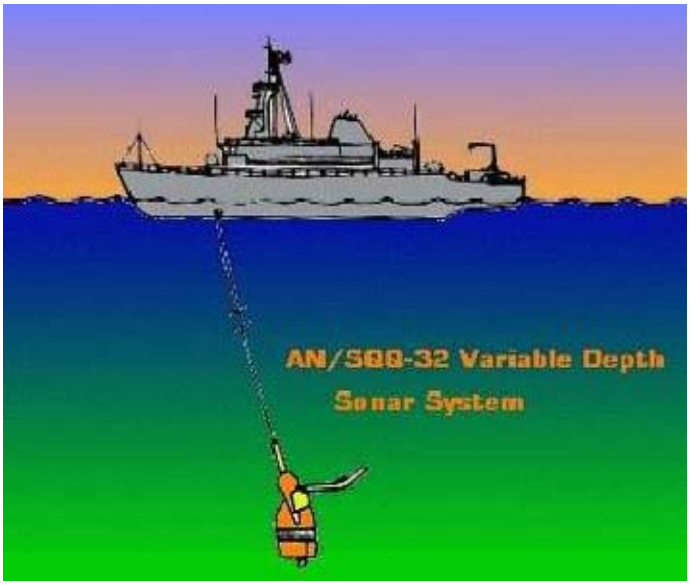

Figure 3. Minehunting ship with Sonar (From GlobalSecurity.org, 2007)

Minesweeping (Figure 4) is conducted by ships and aircraft. There are several types of minesweeping. Mechanical sweeps are designed to sever the cables of moored mines. With this method, a sweep wire is towed by the vessel with the objective of snagging the tether cable of a mine and severing the cable through abrasive action or with explosive cutters located along the sweep wire. Disengaged mines float to the surface and may be deactivated by gunfire or an Explosive Ordnance Disposal (EOD) team. Bottom mines may be dragged away from the minefield by use of nets.

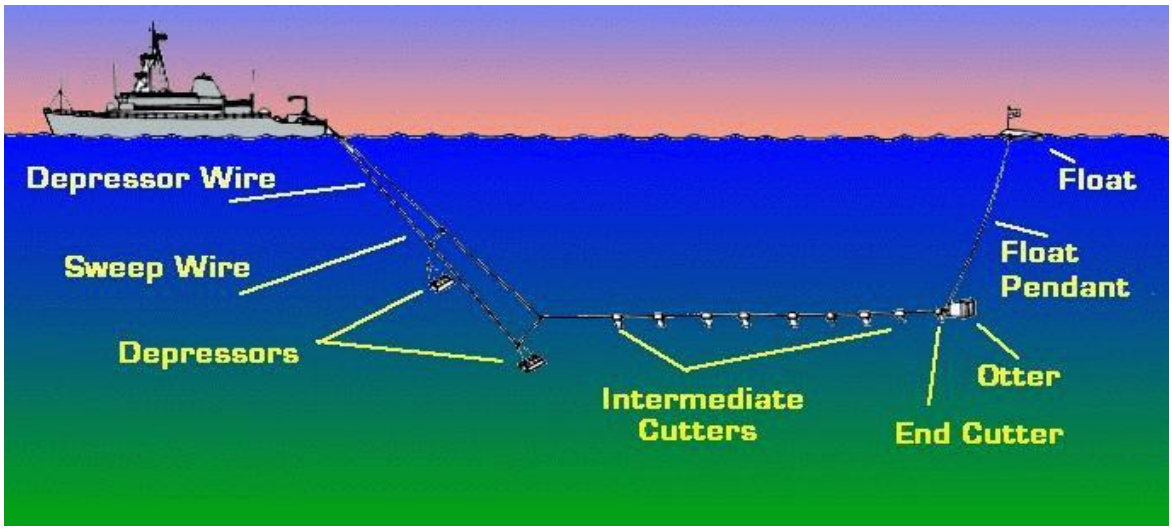

Figure 4. Minesweeping ship with trailing wire (From GlobalSecurity.org, 2007)

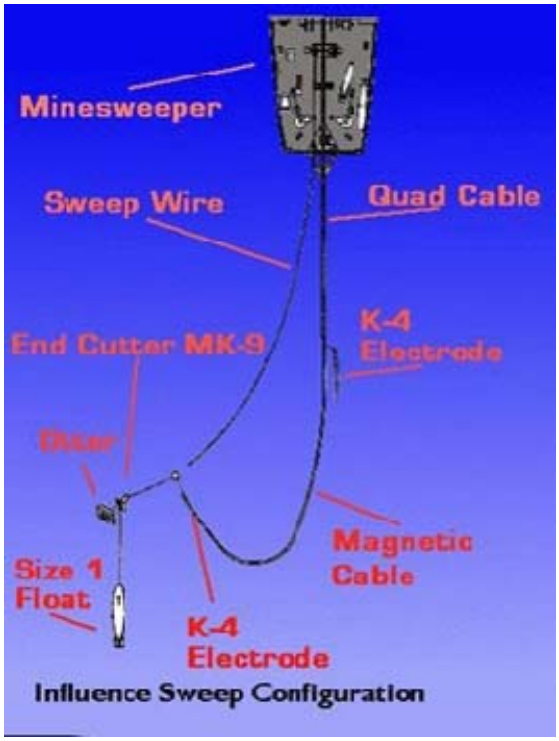

Figure 5. Influence sweep configuration (From GlobalSecurity.org, 2007)

Influence Sweeps (Figure 5) involve simulating the passage of a ship in order to "trick" the mines into detonating. In this case, a magnetic or acoustic sweep system is towed by a ship or aircraft. Mines that detect the simulated ship detonate themselves.

Magnetic sweeps employ a simulated magnetic field that replicates that of a Naval ship. The magnetic field can be produced via an electrical current passing through two non-insulated cables. The resultant magnetic field similar to the ship's magnetic field will induce magnetic mines to detonate.

An acoustic sweep is conducted by simulating the sounds created by a target ship. Various noise makes utilizing compressed air, explosives, hammers or propellers are towed near acoustic mines to detonate them.

Pressure Minesweeping involves sending a large object such as a barge or derelict ship into a minefield to purposely strike mines. This method is not currently practiced.

A combination of different methods of countermeasures is called a combination sweep. A common permutation is a magnetic/acoustic sweep, which simulates the sound and magnetic field of a passing ship.

MCM strategies and mine warfare can be complicated operations. The risk in losing a ship or submarine to a mine is very scenario dependent, and is sensitive to many parameters including:

1. Density of mines in the field (number per square kilometer),
2. Availability of mine hunting and sweeping platforms in theater and their effectiveness in the specific ocean environment,
3. Mission plans and their time constraints,
4. Required length and width of the "Q" route (transit lane) and area needed to conduct operations,
5. Susceptibility of combatants to actuating a mine during their transit through the field,
6. Vulnerability of the vessel to damage from the mine's explosive charge if it donates. (Holmes, 2006)

While the absolute effectiveness of mine-clearing operations and its impact on the overall mission depends highly on the parameters listed, the practical relationship of combatant losses to MCM tactics and technologies has a well-defined trend despite the scenario details.

C. MAGNETIC MINES

Within the last 20 years, mines have damaged 17 U.S. Navy ships, whereas air and missile attacks have damaged only four. During the Korean War, mines laid by North Korean forces damaged 11 U.S. naval vessels. While conducting missions in the Persian Gulf, three U.S. military ships have fallen victim to mines. The following figure shows the US Navy's top threat, that of mines. Some sea mines are actuated by successfully detecting the magnetic signature of a target ship. Mines sensitive to the magnetic signature of a ship were originally developed by the British during World War I, although the Germans are believed to have been the first to deploy these mines in actual operations.

A magnetic mine is a mine designed to explode when the metal hull of a passing ship deflects a magnetic needle, closing an electric circuit and the detonating the mine's charge. The magnetic mine, can be moored, floating or lie in wait on the sea bottom. A ship passing on the water surface above distorts the normal Earth's magnetic field enough (unless degaussed) to trigger the mine. In order to counter magnetic-actuated mines, mine countermeasures forces have developed magnetic mine sweeping capabilities.

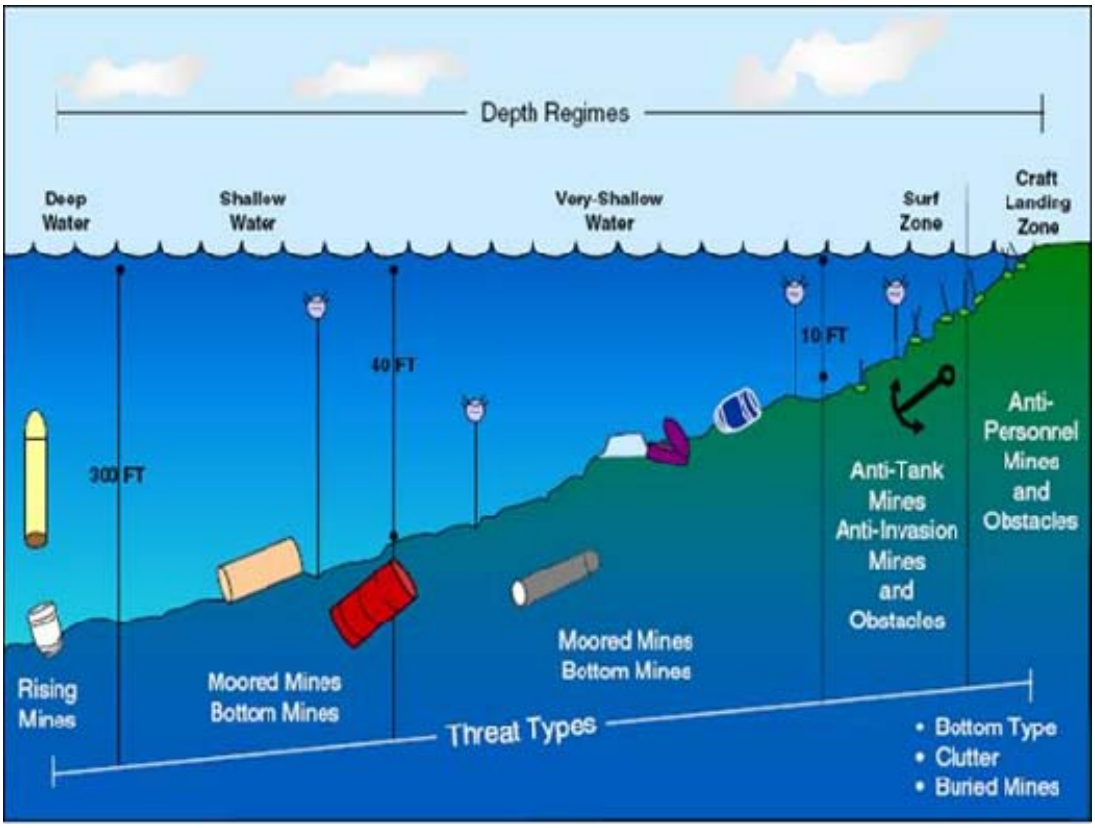

Figure 6. Mine types and associated typical depth regimes (From United States General Accounting Office, 2001)

II. SHIP'S MAGNETIC FIELD SIGNATURES

A basic understanding of the shipboard generating mechanisms of magnetic field signatures, and the physics behind sensing them should reduce some of the mystery of the invisible magnetic field associated with sea going ships. It is difficult at times to picture this magnetic field because it cannot be seen, heard, or felt. The generating mechanism of magnetic fields is rooted in the theory of relativity and more specifically in magnetohydrodynamics. Although the highly non-linear magnetohydrodynamics that takes place in the earth's core is not completely understood (Davidson, 2001), the distribution of its main magnetic field over the world's oceans has been mapped extensively and modeled (McLean, 2004), and is used in the prediction of a vessel's magnetic signature as a function of latitude, longitude, and heading.

To alleviate some of the mystery and get a picture of a magnetic field make this simple visual: Imagine a rectangular magnet placed under a piece of cardboard. When filings or slivers of iron are sprinkled on the cardboard, above the magnet, the filings are magnetized and begin to align with the magnetic field of the magnet below. The patterns that result trace the contours of the magnetic field that cannot be seen directly. Because we do not see this magnetic field it is often difficult to understand how its presence around naval vessels increases the danger of attack by mines and other detection systems.

Like individual handwriting, underwater sound produced by a ship has characteristics that are distinctive to it and thereby can be used to differentiate it from other ships. The term "signature" was coined in the realm of acoustic measurement and detection a vessel's underwater sound pressure field (Holmes 2006). Even though the magnetic field of a seagoing vessel is not as unique as its acoustic, the term signature has been carried over to describe the spatial and temporal distribution of a ship's electromagnetic field.

Surface ship and submarine magnetic field signatures have been exploited for over 80 years by naval influence mines, and both underwater and airborne surveillance systems (Holmes, 2006). Every ship has a magnetic signature, which is caused by its iron

and steel components. These signatures have two parts: a permanent magnetic component, and an induced component. The permanent magnetic component which is acquired at the time the ship is built due to the ferrous steel used in construction. The induced component depends on the instantaneous position and orientation of the ship on the surface of the Earth as well as the local geomagnetic field of the Earth.

As described with the magnet and filings we can determine that magnetic fields are produced by the electric charges in motion. The charges are either positive or negative and can flow linearly, as with electric current or simply about their own axis. The movement of negatively charged electrons is the primary source of all ship and submarine magnetic signatures. A family of hysteresis curves is produced by a field of increasingly larger positive and negative coercive forces.

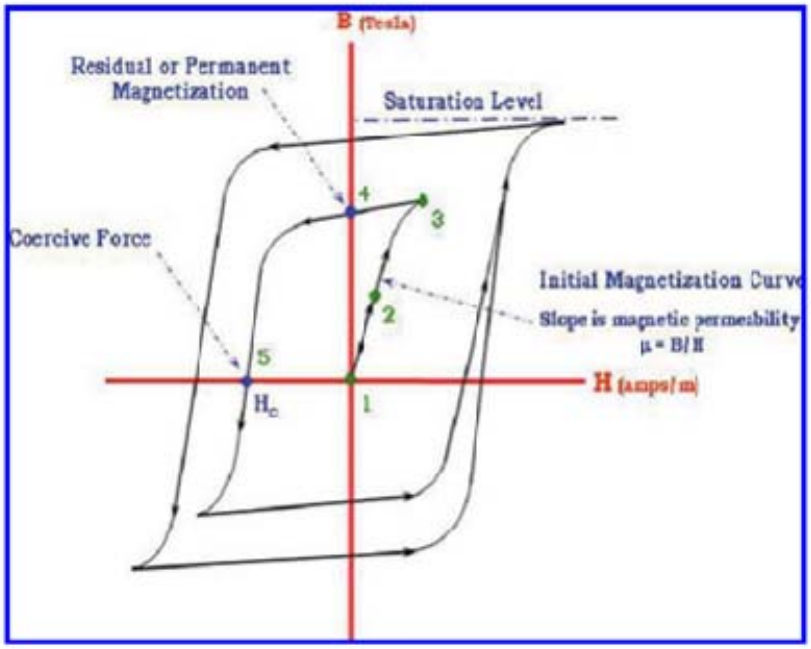

Figure 7. Example of hysteresis curve for ferromagnetic material (From Holmes, 2006)

When a steel bar is placed in a uniform field not only is it magnetized as explained, but this magnetization also distorts the inducing field causing its flux lines to bend toward the steel (Holmes 2006). By principle, the magnetic field leaves the north pole of a magnet and enters its south pole. An anomalous field can be measured as a time-varying signal if the magnetized steel is moved across a sensor or if a sensor is

moved past the steel. This will happen whether the field is produced by an induced magnetization, permanent magnetization, or a combination of the two. This time-varying field is that which is exploited by magnetic mines and submarine surveillance systems.

Magnetization of a ship can occur in each of its three orthogonal directions. Each state of magnetization in-turn produces three magnetic signature vectors called the vertical component (positive down), longitudinal component (positive toward the bow), and transverse or athwartship component (positive abeam). The flux pattern around a uniformly magnetized vessel located at the magnetic North Pole is drawn in Figure 8. Contour plots showing the complete signature patterns of the three components over a rectangular area on the seafloor are included. Dark areas in the plots represent a negative polarity and light areas positive. Induced vertical magnetization (IVM) signature shapes can be gleaned by comparing the contour patterns to those expected from the flux distribution drawn in the upper right corner of the figure.

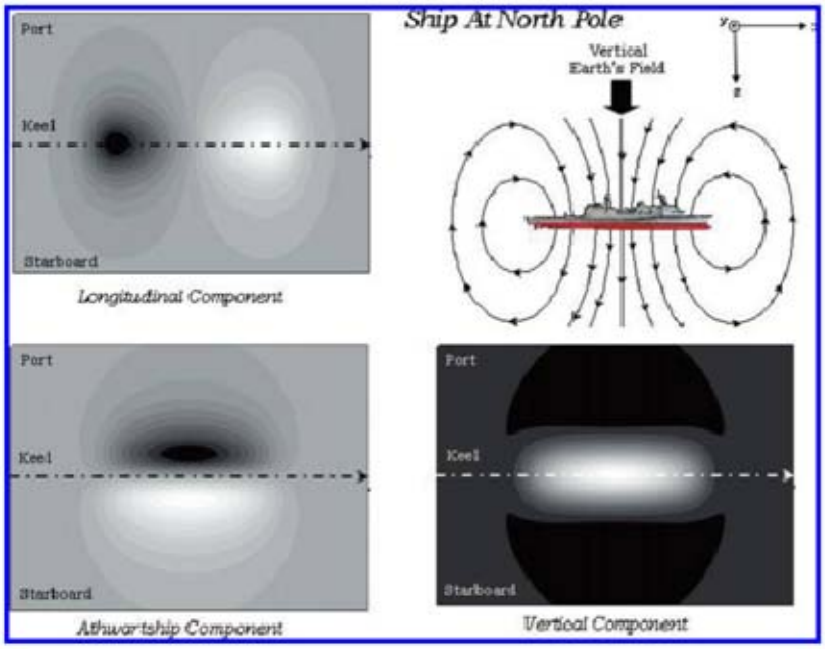

Figure 8. Induced magnetic field signature components of a vertically magnetized ship (From Holmes, 2006)

When a ship is sailing north at the magnetic equator it receives an induced longitudinal magnetization (ILM) from the earth's magnetic field, which turns into an induced transverse magnetization (ITM) when the vessel steams west. These flux patterns and tri-axial signature contour plots are shown in Figures 9 and 10 respectively. Again, the signature shapes can be linked to their respective flux patterns drawn in the upper right of the two figures.

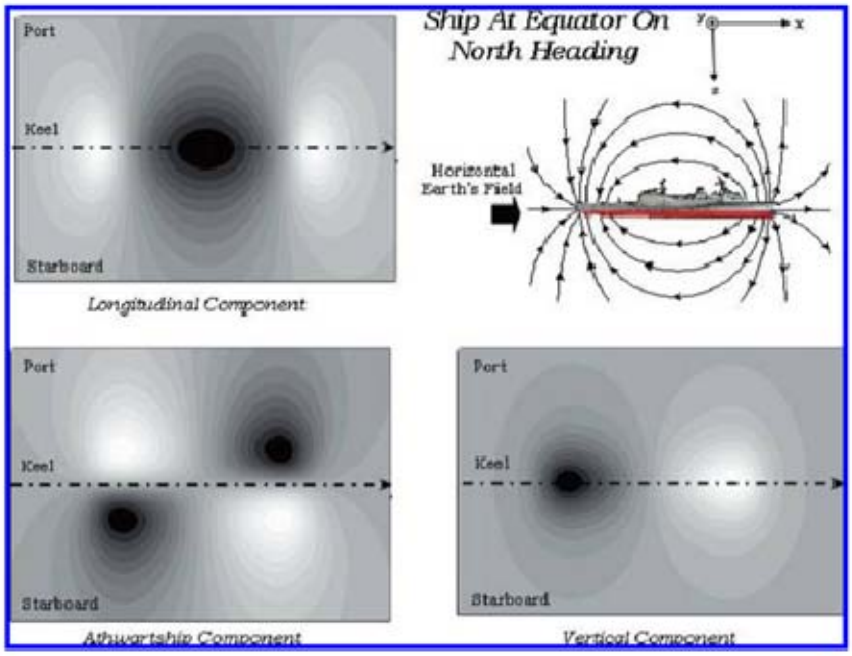

Figure 9. Induced magnetic field signature components of a longitudinally magnetized ship. (From Holmes, 2006)

Naval vessels do not magnetize uniformly. The distribution of steel through out the volume of a ship is irregular and, as a result, so is its magnetization. A ship can be magnetized in its three orthogonal directions simultaneously. Since the maximum amplitude of the earth's magnetic field is small in comparison to the magnetic saturation level of the steel's hysteresis curve, the magnetic permeability can generally be taken as constant (Holmes, 2006). Thus, a sea going vessel arbitrarily located on the globe and sailing on an inter-cardinal heading will have an induced magnetization and signature that is a linear combination of the IVM, ILM, and ITM.

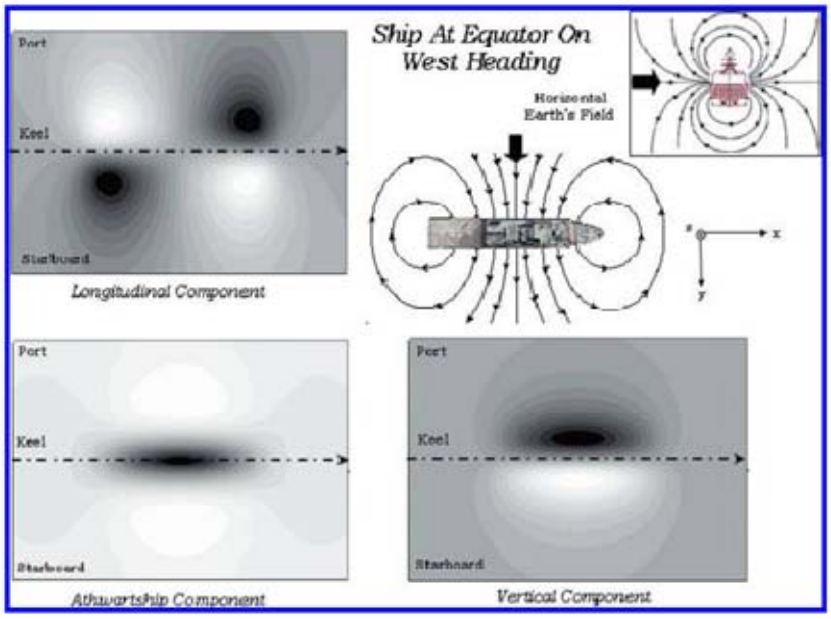

Figure 10. Induced magnetic field signature components of a ship magnetized in the transverse direction. (Holmes, 2006)

Like the induced, a ship's permanent magnetization also follows the three orthogonal directions. The three non-deviating components are called the permanent vertical magnetization (PVM), permanent longitudinal magnetization (PLM), and permanent transverse magnetization (PTM). Each of the three permanent magnetization components generates their own transverse, longitudinal, and vertical magnetic field signatures. Therefore we can identify 18 total ferromagnetic signature components; three each for the ILM, ITM, IVM, PLM, PTM, and PVM.

The tri-axial magnetic field signatures of a 13,300 ton commercial steel hull surface ship were measured at a depth of 25 meters below the vessel, and 67 meters horizontal distance from its keel. The longitudinal, transverse, and vertical signatures were recorded as the vessel sailed by a submerged magnetic field sensor, and are plotted in Figure 11 as a function of time. The earth's background field has been removed from the data. By comparing the field patterns in Figure 10 to those in Figure 8, 9, and 10, it is clear that the vessel is magnetized primarily in its longitudinal and vertical directions. The strengths of these signatures are very large, and exhibit a signal-to-noise ratio greater than 40 db.

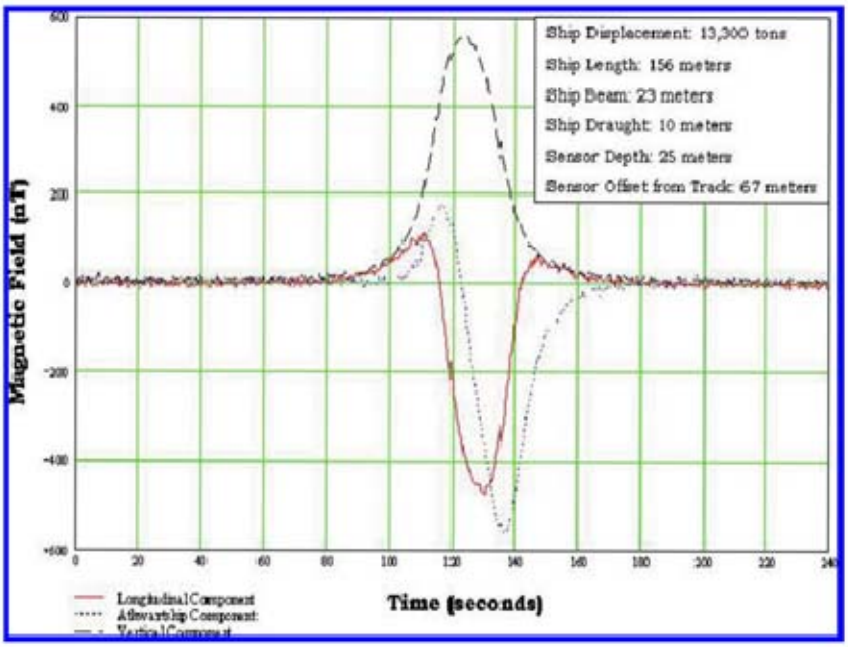

Figure 11. Tri-axial magnetic field signatures of a steel hull surface ship

III. OCEAN CONDUCTIVITY

A. SEA WATER CONDUCTIVITY

Sea water is generally conductive. When the salt concentration of the ocean is about 35 grams per liter, sea water is a very good conductor. Hydrated ions of the dissolved salts in ocean water are great carriers of the electric charge. The conductivity of sea water depends on the amount of ions dissolved per unit volume (salinity) and the mobility of those ions. As with salinity, conductivity increases by the same amount, 1 gram per liter, 1° C temperature change and depth (pressure) increase of 2000 m. Temperature change dominates the change in conductivity with a range of about 2.5 S/m for cold deep water and 6 S/m for warm surface water. A CTD (Conductivity, Temperature, and Depth) is the primary tool used in gathering seawater to determine the essential physical properties. This gives scientists a precise and comprehensive charting of the distribution and variation of water temperature, salinity, and density that helps to understand how magnetic mining is affected by the oceans. CTDs return a conductivity value to represent the amount of dissolved ions in seawater.

Conductivity can be converted to a salinity value of the 1978 Practical Salinity Scale (PSS-78, UNESCO 1981), which is influenced by the ambient temperature and pressure. The conductivity ratio is defined as the ratio between the measured electrical conductivity at a given pressure and temperature against the conductivity of a standard seawater of practical salinity 35 at a temperature of 15°C and atmospheric pressure, defined as 0 decibar. The units for electrical conductivity (EC) are microSiemens per centimeter (µS/cm). The conductivity ratio is calculated by

$$R = \frac{C(S,t,p)}{C(35,15,0)} = \frac{C(S,t,p)}{4.2914\,S\cdot m^{-1}}$$

(3.1)

Here, R is the conductivity ratio, C(S,t,p), {Salinity, temperature and pressure} is the measured electrical conductivity and C(35,15,0) the electrical conductivity of the

standard seawater, which yields 4.2914 $S*m^{-1}$. For electrical conductivities measured in $mS*cm^{-1}$ the value needs to be shifted one decade to 42.914 $mS*cm^{-1}$. For this experiment a standard MATLAB code was used for the conversion. Using the same variables as in Equation (3.1) we have the Sea Water Conductivity ratio as:

SW_CNDR; R = C(S,T,P)/C(35,15,0)

to calculate the conductivity ratio from collected S, T, P.

Reference Appendix A to see this code; % represent comment lines, all else is code.

B. SEDIMENT CONDUCTIVITY

The solid earth materials of the ocean floor do not have the same conductivity as the ocean above it. Ocean sediment structure is characterized in two ways. The first method is observing sediment properties by collecting core samples using in-situ instrumentations. The other method uses remote techniques to estimate the acoustic properties of the sediment. The reflected sound of these observations is used to invert the sediment thickness and determine sound velocity. The acoustic method may suffer range degradation due to the gas trapped in sediments which will impede the sound propagation. Model based techniques have been developed to illustrate the sediment conductivity and thickness by inversion of electromagnetic data. Since both the speed of sound and the electric conductivity of the sediments are related via Archie's law it is possible to make the same type of sediment characterization from low-frequency electromagnetic fields (Fristedt, et al. 2008).

Let F be the ratio between the conductivity of the water (σ_W) and the conductivity of the sediment (σ_T),

$$F = \frac{\sigma_W}{\sigma_T} \tag{3.2}$$

This ratio depends on the sediment porosity (n) with a power law (Archie, 1942) usually called Archie's Law),

$$F = n^{-m}$$

(3.3)

Here, m is the empirical power which equals 1.3 for loose sands and 2 for highly cemented sandstones. For example, Yellow Sea sediment, m = 1.5, in the San Diego Bay sediment m = 1.8. From (3.1) and (3.2) we have

$$\sigma_T = \sigma_W n^m$$

(3.4)

With the known water conductivity (σ_W), sediment porosity (n), and sediment type (m), we are then able to compute the sediment conductivity (σ_T)

The coefficient of proportionality depends on porosity and fabric (sediment). Archie(1942) defined the formation factor F, as the resistivity of the saturated soil, T, divided by the resistivity of the saturating solution, W, that is where W and T are the electrical conductivities of the pore water and saturated soil, respectively. An empirical correlation between the formation factor and porosity for clean sands is given when n is porosity, and m equals values on a given scale.

THIS PAGE INTENTIONALLY LEFT BLANK

IV. NAVY LAYERED MAGNETIC MODEL FOR PREDICTING AN OCEAN MAGNETIC FIELD

There are essentially three different magnetic minesweeps currently in use by the U.S. Navy. These are illustrated in Figure 12. The N-layered model can be used to compute the vector components of the magnetic field produced by each of three sweep types, straight tailed, open loop & closed loop. For each sweep, the magnetic field is produced by the circulation of an electric current. The straight tailed sweep's electric current is generated onboard the minesweeper. Current flows down a twisted pair of insulated cable from one electrode to another via seawater paths and is returned to the twisted pair by a straight, insulated single conductor. The open loop sweep is similar to the straight loop sweep except that one of the electrodes is offset. This minimizes the magnetic field beneath the sweeper. Current from the rear to forward electrodes takes place through the catenary shaped, insulated conductor. Both the straight tailed and open loop sweeps require current flow through the surrounding seawater. If the salinity of the seawater is too low, then it cannot conduct enough current to produce a magnetic field of sufficient strength to actuate mines. Thus, both the straight and open loop sweeps depend on the ocean environment.

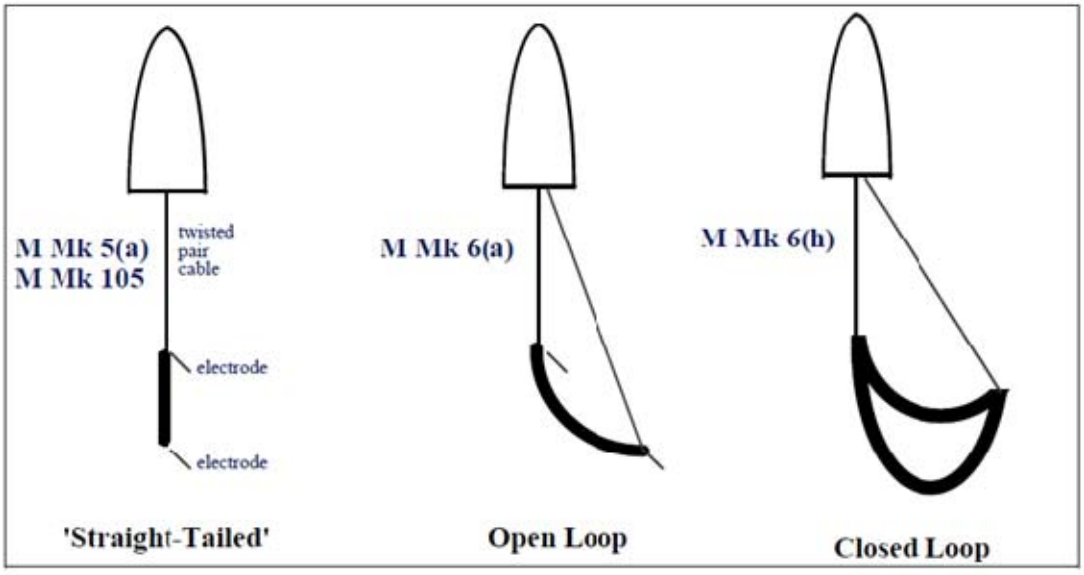

Figure 12. Magnetic sweep types which can be modeled with the N-Layered Magnetic

Model (From Software Design Description for the N-Layered Magnetic Model)

Magnetic minesweeping configurations used by U.S. Forces can be categorized as either straight-tailed, open loop, or closed loop. The modeling capability described must be able to calculate swept path for each of these. There are also a number of other magnetic minesweeping systems which are in use by foreign navies. As a secondary requirement, it is highly desirable that the model be able to calculate performance ranges for non-U.S. systems which are likely to be used in proximity to U.S. forces during periods of littoral or regional warfare.

The NLMM:

- Uses algorithms to predict the performance of magnetic minesweeping equipment
- The conductivity of seawater depends upon both the amount of dissolved salt and the water temperature.
- The ocean environment can be assumed to consist of two simple layers, or of *N layers*, each of constant conductivity, and an underlying half space, also of constant conductivity.

These environments are shown next. Note that when N=2, the N-Layered Magnetic Model environment reduces to the two-layered environment shown on the right hand side of the figure. The MKS unit of conductivity is the mho. A nominal value for salty water is 4 mho. In brackish water, conductivity falls to 2 mho and less. Conductivity in ocean sediments varies over a wide range.

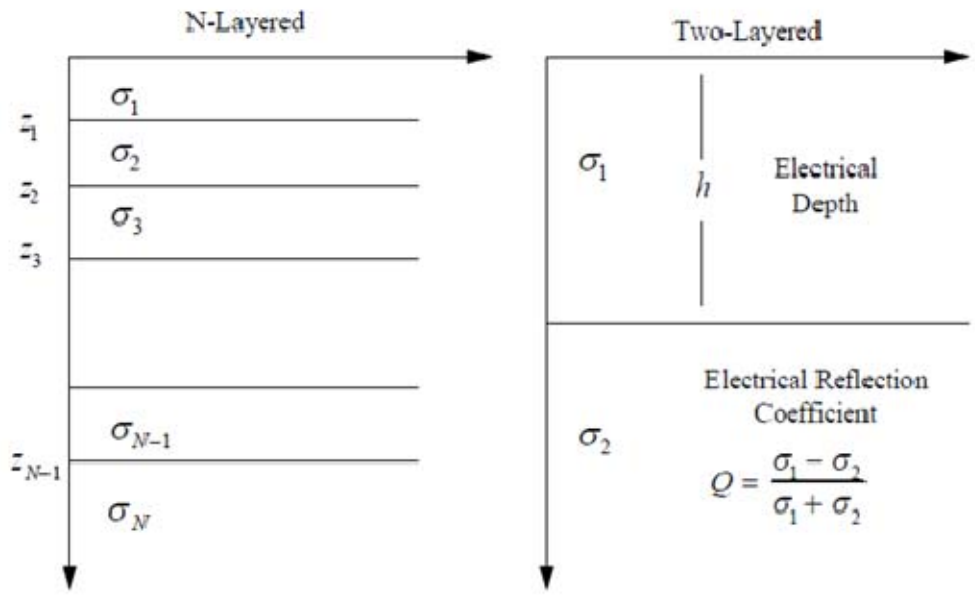

Figure 14. Variation of conductivity versus depth used in the N-Layered Magnetic model

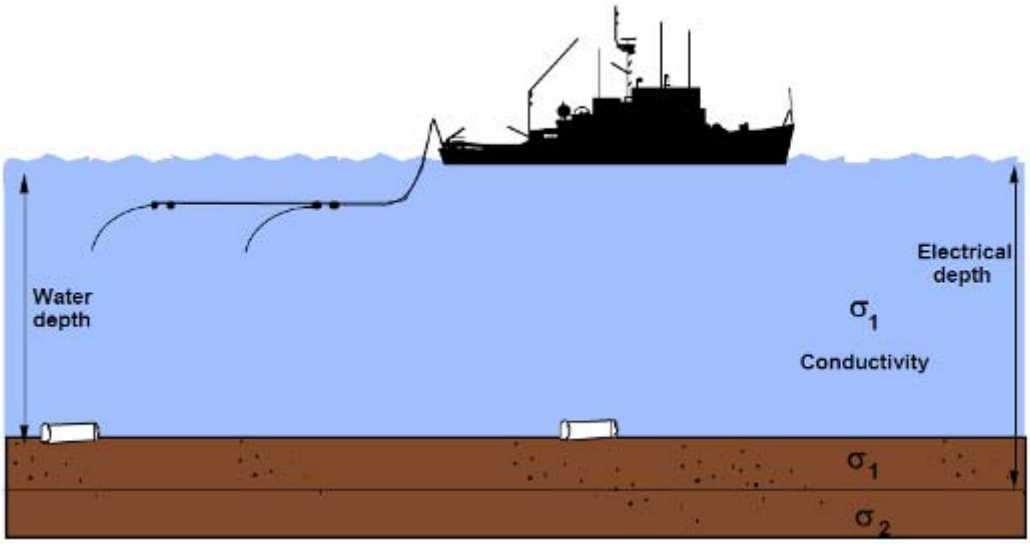

Figure 15. Minesweeping with a straight-tailed sweep

Water column conductivity and sediment conductivity are shown as constants. In complex, littoral waters these may actually be more multifaceted functions of depth. For

a simple, two-layered environment, the electrical depth is the depth at which there is an appreciable change in conductivity.

A. SWEEP DESCRIPTIONS

1. Straight Tail

Let (x, y) be the horizontal coordinates of the sweeper along the y-axis and z be the vertical coordinate. The coordinate origin is located at the middle of the two electrodes along the y-axis (i.e., the axis of the sweeper). The basic geometry of the straight tailed sweep is shown in Figure 16. The magnetic field produced by the straight tailed sweep is the vector sum of the magnetic field produced by the straight wire and the magnetic field produced by the circulating currents.

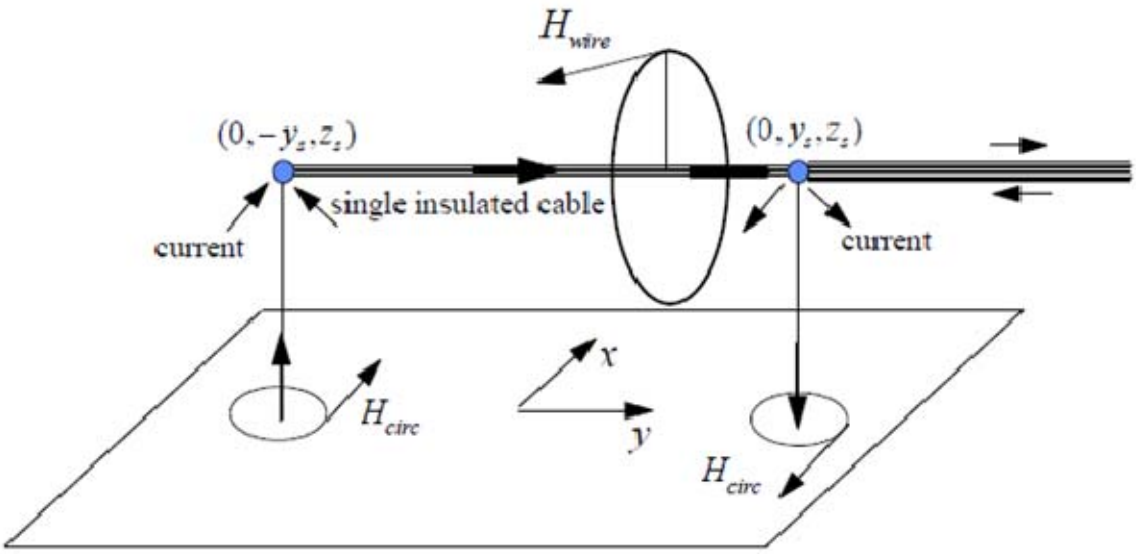

Figure 16. Geometry of a straight tailed sweep

Current is provided to the forward electrode by a twisted pair cable connected to a generator onboard. It escapes into the ocean via an exposed electrode and returns through the rear electrode completing the electrical loop. The wire produces an x-component and a z-component, but no y-component. For a horizontally stratified environment, the circulating currents produce x and y-components but no z-component. The three vector components at the point r =(*x*, *y*,*z)* are as follows:

$$\mathbf{H}(\mathbf{r}) = \frac{1}{4\pi}\int_{straight\ wire} \nabla \times \frac{\mathbf{I}(\mathbf{r}')}{|\mathbf{r}-\mathbf{r}'|}ds' + \frac{1}{4\pi} \underset{\substack{Vol \\ \text{pos electrode}}}{\iiint} \nabla \times \frac{\mathbf{J}(\mathbf{r}')}{|\mathbf{r}-\mathbf{r}'|}dx'dy'dz'$$

$$-\frac{1}{4\pi} \underset{\substack{Vol \\ \text{neg electrode}}}{\iiint} \nabla \times \frac{\mathbf{J}(\mathbf{r}')}{|\mathbf{r}-\mathbf{r}'|}dx'dy'dz'$$

(4.1)

Straight tailed sweep (Software Design Description for the N-Layered Magnetic Model 1997). H(r)is the given integral. J(r) is related to the scalar electric potential V(r) via the relationship $\mathbf{J}(\mathbf{r}) = -\sigma\nabla V(\mathbf{r})$, where Sigma is conductivity. The potential V(r) can be found by solving V^2V =0 together with the appropriate boundary conditions. I(r') is the vector current.

$$\mathbf{J}(\mathbf{r}) = -\sigma\nabla V(\mathbf{r})$$

(4.2)

2. Open Loop

Similar to the straight tail, (x, y) are the horizontal coordinates of the sweeper along the y-axis and z is the vertical coordinate. The magnetic field produced by the open loop sweep is the vector sum of the magnetic field produced by the catenary shaped wire shown in Figure 16 the magnetic field formed by the circulating currents.

$$\mathbf{H}(\mathbf{r}) = \frac{1}{4\pi}\int_{catenary\,1} \nabla \times \frac{\mathbf{I}(\mathbf{r}')}{|\mathbf{r}-\mathbf{r}'|}ds' + \frac{1}{4\pi}\int_{catenary\,2} \nabla \times \frac{\mathbf{I}(\mathbf{r}')}{|\mathbf{r}-\mathbf{r}'|}ds'$$

(4.3)

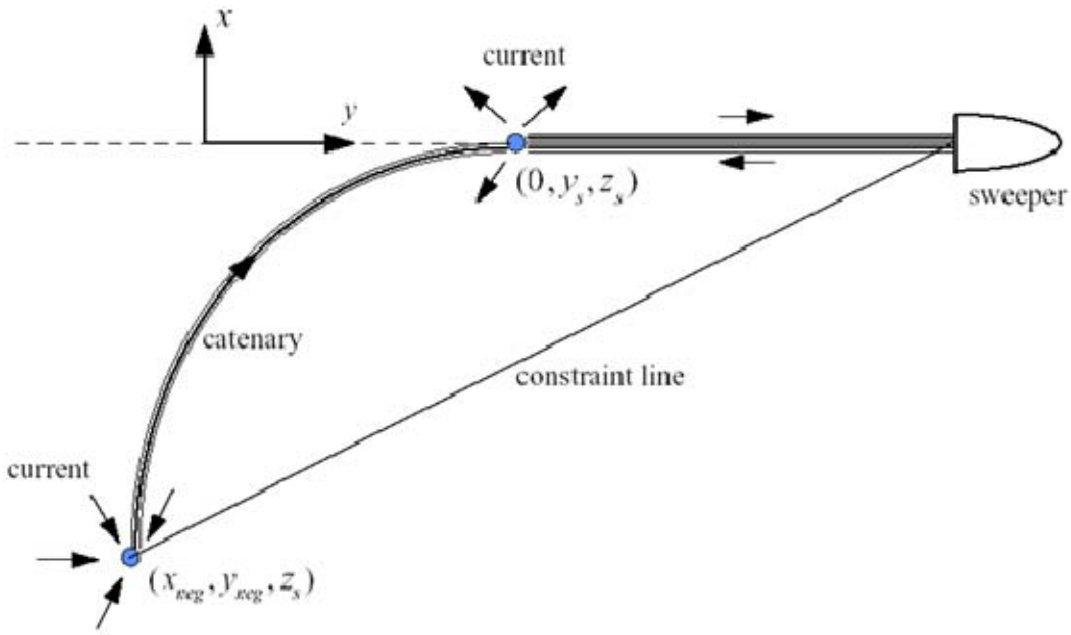

Figure 18. Plan view geometry of the open loop sweep

In this case the curved shape of the wire creates the x, y, and z components. For a horizontally stratified environment the circulating currents produce only x and y components. Current is provided to the forward electrode by twisted pair cable connected to generator onboard the sweeper. It escapes into the ocean via an exposed electrode. Current returns via the rear electrode and flows through the single insulated cable (catenary shaped segment) to complete the electrical loop.

> In order to calculate the swept path width for magnetic minesweeping systems currently in use the US mine Warfare forces, it is necessary to calculate the vector components of the magnetic field which are generated by each of the possible sweep configurations. (N-Layered Magnetic Model Software Requirement Specification 1997)

The four functional routines needed to perform this calculation are:

Compute:

- The shape that is assumed by the buoyant current carrying cables towed behind a minesweeping platform.

- Magnetic fields generated by a current flowing in a known cable shape.
- A single electrode contribution to the magnetic field due to the ocean return path.

and combine:

- All magnetic field contributions due to currents flowing in both wires and the ocean, into a system performance estimate for specific minesweeping configurations.

Additionally, there are environmental factors that impact magnetic sweeping systems. The most critical of these is salinity, as previously discussed. Conductivity values that are low due to water column salinity values will not support open loop sweeping. Environmental conditions which have the most impact on magnetic mine sweeping can be seen in Table 1.

Environmental Category	Environmental Parameter	Typical Effect
Bathymetry	Water Depth	Swept path calculations are not valid in regions of highly variable bathymetry, as these calculations assume constant water depth.
	Bottom Slope	Can cause shielding effects, thereby degrading sweep performance.
Water Column Characteristics	Conductivity and Salinity	Open-loop configurations of sweeps depend on the conductivity of sea water to complete the return of electrical current.
Internal velocity fields	Currents	Deployment of cabling configurations may be difficult
Ocean Bottom Characteristics	Sediment Conductivity	Current flow from open loop sweeps can be altered by variations of conductivity in the ocean bottom thereby perturbing magnetic field produced by the sweep.

Table 1. Environmental parameters which impact magnetic mine sweeping (From N-layered magnetic Model SRS, 1997)

B. NAVAL OCEANOGRAPHIC OFFICE (NAVO) 2 LAYER MODEL

In the theory of calculating magnetic fields of electrode sweeps in minesweeping an environmental model of two conducting layers (Figure 17) is normally assumed. The magnetic field of an electrode sweep, typically open loop sweeps, is affected by the

environment, because the sea water and sea bottom are part of the path of the current. The name "two-layer" model is due to there being two conducting layers, later we will show model results from multiple layers. There also is a non-conducting air layer above the water's surface, but the magnetic field of the sweep is not going to be computed there. There are two boundaries: the first one being at the air-water interface, the second one at depth ED. These parameters pertain to the boundary between the upper conducting layer and the lower conducting layer (Two-Layer Model for Magnetic Field for Electrode Minesweeping, Jones 2004).

> Concerning the relationship between ED and AD, the normal situation is ED≥AD, but the situation ED<AD can occur. If ED≥AD, moored magnetic mines and bottom mines will be in the upper layer of the two-layer model. The case ED<AD is considered anomalous. If ED<AD occurs, then bottom mines are in the lower layer of the two-layer model but moored mines could be in the upper layer. (Two-Layer Model for Magnetic Field for Electrode Minesweeping, Jones 2004)

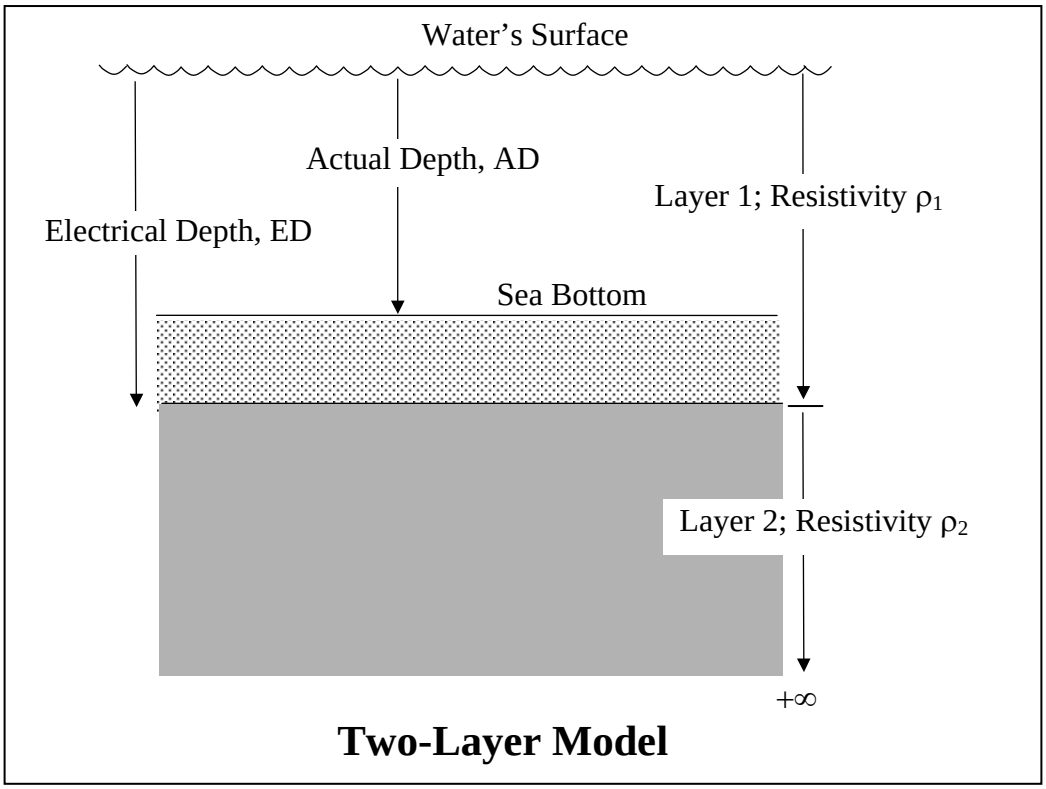

Figure 19. Two-layer model for electrode sweep minesweeping

$$Q = \frac{\rho_2 - \rho_1}{\rho_1 + \rho_2}; \quad 0 < Q \leq 1$$

(4.4)

The strength of the magnetic field that a sea mine will sense are water column conductivity, sediment conductivity, water depth, and bottom slope and denoted by the following input parameters:

- Resistivity of water column / sediment (Q)
- Electrical Depth vs Actual Depth ratio (ED/AD)
- Water Depth
- Water Conductivity (vertical profile)
- Cable Configuration
- Sweep Setting (cable amperage, pulse settings, etc.)
- Assumed Mine Type / Settings

The two layer model is characterized by two of the most important parameters above, ED and Q. The third value of AD is used in the ED/AD ratio and is also essential. Surveys known as Magnetic Capability and Safety (MACAS) surveys are used to obtain ED/AD and Q values. This is done by measuring voltages in the water produced by a pulsing magnetic tail. Survey efforts are time consuming and sometimes produce few ED/AD and Q data compared to the amount of priority littoral regions in which the U.S. Navy needs to operate.

In the two-layer model used by NAVO positive z is down, and the potential, V, at a point in space (on an electrode) is a function of Q and ED. As denoted previously, a point (r,z) will be taken at a horizontal radius r from the electrode and at a depth z below the surface. Values of Q and ED need to be known for an oceanographic area that is to be swept, in order to predict $\vec{H}$ of the sweep accurately in the area. When H is determined and a magnetic mine is present, the swept path to conduct a sweep against the mine can be predicted. Using the sediment and water conductivity profile as input most water columns can be reduced to a 2-layer case and thus able to compute Q and ED/AD.

THIS PAGE INTENTIONALLY LEFT BLANK

V. APPLICATION FOR MAGNETIC MINE NEUTRALIZATION

A. AREAS OF INTEREST

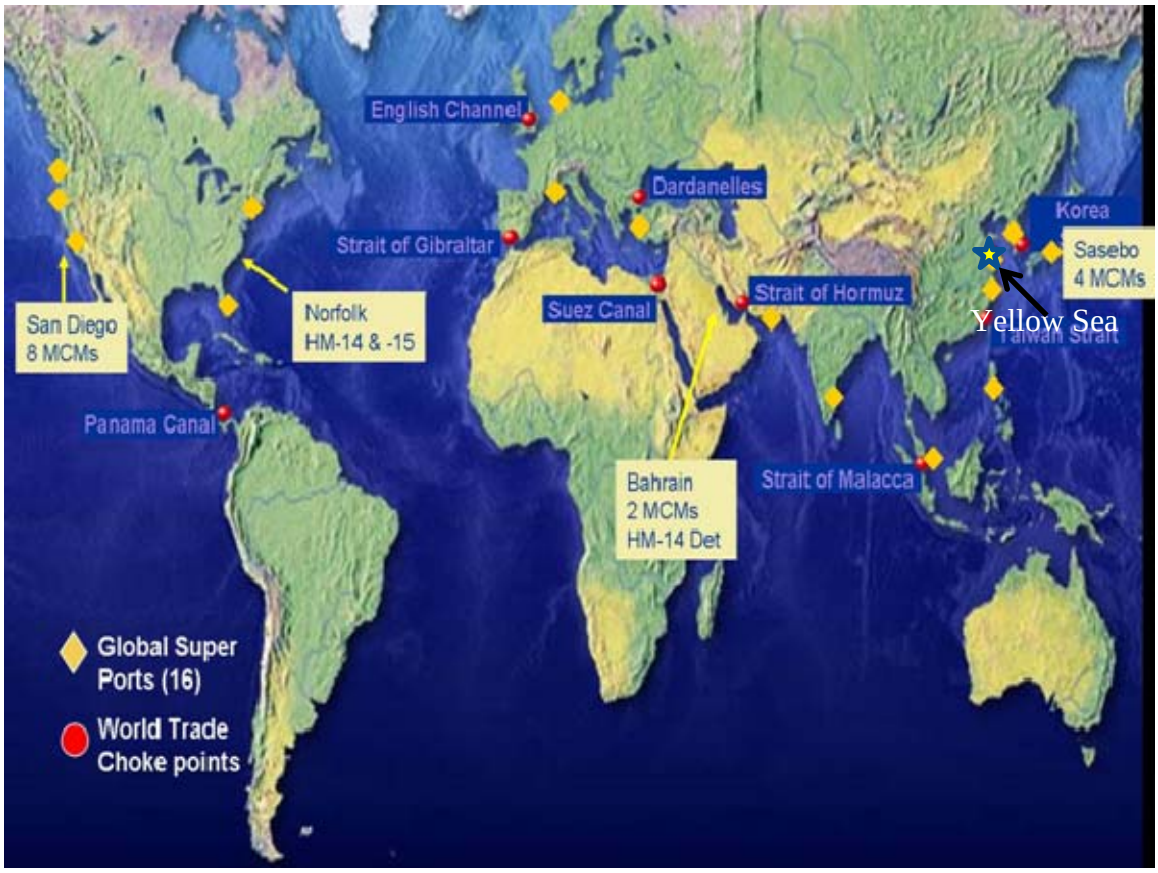

Figure 20. World map: major seaports and possible trade choke points (After Naval War College, 2009)

In this project we had two Areas of Interest (AOI), San Diego and the Yellow Sea. Both of these areas are important for their strategic locations and significance to economics. The oceans support 90% of the world's trade and two-thirds of its petroleum transport. The global economy in which we prosper is due primarily to the free movement of goods and services secured by the world's navies, most specifically, our own. Open sea lanes world wide and the supporting shore structure are lifelines to this free movement. Shutting down a single port can prove devastating to a nation's financial system. The enormity of economic damage a port closure would have could cause a

ripple effect around the globe. There is an undeniable link between the prosperity a country enjoys and its security, the two go hand in hand. Control of the sea and the harbors leading to port trade is vital to our existence. Laying mines is a simple method that can interrupt and deny this control. During operations other than peace time, ports and chokepoints are not the only places vulnerable to disruption. Sea lanes for support, sea lines of communication and beaches for amphibious landings are often targets for mining our adversaries.

1. San Diego

San Diego Bay is home port to a substantial fraction of the Navy's Fleet. Supporting large numbers of ships and facilities requires a balance between the Navy's requirements and the natural, recreational, and commercial uses of the bay. It is clear that the many ports near San Diego, California are vital to U.S. trade and military operations. The water leading into this area can vary greatly around the small islands near the coast. Water depth in the area of our study was as deep at 216 meters. For our observations we selected a location with water depth of 50 meters. The sediments of the San Diego Bay consist primarily of gray, brown, or black mud, silt, gravel and sand. The bottom sediment for our area is a sandy mud mixture.

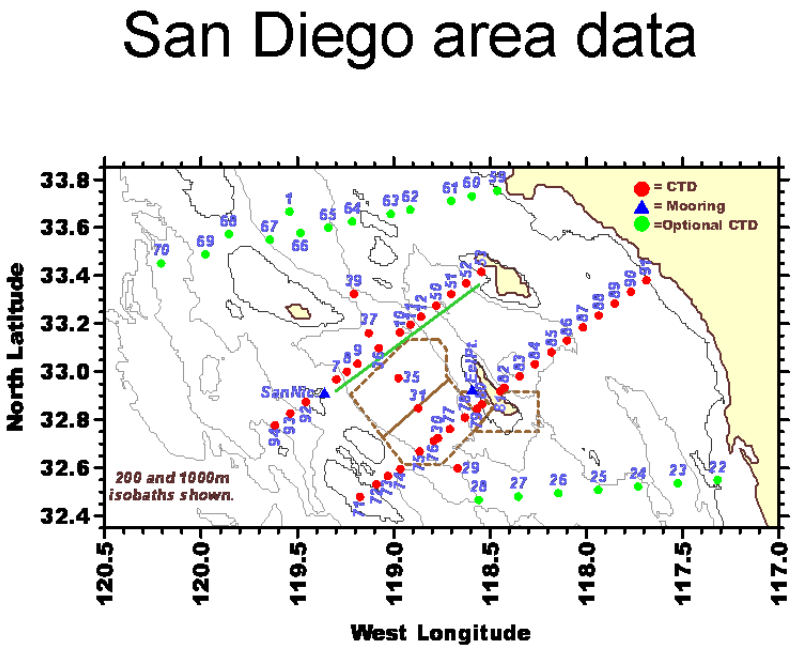

Figure 21. San Diego area CTD drop points Sept 2009

2. Yellow Sea

U.S. operations in the Yellow Sea take place in international waters and have for many years. While the Yellow Sea covers a relatively large area, it is quite shallow. The water depth over most of the area is less than 50 meters and having a maximum depth of about 140 meters, with a very small slope gradient. This makes it prime for possible minefields. However, operations in the Yellow Sea west of South Korea have been the site of repeated naval clashes between the two Koreas over the past 10 years, most recently in November 2009. The Navy's presence in the Yellow Sea isn't new, nor has China previously so vehemently opposed U.S. operations there. China's efforts to rid its coastal waters of U.S. influence are not new, having manifested themselves several times in recent years. Knowing more about the water characteristics provides information that can be used in future operations.

We know the depth of the Yellow Sea and have gathered data on the S, T, and P, for which we use to determine conductivity. The remaining environmental parameter we need to make our model accurate is the sediment conductivity. This data is somewhat sparse but very critical. For our area in the central and western regions the sediment consists mainly of mud, whereas the in the eastern region it is primarily sand.

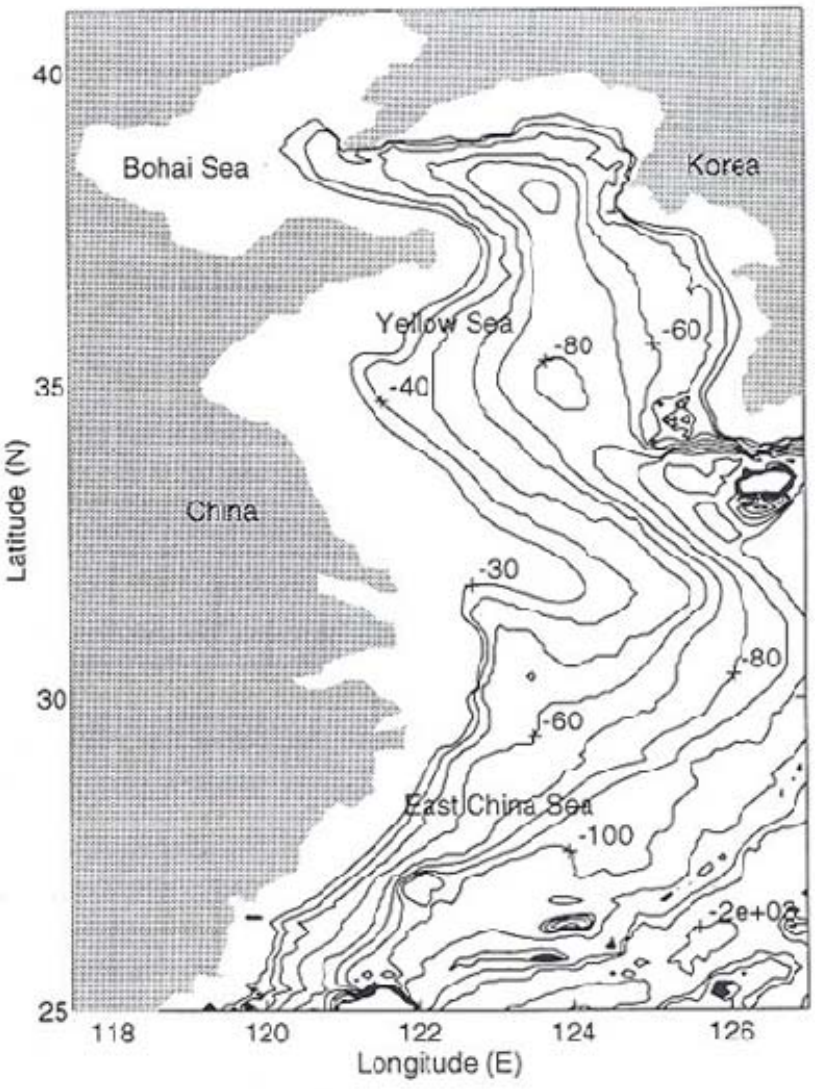

Figure 22. Yellow Sea bottom topography

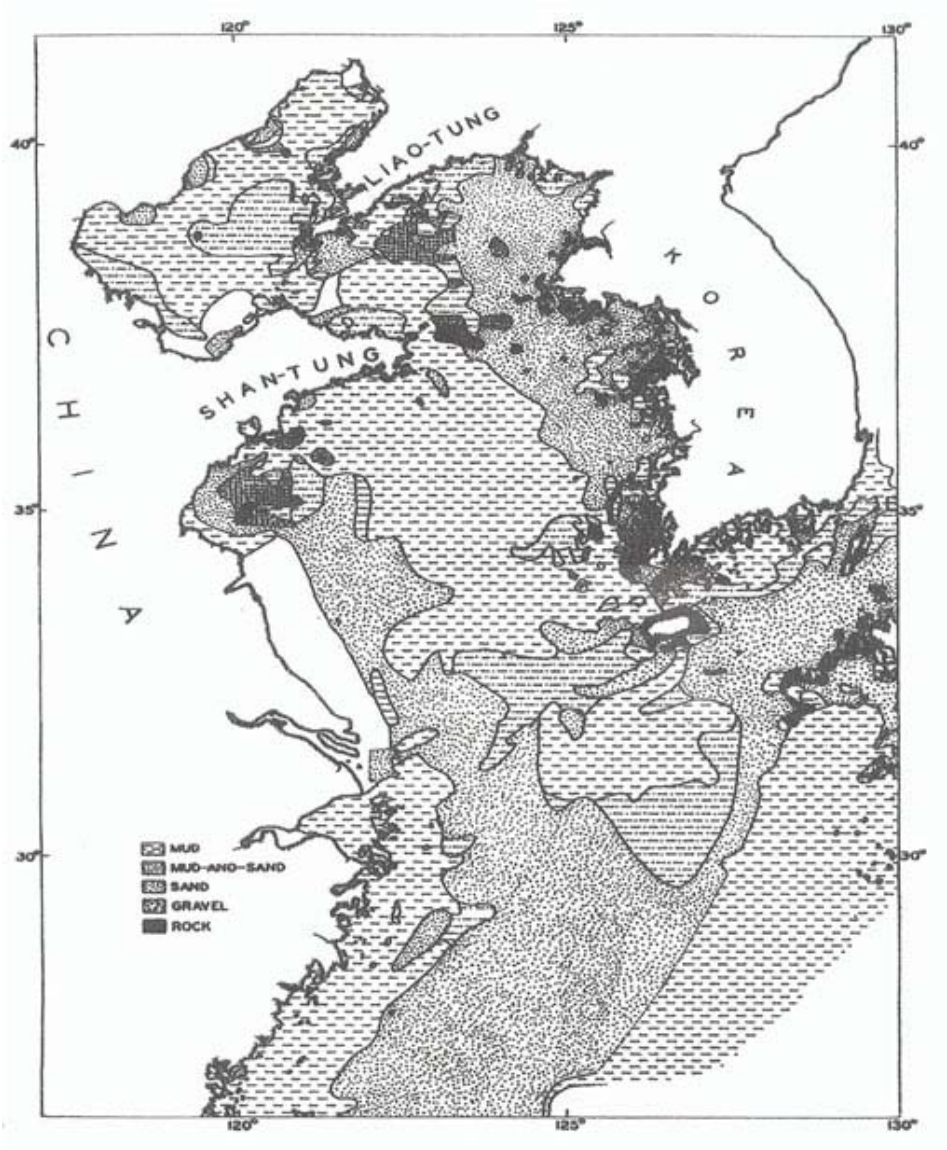

Figure 23. Yellow Sea Bottom Sediment

B. MODEL INPUT

1. Parameters NLMM Type I/ 2-layer

1000.0	Wire current (amp) {Does not change for our model}
100.0	Wire length (m) {Does not change for our model}
1.0	Wire depth (m) {Does not change for our model}
10	Mine Depth (m)
2	Maximum spatial wave number (m)
200	Number of wave numbers
1	Number of layers
xx.x	Layer 1 Bottom Depth (m)
x.xxxx	Layer 1 Bottom Conductivity (mho)
x.xxxx	Seafloor conductivity (mho) 100m
4	Output option
-100.0	Minimum output range X (m)
100.0	Maximum output range X (m)
101	Number of X values
-100.0	Minimum output range Y (m)
100.0	Maximum output range Y (m)
101	Number of Y values
-50.0	X-axis offset (for profiles)
50.0	Y-axis offset (for profiles)

Case#	Water Depth (m)	Mine Depth (m)	Layer 1 Bottom Depth (m)	Layer 1 Bottom Conductivity (mho)	Seafloor Conductivity (mho)
1	50	10	10	4.5333	1.2592
2	50	20	20	4.1719	1.2592
3	50	30	30	3.9451	1.2592
4	50	40	40	3.8911	1.2592
5	50	10	50	3.8749	1.2592

Table 2. San Diego Type I (Straight Tail) 2-layer

Figure 24 (left) shows the spatial variability along the x-axis of the three components of the magnetic field generated by the mine sweeper at the mine depth (z_m) for y = 50 m relative to the mine location: H_x(x, 50 m, z_m), H_y(x, 50 m, z_m), and H_z(x, 50 m, z_m). Figure 24 (right) shows the spatial variability along the y-axis (i.e., the axis of

the sweeper) of the three components of the magnetic field generated by the mine sweeper at the mine depth (z_m) for x = 50 m relative to the mine location: H_x(50 m, y, z_m), H_y(50 m, y, z_m), and H_z(50 m, y, z_m). Because the sweeper is moving, the magnetic components Hx, Hy and Hz as seen by the mine change with (x, y). Voltage produced in the mine's induction coil detector will depend upon the location of these components as well as mine heading, tilt, sweeper heading and speed.

For the straight-tailed sweep, the components H_x and H_y will depend on the environment. For this sweep type the component H_z is generated only by the straight wire and does not depend on the environment. Figure 24 also shows that H_z is much smaller than H_x and H_y. H_x(x, 50 m, z_m) has maximum value (9.0 Amp/m) at x = 0 and decreases away from the mine. H_x(50 m, y, z_m) has maximum value (1.0 Amp/m) at y = 0 and decrease as away from the mine. However, H_y(x, 50 m, z_m) is zero at x = 0 and has maximum magnitudes (±4.3 Amp/m) at around x = 5 m. H_y(50 m, y, z_m) has a minimum value (2.1 Amp/m) at y = 0 and decreases away from the mine.

Figure 25 shows the horizontal distributions of the three magnetic components at the mine depth: H_x(x, y, z_m), H_y(x, y, z_m), and H_z(x, y, z_m). Regions of high positive strength are shown in red. Regions of high negative strength are shown in blue.

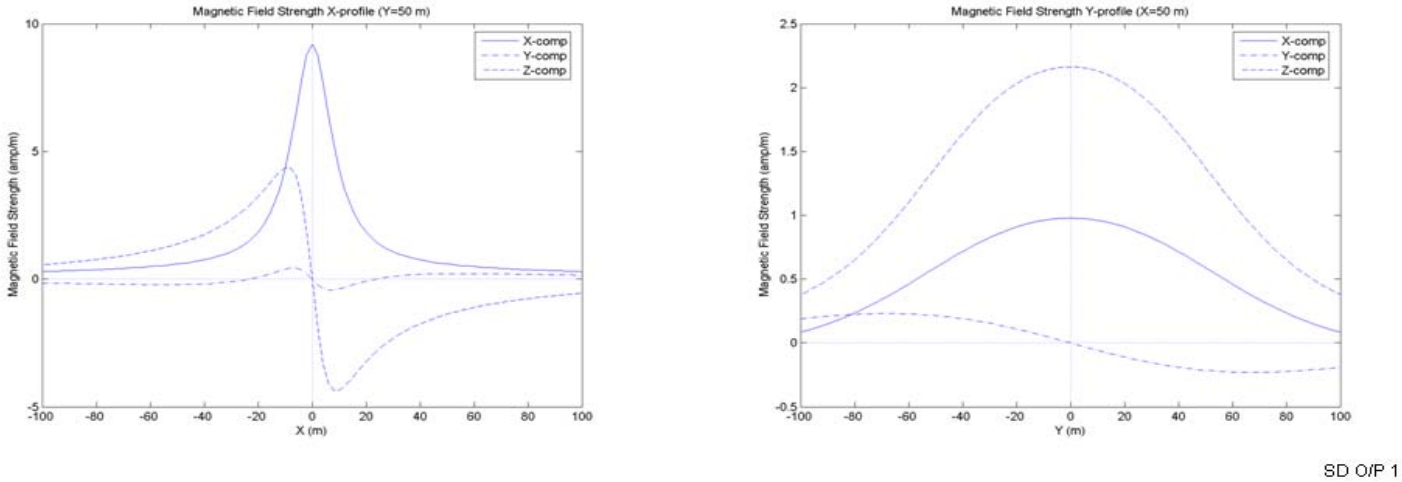

Figure 24. San Diego Type I Case 1 Output (Components *Hx*, *Hy* and *Hz* of the magnetic sweep produced by a straight-tailed sweep viewed at a mine)

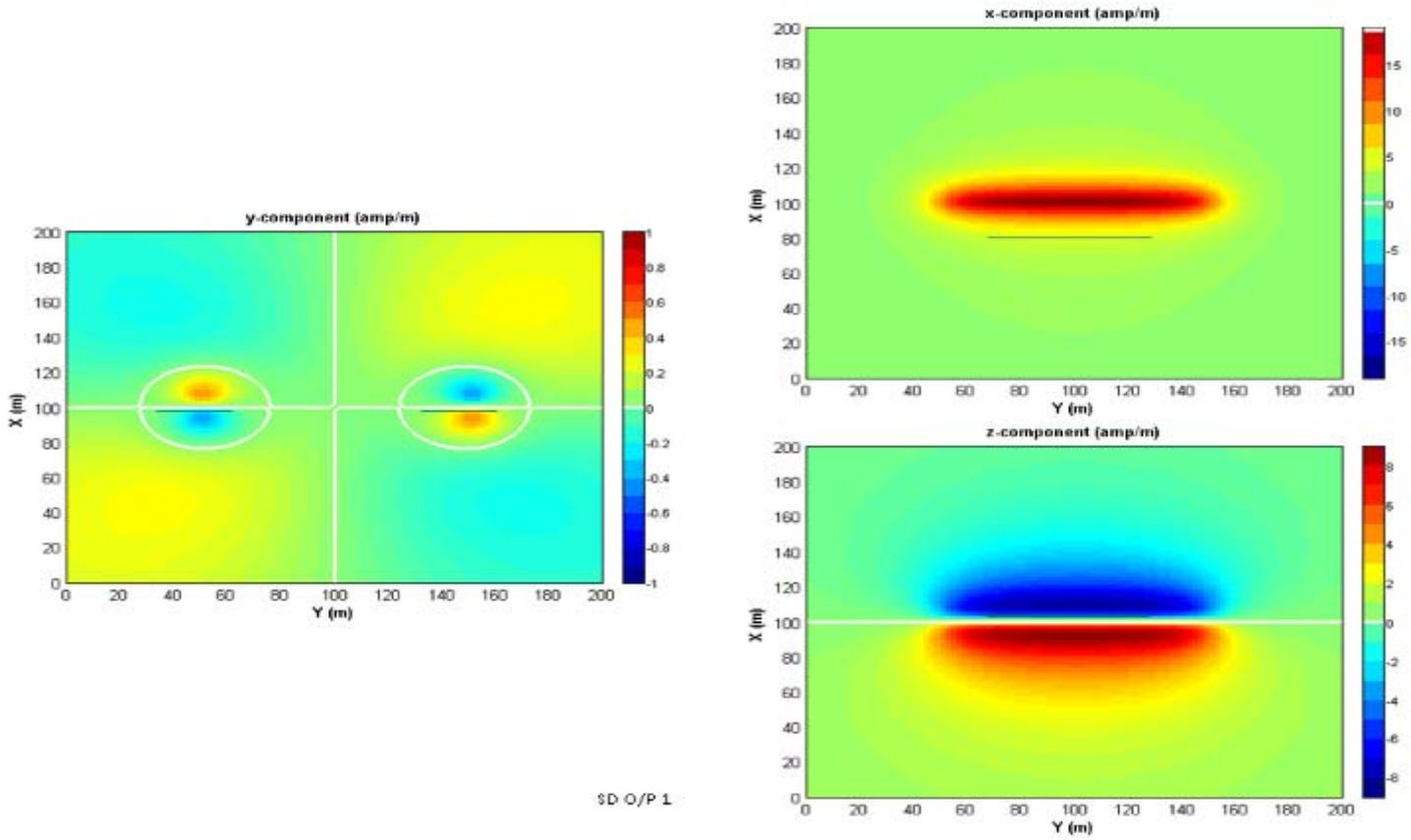

Figure 25. San Diego Type I Case 1 Magnetic Field Individual magnetic field components for a straight-tailed sweep. Depth of mine is 10 m. Single current carrying cable is shown as a green line

Figure 26 (left) shows the spatial variability along the x-axis of the three components of the magnetic field generated by the mine sweeper at the mine depth (z_m) for y = 50 m relative to the mine location: H_x(x, 50 m, z_m), H_y(x, 50 m, z_m), and H_z(x, 50 m, z_m). Figure 26 (right) shows the spatial variability along the y-axis (i.e., the axis of the sweeper) of the three components of the magnetic field generated by the mine sweeper at the mine depth (z_m) for x = 50 m relative to the mine location: H_x(50 m, y, z_m), H_y(50 m, y, z_m), and H_z(50 m, y, z_m). Because the sweeper is moving, the magnetic components Hx, Hy and Hz as seen by the mine change with (x, y). Voltage produced in the mine's induction coil detector will depend upon the location of these components as well as mine heading, tilt, sweeper heading and speed.

For the straight-tailed sweep, the components H_x and H_y will depend on the environment. For this sweep type the component H_z is generated only by the straight wire and does not depend on the environment. Figure 26 also shows that H_z is much smaller than H_x and H_y. H_x(x, 50 m, z_m) has maximum value (9.0 Amp/m) at x = 0 and decreases away from the mine. H_x(50 m, y, z_m) has maximum value (1.0 Amp/m) at y = 0 and decrease as away from the mine. However, H_y(x, 50 m, z_m) is zero at x = 0 and has maximum magnitudes (±4.3 Amp/m) at around x = 5 m. H_y(50 m, y, z_m) has a minimum value (2.1 Amp/m) at y = 0 and decreases away from the mine.

Figure 27 shows the horizontal distributions of the three magnetic components at the mine depth: H_x(x, y, z_m), H_y(x, y, z_m), and H_z(x, y, z_m). Regions of high positive strength are shown in red. Regions of high negative strength are shown in blue.

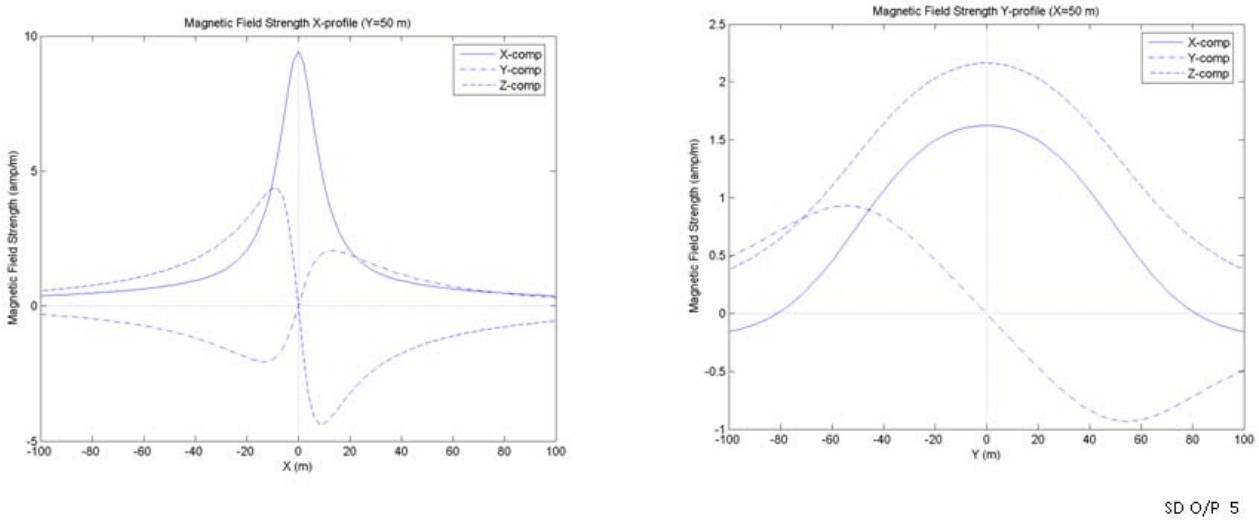

Figure 26. San Diego Type I Case 5 Output

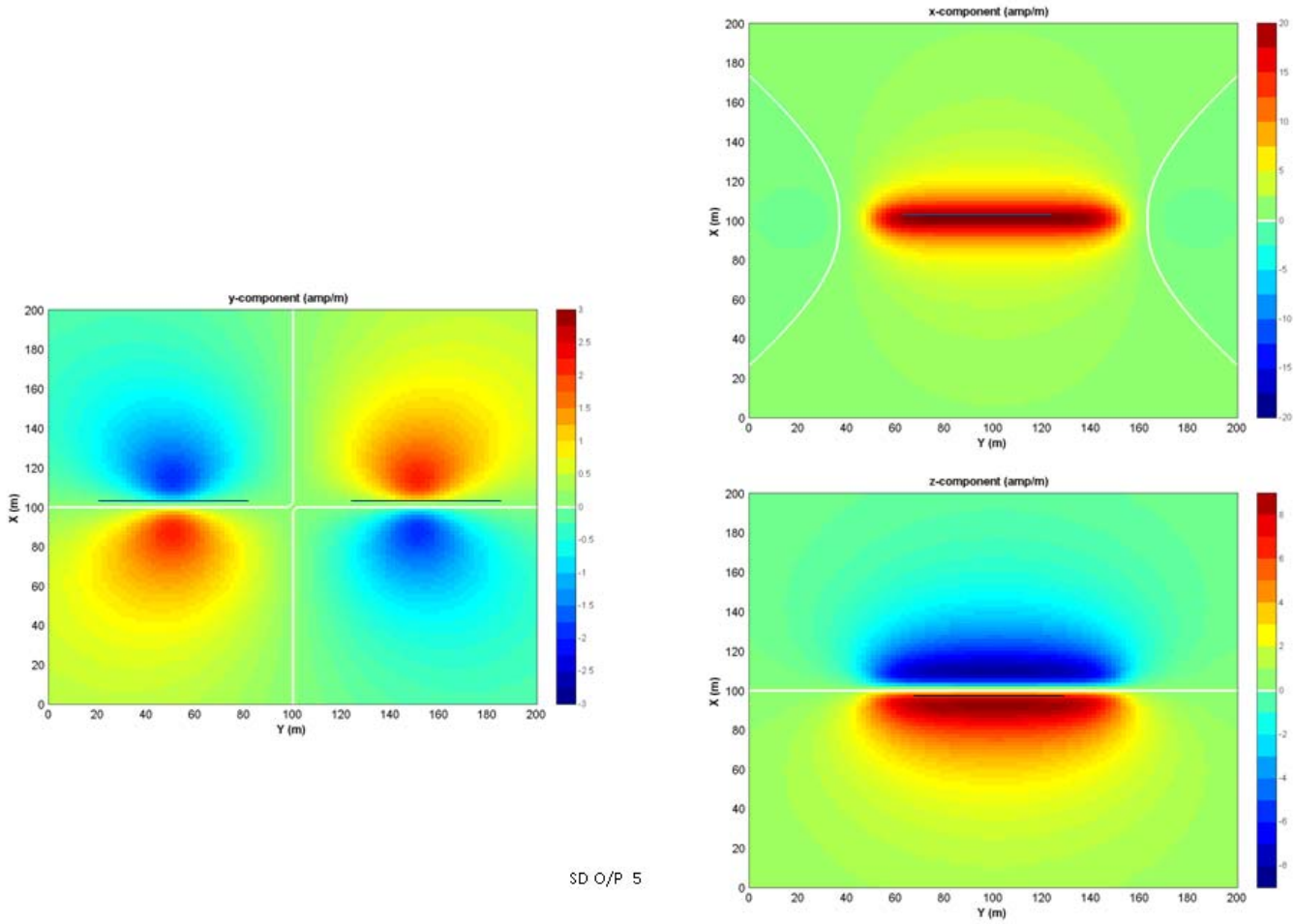

Figure 27. San Diego Type I Case 5 Magnetic Field

Observation#	Water Depth (m)	Mine Depth (m)	Layer 1 Bottom Depth (m)	Layer 1 Bottom Conductivity (mho)	Seafloor Conductivity (mho)
1	50	5	5	3.4251	1.0086
2	50	20	20	3.7589	1.0086
3	50	50	50	3.6569	.9813

Table 3. Yellow Sea Type I (Straight Tail)2-layer

Figures 28, 30 and 32 (left) show the spatial variability along the x-axis of the three components of the magnetic field generated by the mine sweeper at the mine depth (z_m) for y = 50 m relative to the mine location: H_x(x, 50 m, z_m), H_y(x, 50 m, z_m), and H_z(x, 50 m, z_m). Figures 28, 30, and 32 (right) show the spatial variability along the y-axis (i.e., the axis of the sweeper) of the three components of the magnetic field generated by the mine sweeper at the mine depth (z_m) for x = 50 m relative to the mine location: H_x(50 m, y, z_m), H_y(50 m, y, z_m), and H_z(50 m, y, z_m). Because the sweeper is moving, the magnetic components Hx, Hy and Hz as seen by the mine change with (x, y). Voltage produced in the mine's induction coil detector will depend upon the location of these components as well as mine heading, tilt, sweeper heading and speed.

For the straight-tailed sweep, the components H_x and H_y will depend on the environment. For this sweep type the component H_z is generated only by the straight wire and does not depend on the environment. Figures 28, 30, and 32 each show that H_z is significantly smaller than H_x and H_y. H_x(x, 50 m, z_m) at y = 0 and decreases as away from the mine. However, H_y(x, 50 m, z_m) is zero at x = 0 at y = 0 and also decreases away from the mine in each case.

Figures 29, 31, and 33 show the horizontal distributions of the three magnetic components at the mine depth: H_x(x, y, z_m), H_y(x, y, z_m), and H_z(x, y, z_m). Regions of high positive strength are shown in red. Regions of high negative strength are shown in blue.

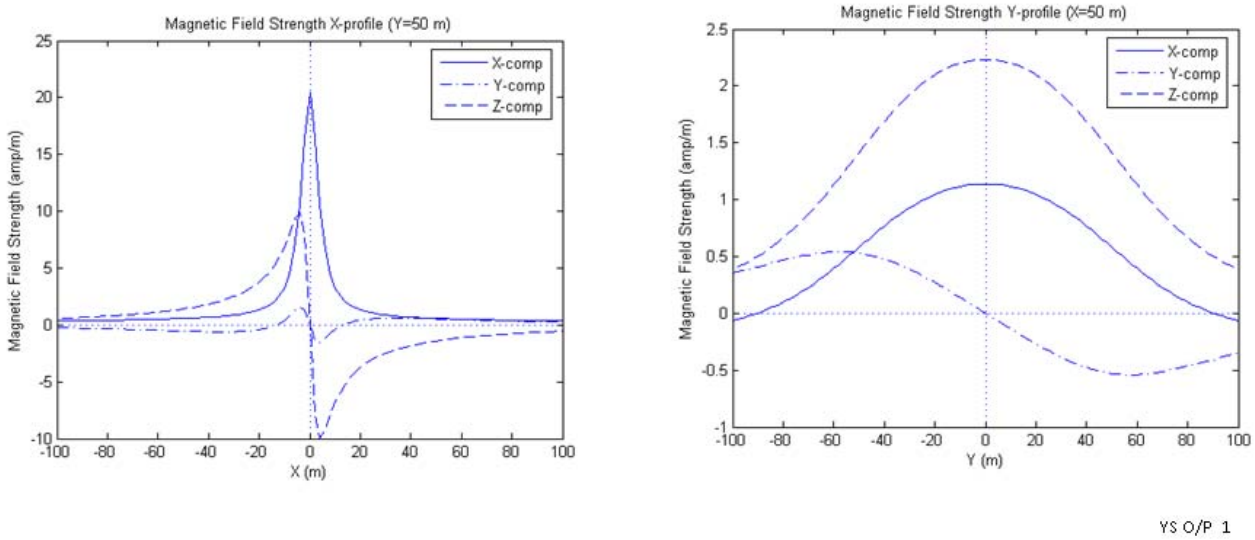

Figure 28. Yellow Sea Type I Case 1 Output

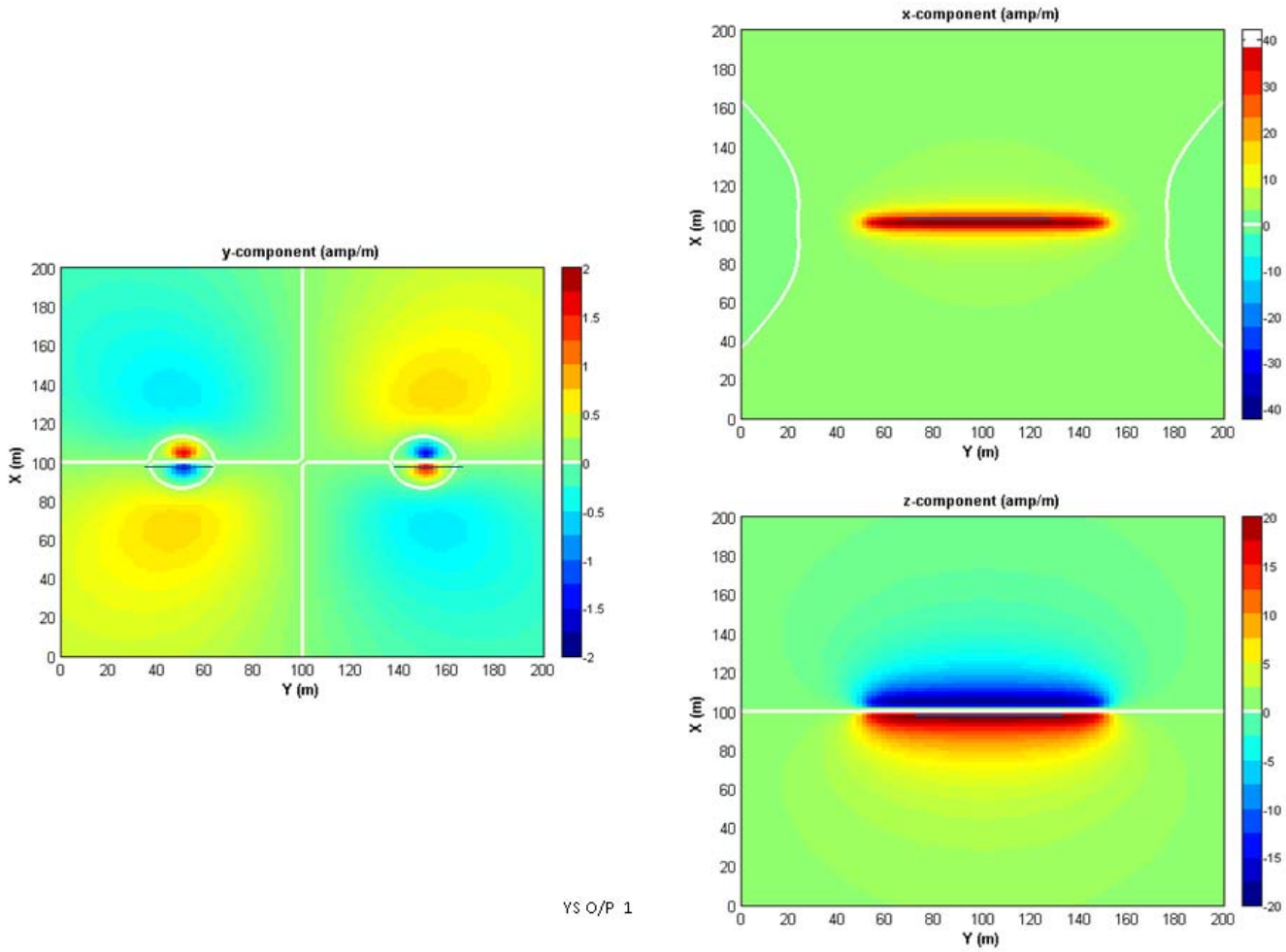

Figure 29. Yellow Sea Type I Case 1 Magnetic Field

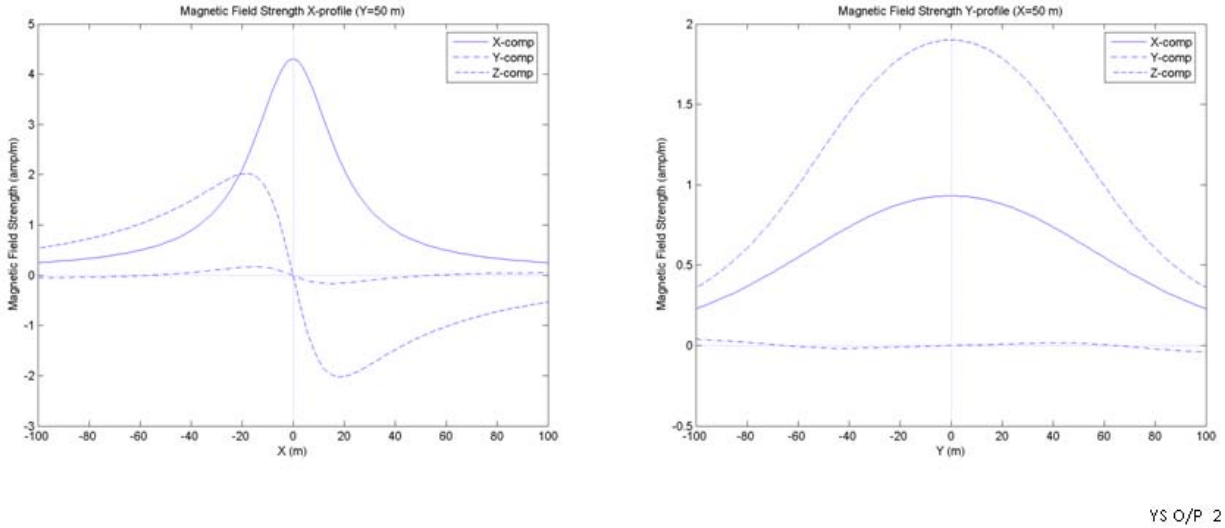

Figure 30. Yellow Sea Type I Case 2 Output

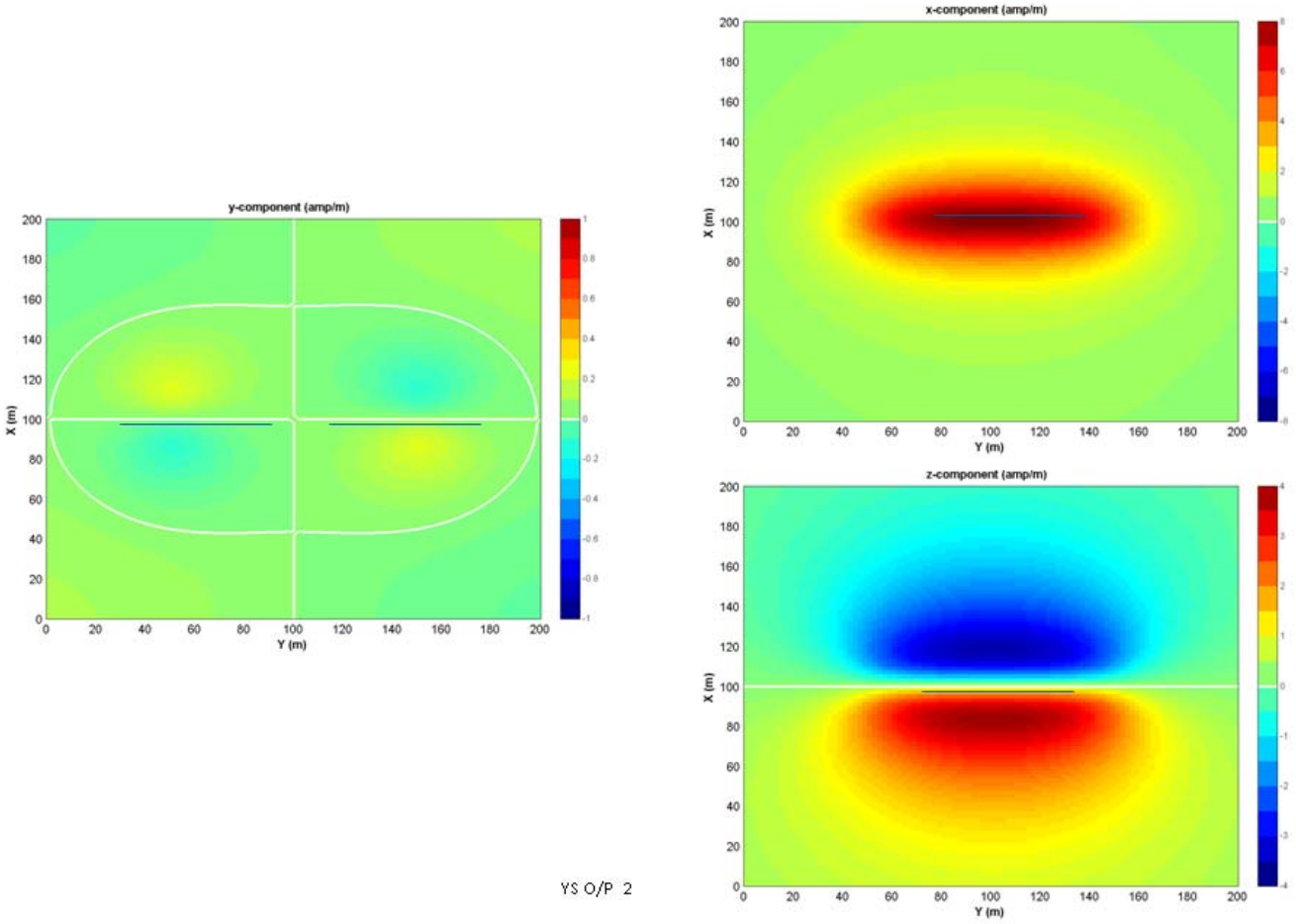

Figure 31. Yellow Sea Type I Case 2 Magnetic Field

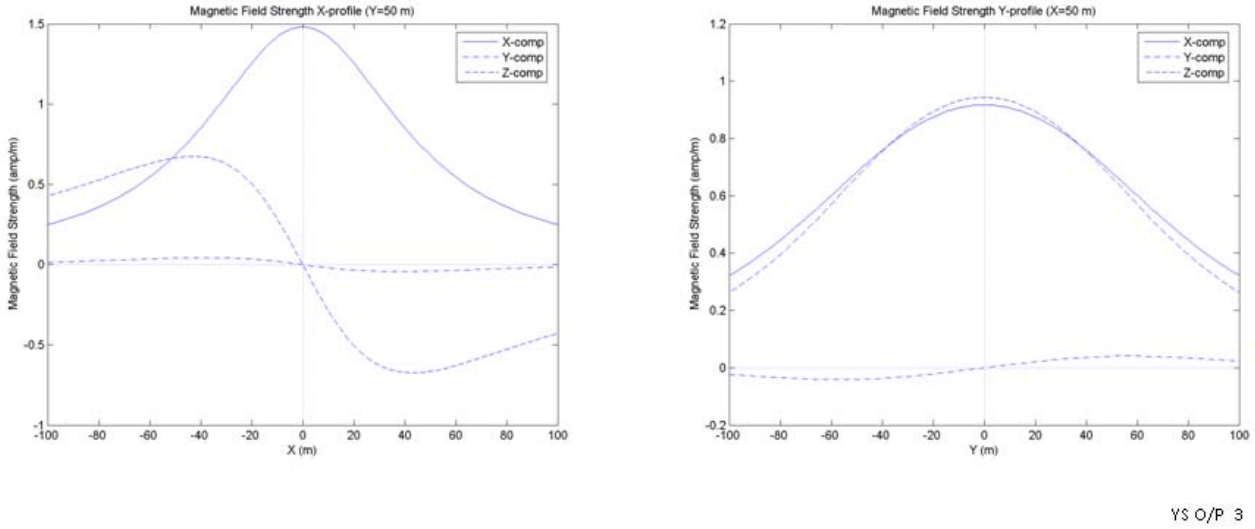

Figure 32. Yellow Sea Type I Case 3 Output

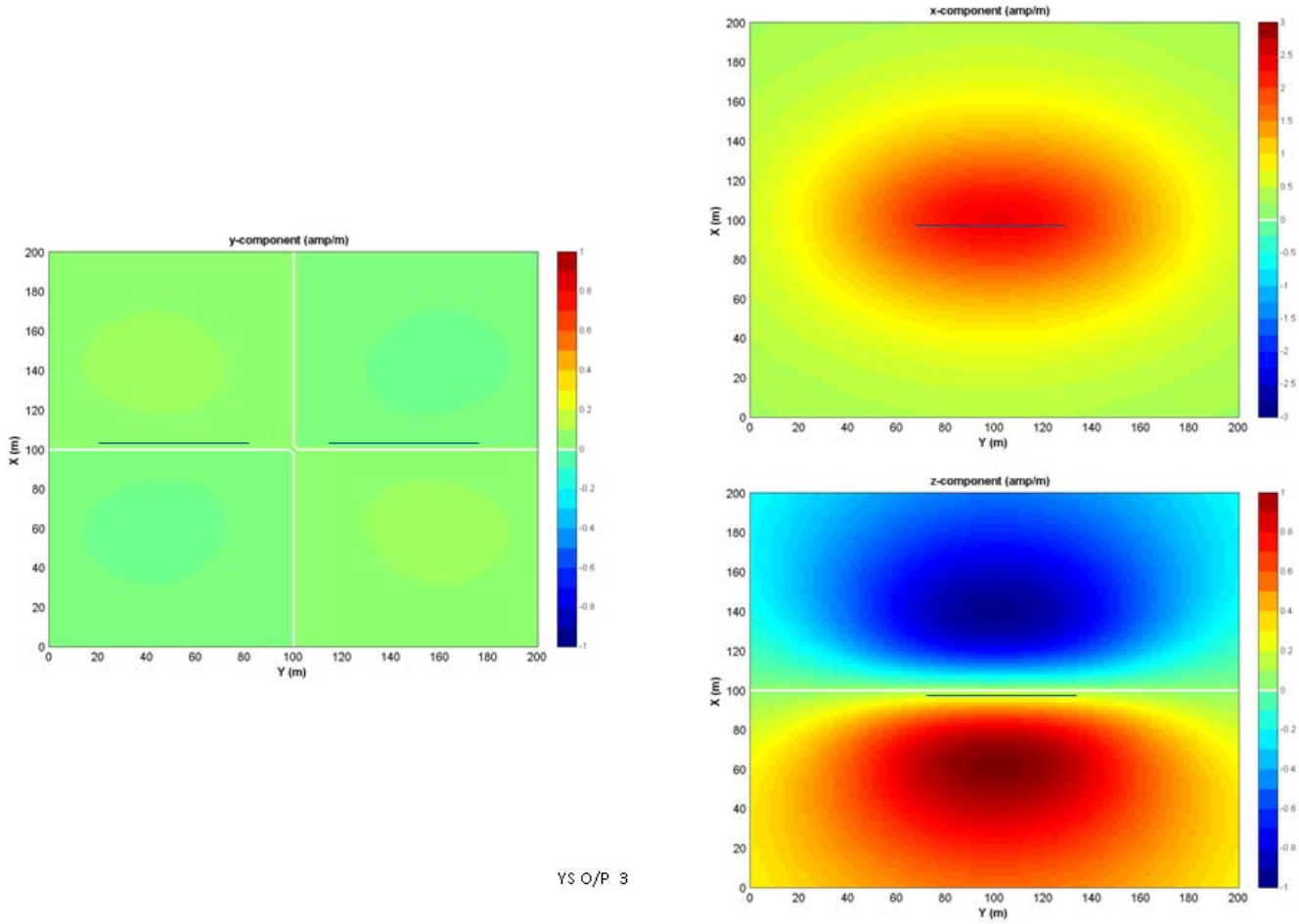

Figure 33. Yellow Sea Type I Case 3 Magnetic Field

2. Parameters NLMM Type I/ 4-layer

1000.0		Wire current (amp) {Does not change for our model}
100.0		Wire length (m) {Does not change for our model}
1.0		Wire depth (m) {Does not change for our model}
xx		Mine Depth (m)
2		Maximum spatial wave number (m)
200		Number of wave numbers
3		Number of layers
x.x	x.xxxx	Layer 1 Bottom Depth(m) and Conductivity(mho)
x.xx	x.xxxx	Layer 2 Bottom Depth (m) Layer 2 Bottom Conductivity (mho)
x.xx	x.xxxx	Layer 3 Bottom Depth (m) Layer 3 Bottom Conductivity (mho)
x.xxxx		Seafloor conductivity (mho)
4		Output option
-100.0		Minimum output range X (m)
100.0		Maximum output range X (m)
101		Number of X values
-100.0		Minimum output range Y (m)
100.0		Maximum output range Y (m)
101		Number of Y values
-50.0		X-axis offset (for profiles)
50.0		Y-axis offset (for profiles)

Case #	Water Depth (m)	Mine Depth (m)	Layer 1 Bottom Depth (m)	Layer 1 Bottom Conductivity	Layer 2 Bottom Depth (m)	Layer 2 Bottom Conductivity	Layer 3 Bottom Depth (m)	Layer 3 Bottom Conductivity	Seafloor Conductivity
6	1,10,20	10	1	4.6602	10	4.5333	20	4.1719	1.3265
7	10,20,30	10	10	4.5333	20	4.1719	30	3.9451	1.3265
8	10,20,40	20	10	4.5333	20	4.1719	40	3.8911	1.3265
9	10,20,50	20	10	4.5333	20	4.1719	50	3.8749	1.3265
10	10,30,50	30	10	4.5333	30	3.9451	50	3.8749	1.3265

Table 4. San Diego Type I (Straight Tail) 4-layer

Figure 34 (left) shows the spatial variability along the x-axis of the three components of the magnetic field generated by the mine sweeper at the mine depth (z_m) for y = 50 m relative to the mine location: H_x(x, 50 m, z_m), H_y(x, 50 m, z_m), and H_z(x, 50 m, z_m). Figure 34 (right) shows the spatial variability along the y-axis (i.e., the axis of the sweeper) of the three components of the magnetic field generated by the mine sweeper at the mine depth (z_m) for x = 50 m relative to the mine location: H_x(50 m, y, z_m), H_y(50 m, y, z_m), and H_z(50 m, y, z_m). Because the sweeper is moving, the magnetic components Hx, Hy and Hz as seen by the mine change with (x, y). Voltage produced in the mine's induction coil detector will depend upon the location of these components as well as mine heading, tilt, sweeper heading and speed.

For the straight-tailed sweep, the components H_x and H_y will depend on the environment. For this sweep type the component H_z is generated only by the straight wire and does not depend on the environment. Figure 34 also shows that H_z is much smaller than H_x and H_y. H_x(x, 50 m, z_m) has maximum value (9.0 Amp/m) at x = 0 and decreases away from the mine. H_x(50 m, y, z_m) has maximum value (1.0 Amp/m) at y = 0 and decrease as away from the mine. However, H_y(x, 50 m, z_m) is zero at x = 0 and has maximum magnitudes (±4.3 Amp/m) at around x = 5 m. H_y(50 m, y, z_m) has a minimum value (2.1 Amp/m) at y = 0 and decreases away from the mine.

Figure 35 shows the horizontal distributions of the three magnetic components at the mine depth: H_x(x, y, z_m), H_y(x, y, z_m), and H_z(x, y, z_m). Regions of high positive strength are shown in red. Regions of high negative strength are shown in blue.

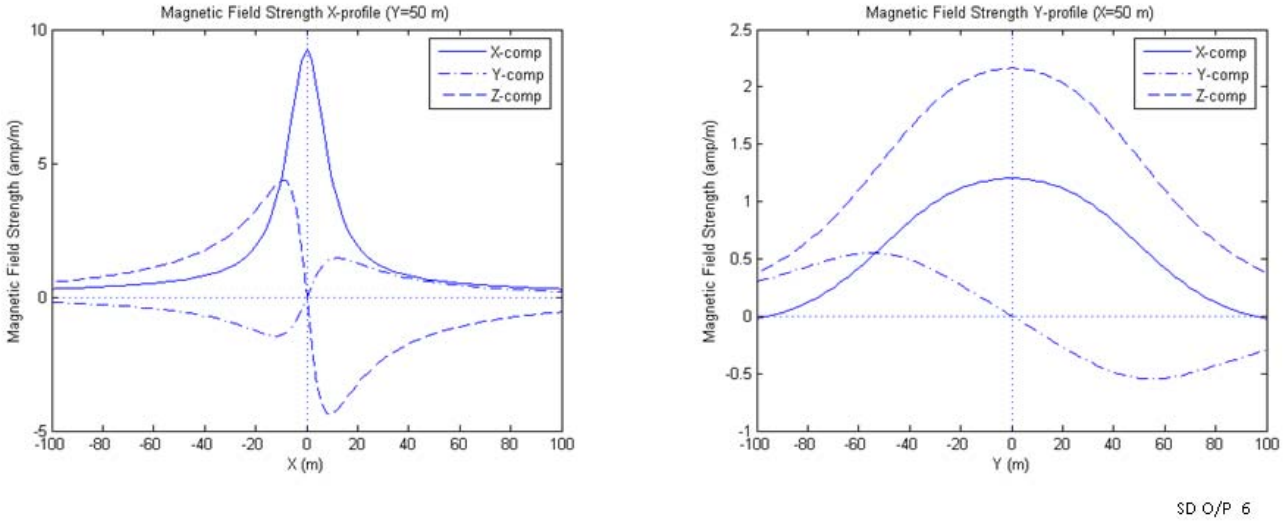

Figure 34. San Diego Type I Case 6 Output

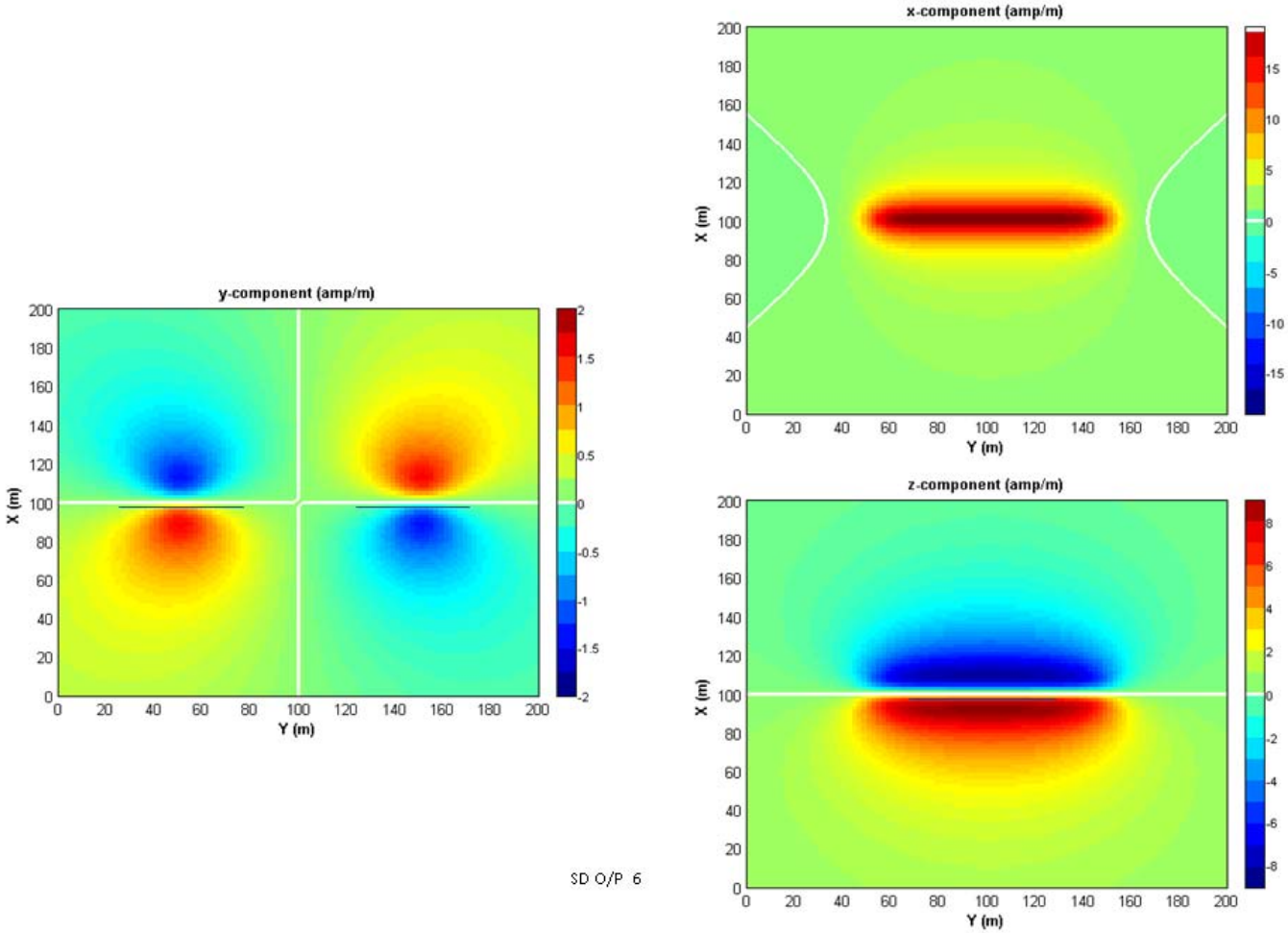

Figure 35. San Diego Type I Case 6 Magnetic Field

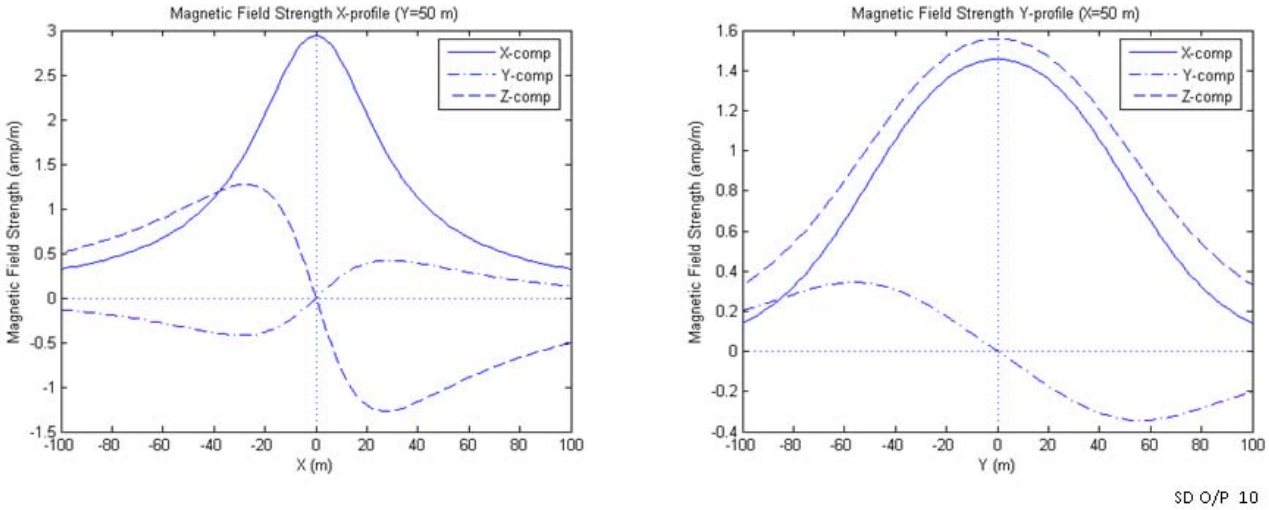

Figure 36. San Diego Type I Case 10 Output

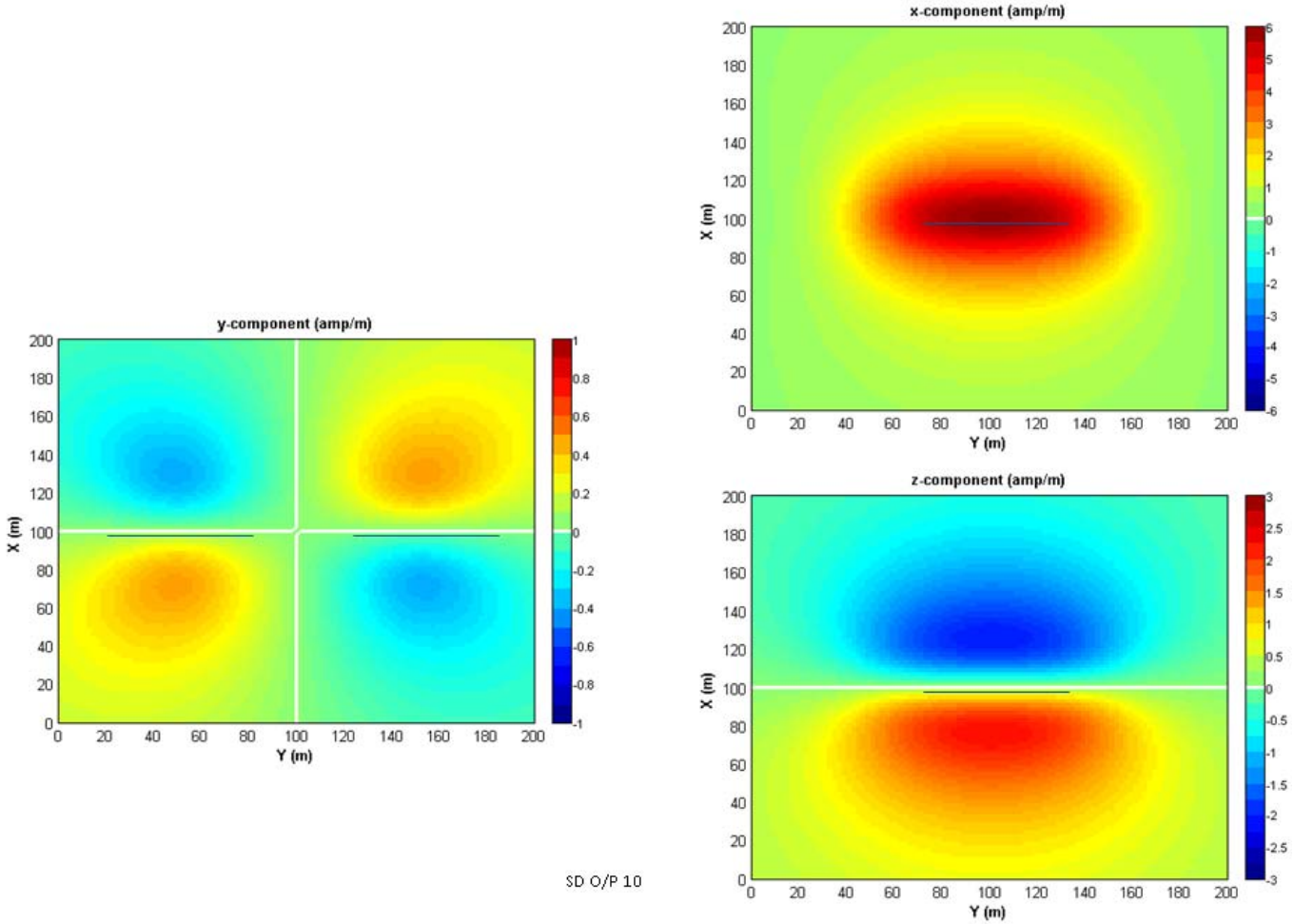

Figure 37. San Diego Type I Case 10 Magnetic Field

3. Parameters NLMM Type II/ 2-layer

1000.0	Wire Curent (amp)
100.0	S-Cable Length (m)
200	No. of Points in Catenary
75.0	Straight Line Interelectrode distance (m)
135.0	Aft Eletrode Bearing Angle(deg)
1.0	Electrode and Catenary Depth(m)
xx.x	Mine Depth(m)
4.0	Maximum Spatial Wavenumber(1/m)
200	No. of Spatial Wavenumbers
1	Number of Layers
xx.x	Layer Bottom Depth(m)
x.xxxx	Layer Bottom Conductivity(mho)
x.xxxx	Seafloor Conductivity(mho)
4	Output Option
-100.0	Minimum Output Range X(m)
100.0	Maximum Output Range X(m)
101	No. of X values
-100.0	Minimum Output Range Y(m)
100.0	Maximum Output Range Y(m)
101	No. of Y values
-50.0	X-Axis Offset (for profiles)
-50.0	Y-Axis Offset (for profiles)

Case #	Water Depth (m)	Mine Depth (m)	Layer 1 Bottom Depth (m)	Layer 1 Bottom Conductivity (mho)	Seafloor Conductivity (mho)
1	50	10	10	4.5333	1.2592
2	50	20	20	4.1719	1.2592
3	50	30	30	3.9451	1.2592
4	50	40	40	3.8911	1.2592
5	50	10	50	3.8749	1.2592

Table 5. San Diego Type II (Open Loop) 2-layer

Even figures (38-48) in Section 3 represent San Diego cases for the Type II straight tailed and open loop sweeps. Panels on the left show the spatial variability along the x-axis of the three components of the magnetic field generated by the mine sweeper at the mine depth (z_m) for y = 50 m relative to the mine location: H_x(x, 50 m, z_m), H_y(x, 50

m, z_m), and H_z(x, 50 m, z_m). Type II straight tailed sweep panels on the right show the spatial variability along the y-axis (i.e., the axis of the sweeper) of the three components of the magnetic field generated by the mine sweeper at the mine depth (z_m) for x = 50 m relative to the mine location: H_x(50 m, y, z_m), H_y(50 m, y, z_m), and H_z(50 m, y, z_m). Because the sweeper is moving, the magnetic components Hx, Hy and Hz as seen by the mine change with (x, y). Voltage produced in the mine's induction coil detector will depend upon the location of these components as well as mine heading, tilt, sweeper heading and speed.

For the straight-tailed sweep, the components H_x and H_y will depend on the environment. For this sweep type the component H_z is generated only by the straight wire and does not depend on the environment. H_x(x, 50 m, z_m) has maximum value at x = 0 and decreases away from the mine. H_x(50 m, y, z_m) has maximum value at y = 0 and decrease as away from the mine.

Odd figures (39-49) in Section 3 below represent San Diego cases for the Type II straight tailed and open loop sweeps. They show the horizontal distributions of the three magnetic components at the mine depth: H_x(x, y, z_m), H_y(x, y, z_m), and H_z(x, y, z_m). Regions of high positive strength are shown in red. Regions of high negative strength are shown in blue.

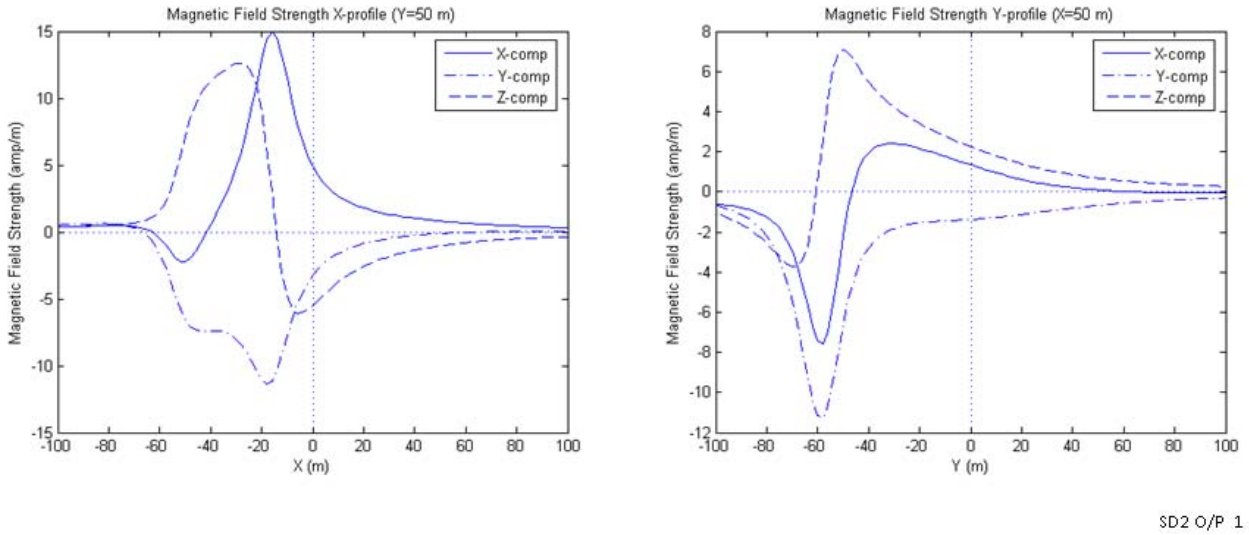

Figure 38. San Diego Type II Case 1 Output

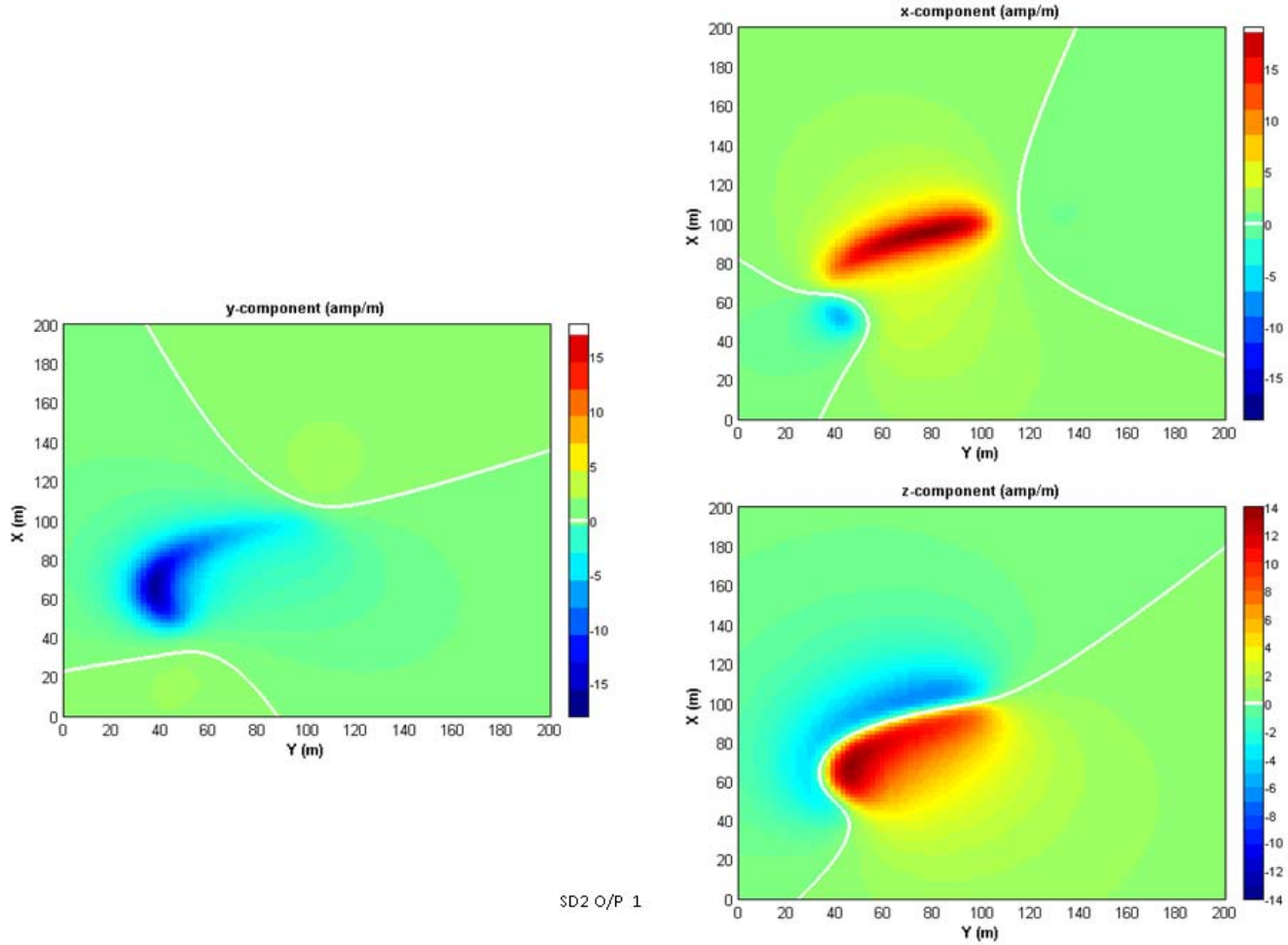

Figure 39. San Diego Type II Case 1 Magnetic Field

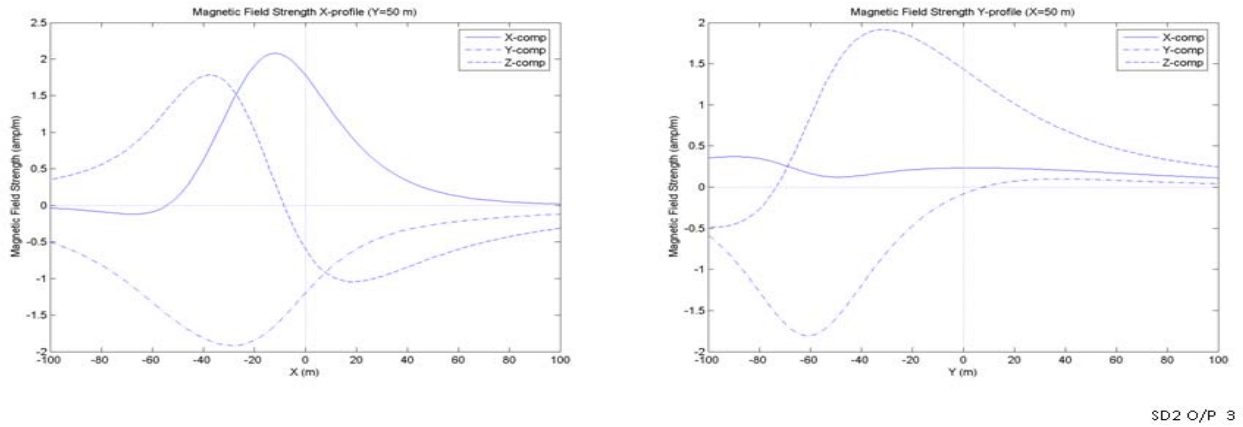

Figure 40. San Diego Type II Case 3 Output

Figure 41.

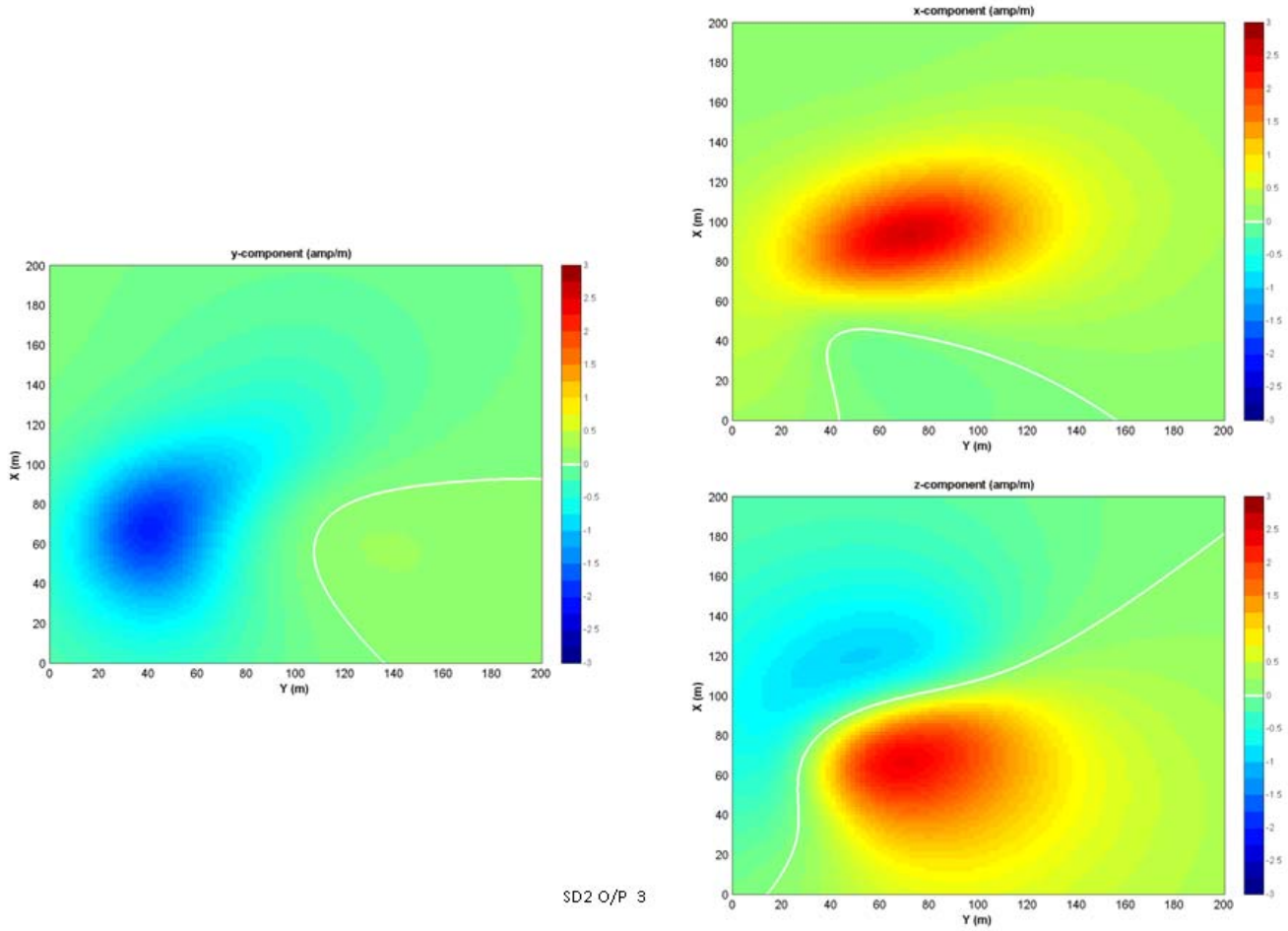

Figure 42. San Diego Type II Case 3 Magnetic Field

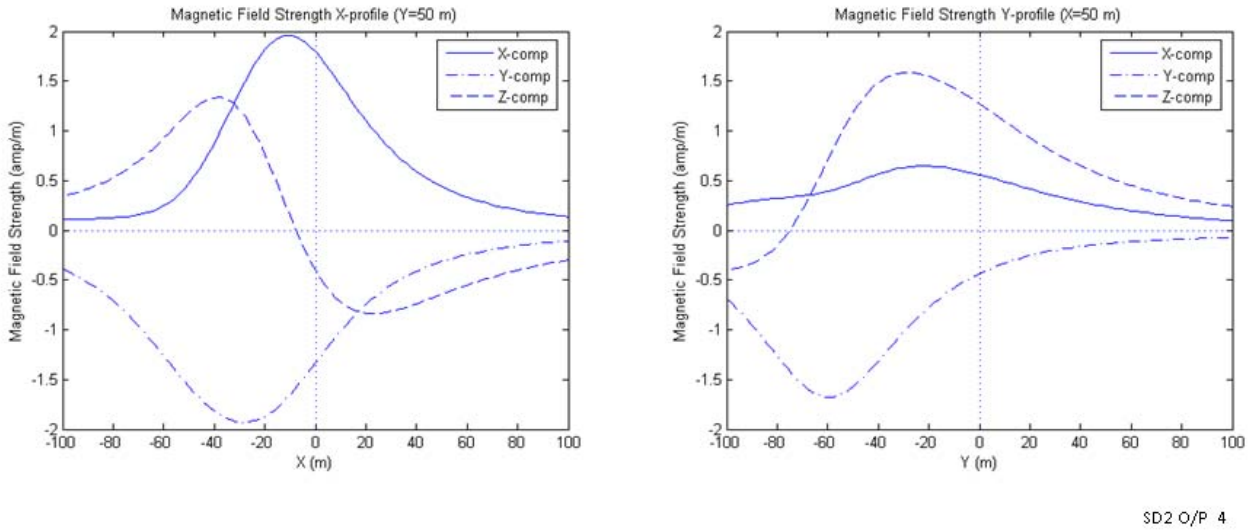

Figure 43. San Diego Type II Case 4 Output

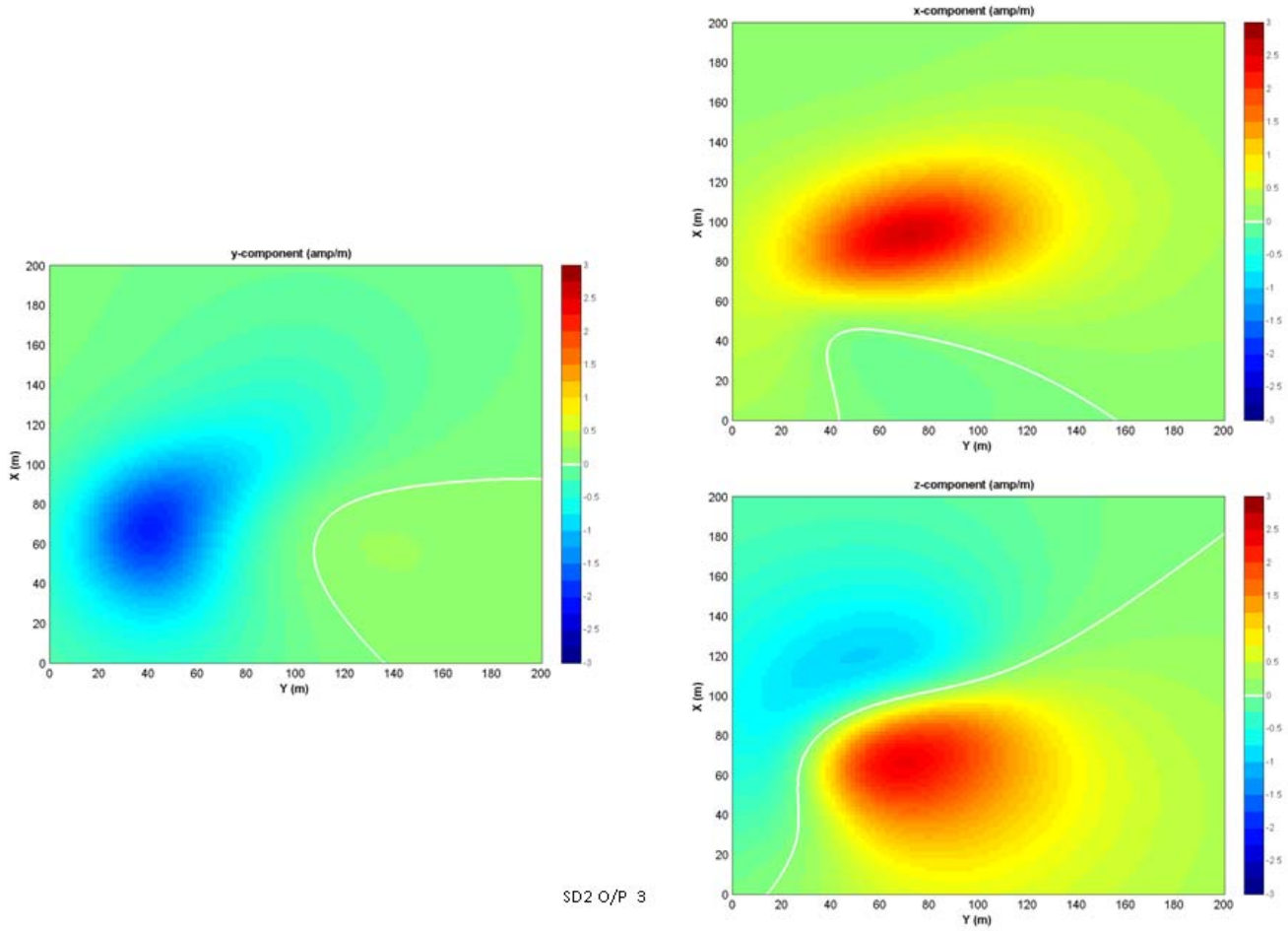

Figure 44. San Diego Type II Case 4 Magnetic Field

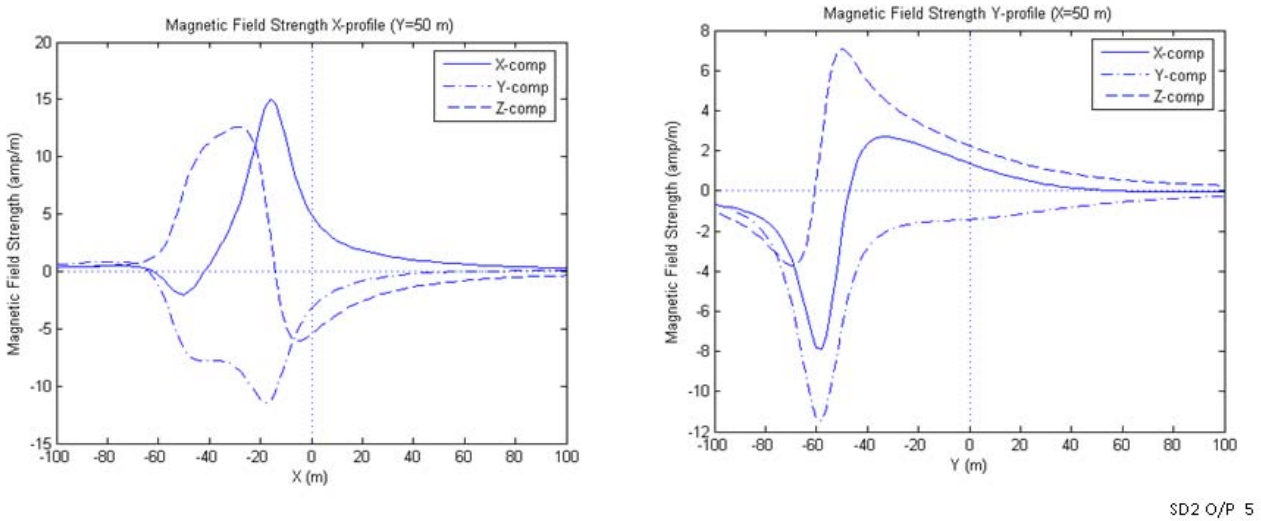

Figure 45. San Diego Type II Case 5 Output

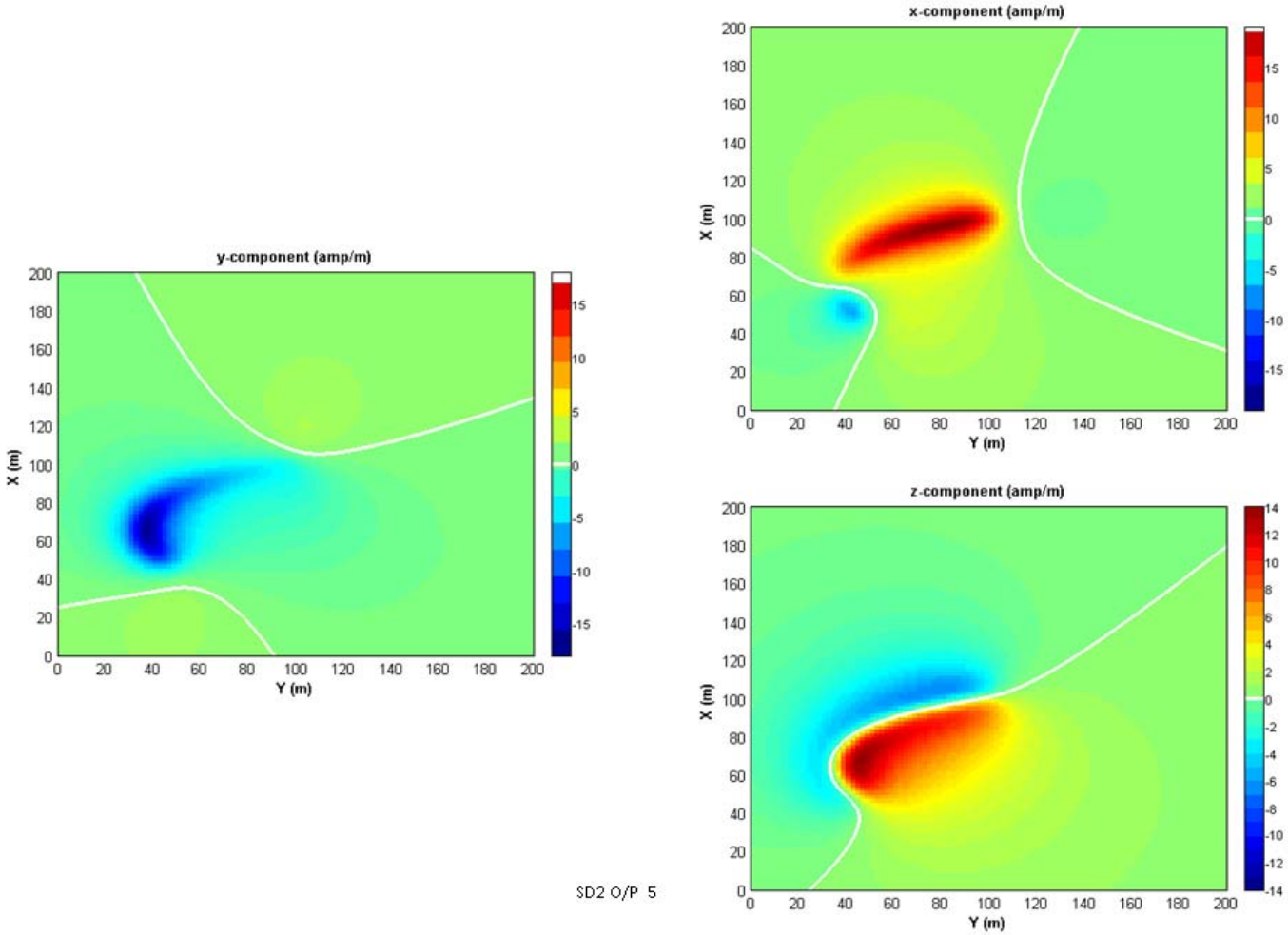

Figure 46. San Diego Type II Case 5 Magnetic Field

4. Parameters NLMM Type II/ 4-layer

1000.0	Wire Curent (amp)
100.0	S-Cable Length (m)
200	No. of Points in Catenary
75.0	Straight Line Interelectrode distance (m)
135.0	Aft Eletrode Bearing Angle(deg)
1.0	Electrode and Catenary Depth(m)
xx.x	Mine Depth(m)
4.0	Maximum Spatial Wavenumber(1/m)
200	No. of Spatial Wavenumbers
3	Number of Layers
x.x x.xxxx	Layer 1 Bottom Depth(m) and Conductivity(mho)
x.x x.xxxx	Layer 2 Bottom Depth (m) Layer 2 Bottom Conductivity (mho)
x.x x.xxxx	Layer 3 Bottom Depth (m) Layer 3 Bottom Conductivity (mho)
1.0619	Seafloor Conductivity(mho)
4	Output Option
-100.0	Minimum Output Range X(m)
100.0	Maximum Output Range X(m)
101	No. of X values
-100.0	Minimum Output Range Y(m)
100.0	Maximum Output Range Y(m)
101	No. of Y values
-50.0	X-Axis Offset (for profiles)
-50.0	Y-Axis Offset (for profiles)

Case #	Water Depth (m)	Mine Depth (m)	Layer 1 Bottom Depth (m)	Layer 1 Bottom Conductivity	Layer 2 Bottom Depth (m)	Layer 2 Bottom Conductivity	Layer 3 Bottom Depth (m)	Layer 3 Bottom Conductivity	Seafloor Conductivity
6	1,10,20	10	1	4.6602	10	4.5333	20	4.1719	1.3265
7	10,20,30	10	10	4.5333	20	4.1719	30	3.9451	1.3265
8	10,20,40	20	10	4.5333	20	4.1719	40	3.8911	1.3265
9	10,20,50	20	10	4.5333	20	4.1719	50	3.8749	1.3265
10	10,30,50	30	10	4.5333	30	3.9451	50	3.8749	1.3265

Table 6. San Diego Type II (Open Loop) 4-layer

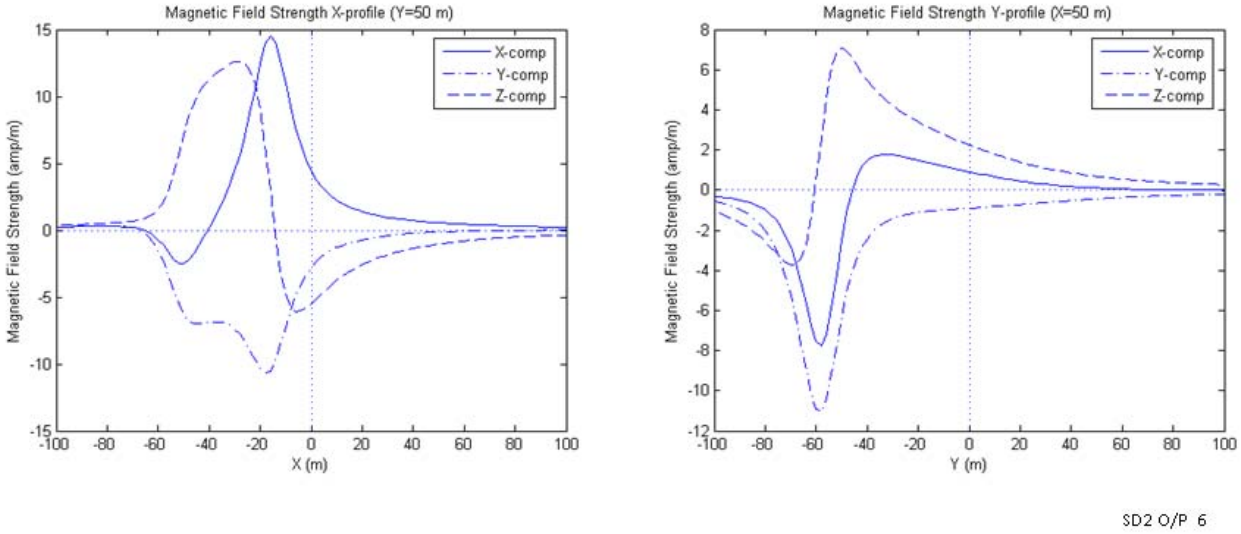

Figure 47. San Diego Type II Case 6 Output

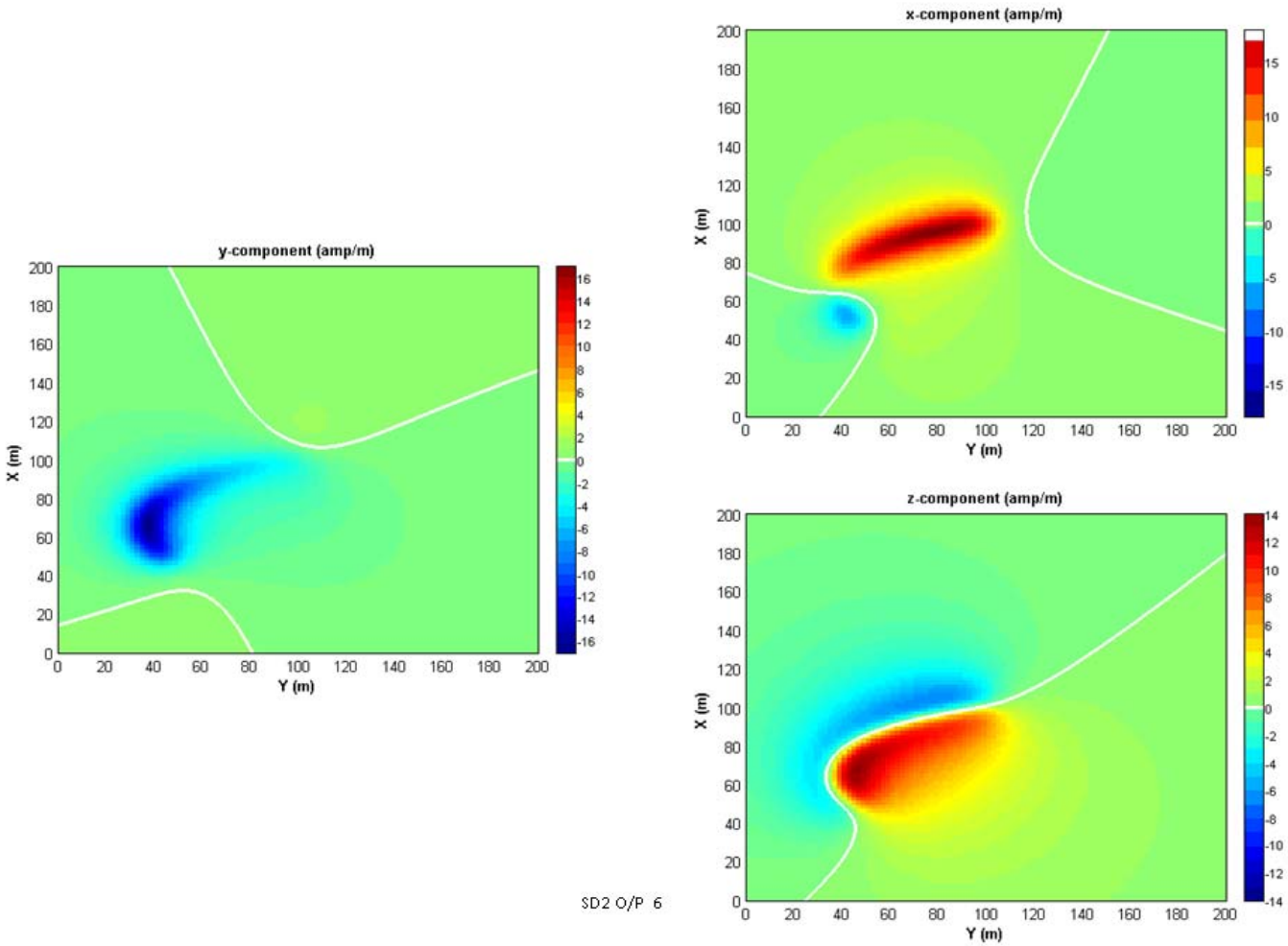

Figure 48. San Diego Type II Case 6 Magnetic Field

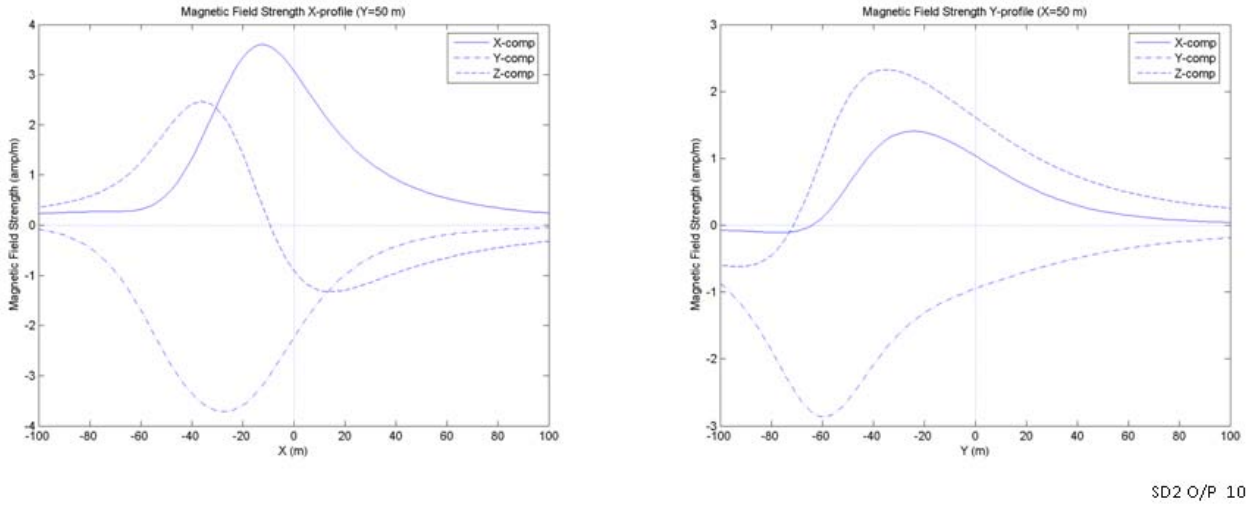

Figure 49. San Diego Type II Case 10 Output

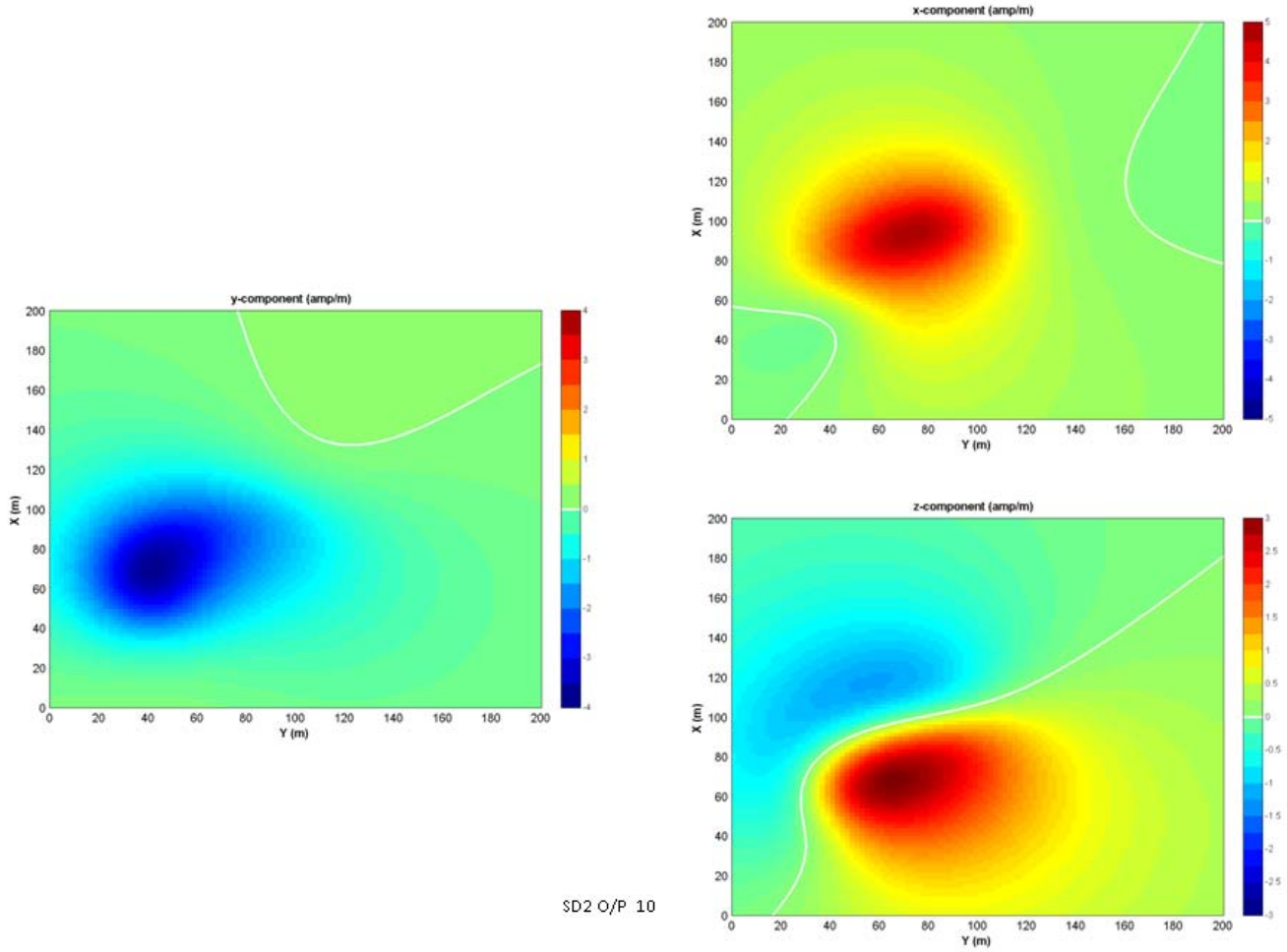

Figure 50. San Diego Type II Case 10 Magnetic Field

5. NAVO 2-Layer model

The sweep type can be: STRAIGHT = 1, SINGLE JIG = 2, DOUBLE JIG = 3, or MACAS = 4

SWEEP TYPE = 4
The actual water depth in meters
WATER DEPTH = 20
Length of cable between electrodes for the straight and single jig sweeps or the length of the long cable in the double jig sweep (meters)
CABLE LENGTH = 238.6584
MINE DEPTH = xx
Depth of the electrodes (meters)
ELECTRODE DEPTH = 0.5
MACAS Potentiometer depth (meters)
POTENTIOMETER DEPTH = 1.0
Maximum spatial wavenumber in computing Green's Function (1 / meters)
MAXIMUM SPATIAL WAVENUMBER = 0.1
Total number of spatial wavenumbers
NUMBER OF SPATIAL WAVENUMBERS = 400
Conductivity Table

Case #	Water Depth/ Mine Depth	Q (S/m)	ED(m)	ED/AD	Archie exponent, 'm'
1	10m/10m	0.9595410611	33.28824638	3.504025935	1.8
2	20m/20m	0.9675928463	30.98861831	1.589159914	1.8
3	30m	0.9560450221	38.43243398	1.302794372	1.8
4	40m	0.9598807254	45.74053032	1.157988109	1.8
5	50m	0.9469913234	52.65840035	1.063806068	1.8
6	60m	0.9469287757	62.21985968	1.045711927	1.8
7	70m/20m	0.9696113602	76.46574439	1.096283074	1.8
8	80m/20m	0.1392759675	95.78806342	1.204881301	1.8
9	90m/20m	1.130473756	141.3752193	1.575211358	1.8

Table 7. NAVO Model results

VI. DISCUSSION/SUMMARY

If the U.S. Navy is to be adequately prepared to face the growing mine warfare challenge, it must change its disinterested mind-set towards MIW. Planners must appreciate how mine countermeasures can be used to shape the battlefield and facilitate operational maneuvers. Moreover, decision makers must understand mine warfare's limitations and the impact it can have on time factors. Operational commanders also must understand the important role the intelligence of MIW can play in support of mine warfare operations.

The earth's natural magnetic field induces a magnetization in a ship depending on its latitude, longitude, and heading. The magnetic signature of ship is caused by its iron and steel components. These signatures have two parts: a permanent magnetic component, which is acquired at the time the ship is built, and an induced magnetic component. The induced component depends on the instantaneous position and orientation of the ship on the surface of the Earth as well as the local geomagnetic field of the Earth. The induced magnetization can be broken into three orthogonal components that are parallel to the vessel's vertical, longitudinal, and transverse axis. Each of these induced magnetizations in turn generate their own distinguishing flux distributions around the hull. Some of the induced magnetization will be retained as a permanent component due to the mechanical stress on the ship's structure. This does not immediately change with the earths' inducing field. The permanent magnetization can be separated into the ship's three orthogonal directions, thereby producing their own characteristic signatures.

Bottom magnetic influence mines were developed to counter mechanical minesweeping systems that proved to be effective in clearing moored mines during World War I. In shallow, littoral water areas, Naval ship's will always be subject to the possibility of influence mines, specifically that of magnetic mines. Because of the ever present influence of the earth's' magnetic field couple with that of the ship's magnetic field it is necessary to detect magnetic mines and render their damage to a minimum.

Detection of the magnetic signature of a target ship is a common trigger for some sea mines. It has been well known for a century that all waterborne ships induce a magnetic influence field. Mines that respond to the magnetic signature of a ship were originally developed by the British in World War I. Since that time, exploitation of a ship's magnetic signature has been a part of all naval war endeavors for us and our enemies.

In efforts to counter the damage caused by magnetic-actuated mines, mine countermeasures forces have developed magnetic mine sweeping capabilities. A key component of the magnetic mine sweeping mission is for minesweepers to produce target like magnetic signatures. This is accomplished by towing a pair of current producing and receiving electrodes behind the sweeper. Current flows through the wires and from one electrode, through the ocean, and back to another electrode, in order to produce a magnetic field. If the pair of wires is not connected the configuration is described as an 'open loop sweep'.

The Navy's N-Layered Magnetic Model should be applicable to performance evaluations for all standard Navy surface and helicopter magnetic minesweeps. It is necessary for the model to be useful in the assessment of the impact of environmental variability on system performance. Additionally, the magnetic model should predict the individual vector components of the magnetic field, as well as the total magnetic field strength. The output quantities generated by the model should be displayed along user selected lines or in a plan-view format.

APPENDIX A. SALINITY TO CONDUCTIVITY CONVERSION

A. MATLAB CODE FOR SALINITY TO CONDUCTIVITY CONVERSION

```
INPUT:  (all must have same dimensions)

%   S = salinity    [psu (PSS-78) ]
%   T = temperature [degree C (IPTS-68)]
%    P = pressure      [db] (P may have dims 1x1, mx1, 1xn or mxn for
S(mxn) )
% OUTPUT:
%   cndr = Conductivity ratio     R =  C(S,T,P)/C(35,15,0) [no units]
check inputs
%-------------
if nargin~=3
  error('sw_cndr.m: must have 3 input arguments')
end %if
 % CHECK S,T,P dimensions and verify consistent
[ms,ns] = size(S);
[mt,nt] = size(T);
[mp,np] = size(P);
% CHECK THAT S & T HAVE SAME SHAPE
if (ms~=mt) | (ns~=nt)
   error('check_stp: S & T must have same dimensions')
end %if
% CHECK OPTIONAL SHAPES FOR P
if     mp==1  & np==1      % P is a scalar.  Fill to size of S
   P = P(1)*ones(ms,ns);
elseif np==ns & mp==1      % P is row vector with same cols as S
   P = P( ones(1,ms), : ); %   Copy down each column.
elseif mp==ms & np==1      % P is column vector
   P = P( :, ones(1,ns) ); %   Copy across each row
elseif mp==ms & np==ns     % PR is a matrix size(S)
   % shape ok
else
```

```
  error('check_stp: P has wrong dimensions')
end %if
[mp,np] = size(P);
% IF ALL ROW VECTORS ARE PASSED THEN LET US PRESERVE SHAPE ON RETURN.
Transpose = 0;
if mp == 1  % row vector
  P      =  P(:);
  T      =  T(:);
  S      =  S(:);
   Transpose = 1;
end %if
%***check_stp
% BEGIN
del_T = T - 15;
for i = 1:ms
 for j = 1:ns
  % DO A NEWTON-RAPHSON ITERATION FOR INVERSE INTERPOLATION OF Rt FROM S.
   S_loop  = S(i,j);  % S in the loop
   T_loop  = T(i,j);  % T in the loop
   Rx_loop = sqrt(S_loop/35.0);              % first guess at Rx = sqrt(Rt)
   SInc    = sw_sals(Rx_loop.*Rx_loop,T_loop); % S INCrement (guess) from Rx
   iloop   = 0;
   end_loop = 0;
   while ~end_loop
     Rx_loop = Rx_loop + (S_loop - SInc)./sw_salds(Rx_loop,del_T(i,j));
     SInc    = sw_sals(Rx_loop.*Rx_loop,T_loop);
     iloop   = iloop + 1;
     dels    = abs(SInc-S_loop);
     if (dels>1.0e-4 & iloop<10)
       end_loop = 0;
     else
       end_loop = 1;
     end %if
```

```
    end %while
     Rx(i,j) = Rx_loop;
   end %for j
end %for i
% ONCE Rt FOUND, CORRESPONDING TO EACH (S,T) EVALUATE R
```

THIS PAGE INTENTIONALLY LEFT BLANK

APPENDIX B. ADDITIONAL OBSERVATIONS

A. SAN DIEGO

As with the observations described previously, even numbered figures on the left show the spatial variability along the x-axis of the three components of the magnetic field generated by the mine sweeper at the mine depth (z_m) for y = 50 m relative to the mine location: H_x(x, 50 m, z_m), H_y(x, 50 m, z_m), and H_z(x, 50 m, z_m). Even numbered figures on the right show the spatial variability along the y-axis (i.e., the axis of the sweeper) of the three components of the magnetic field generated by the mine sweeper at the mine depth (z_m) for x = 50 m relative to the mine location: H_x(50 m, y, z_m), H_y(50 m, y, z_m), and H_z(50 m, y, z_m). Because the sweeper is moving, the magnetic components Hx, Hy and Hz as seen by the mine change with (x, y). Voltage produced in the mine's induction coil detector will depend upon the location of these components as well as mine heading, tilt, sweeper heading and speed.

Odd numbered figures show the horizontal distributions of the three magnetic components at the mine depth: Hx(x, y, zm), Hy(x, y, zm), and Hz(x, y, zm). Regions of high positive strength are shown in red. Regions of high negative strength are shown in blue.

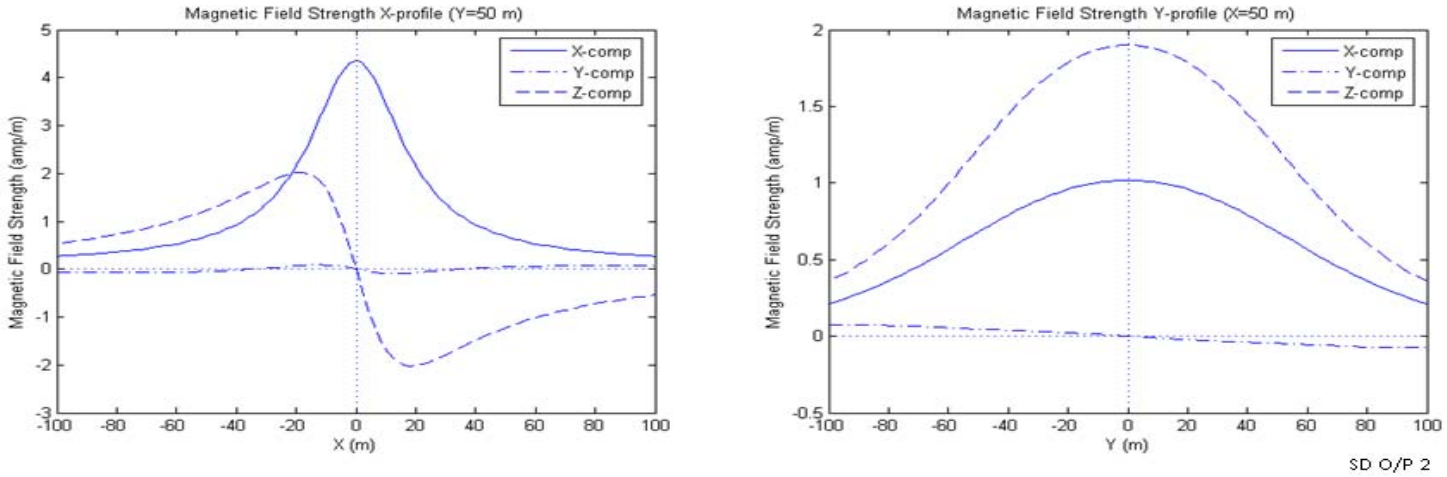

Figure 51. San Diego Type I Case 2 Output (Components *Hx*, *Hy* and *Hz* of the magnetic sweep produced by a straight-tailed sweep viewed at a mine)

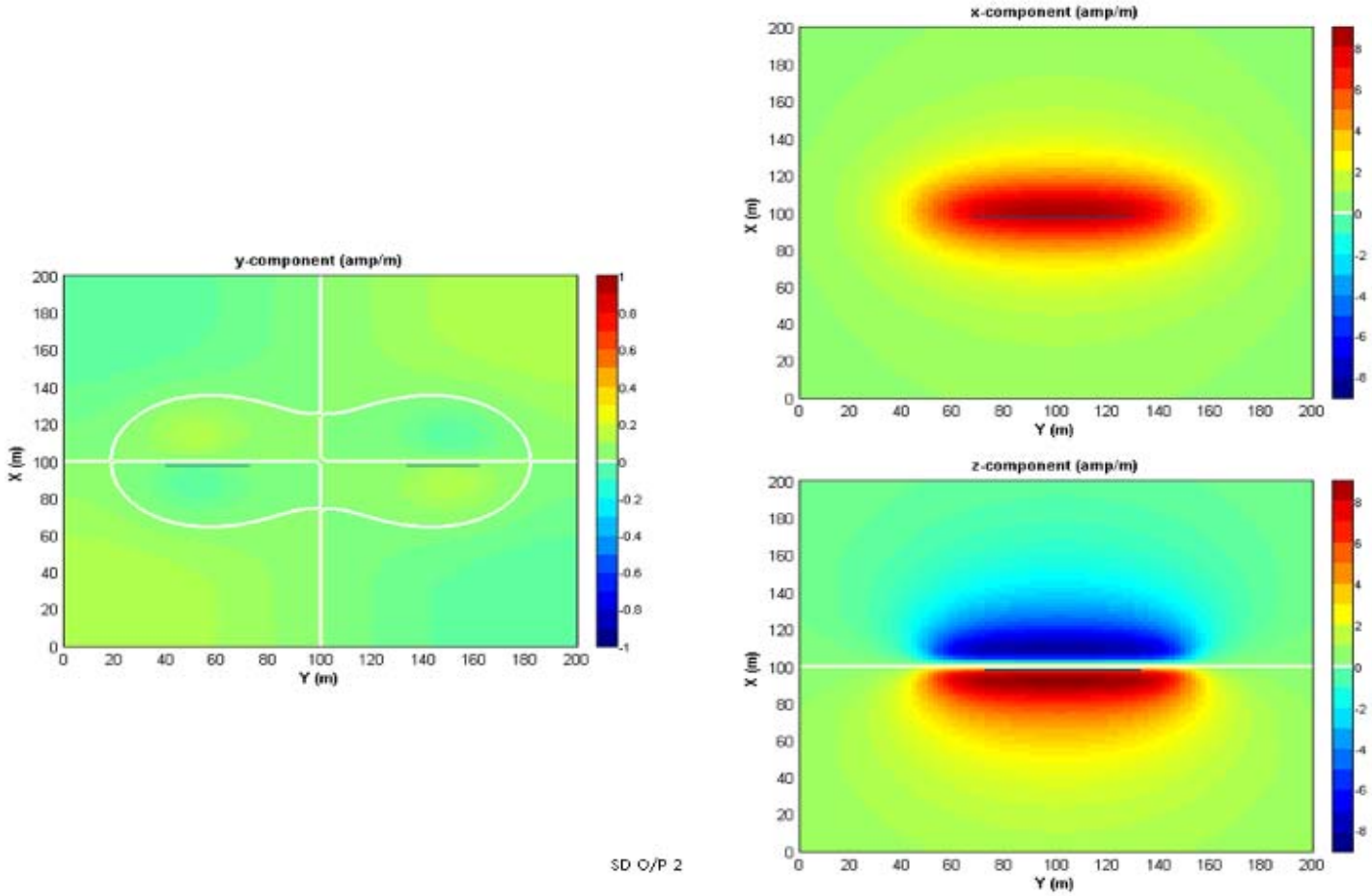

Figure 52. San Diego Type I Case 2 Magnetic Field (Components *Hx*, *Hy* and *Hz* of the magnetic sweep produced by a straight-tailed sweep viewed at a mine)

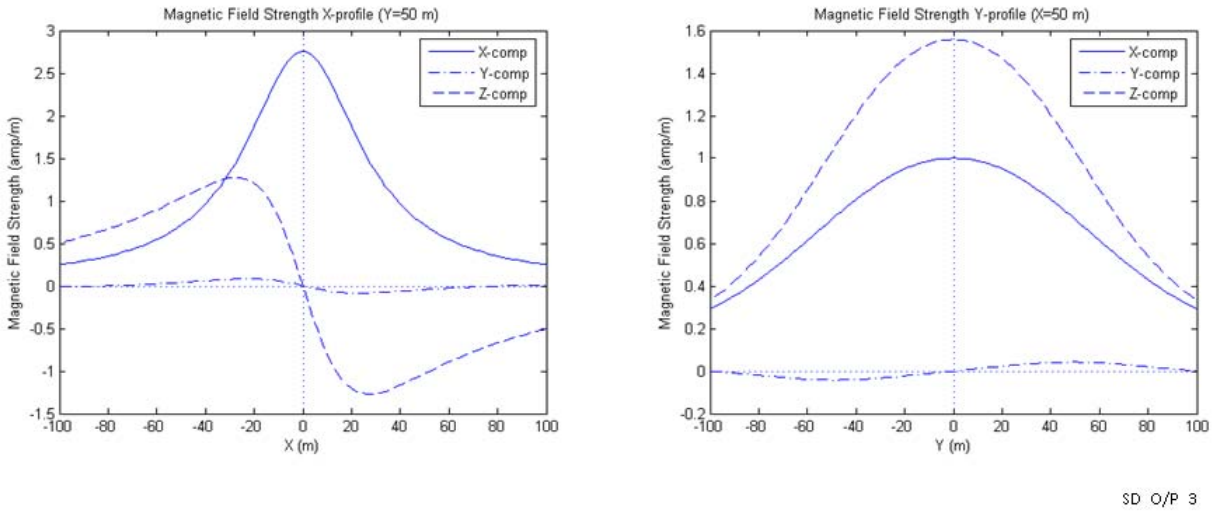

Figure 53. San Diego Type I Case 3 Output

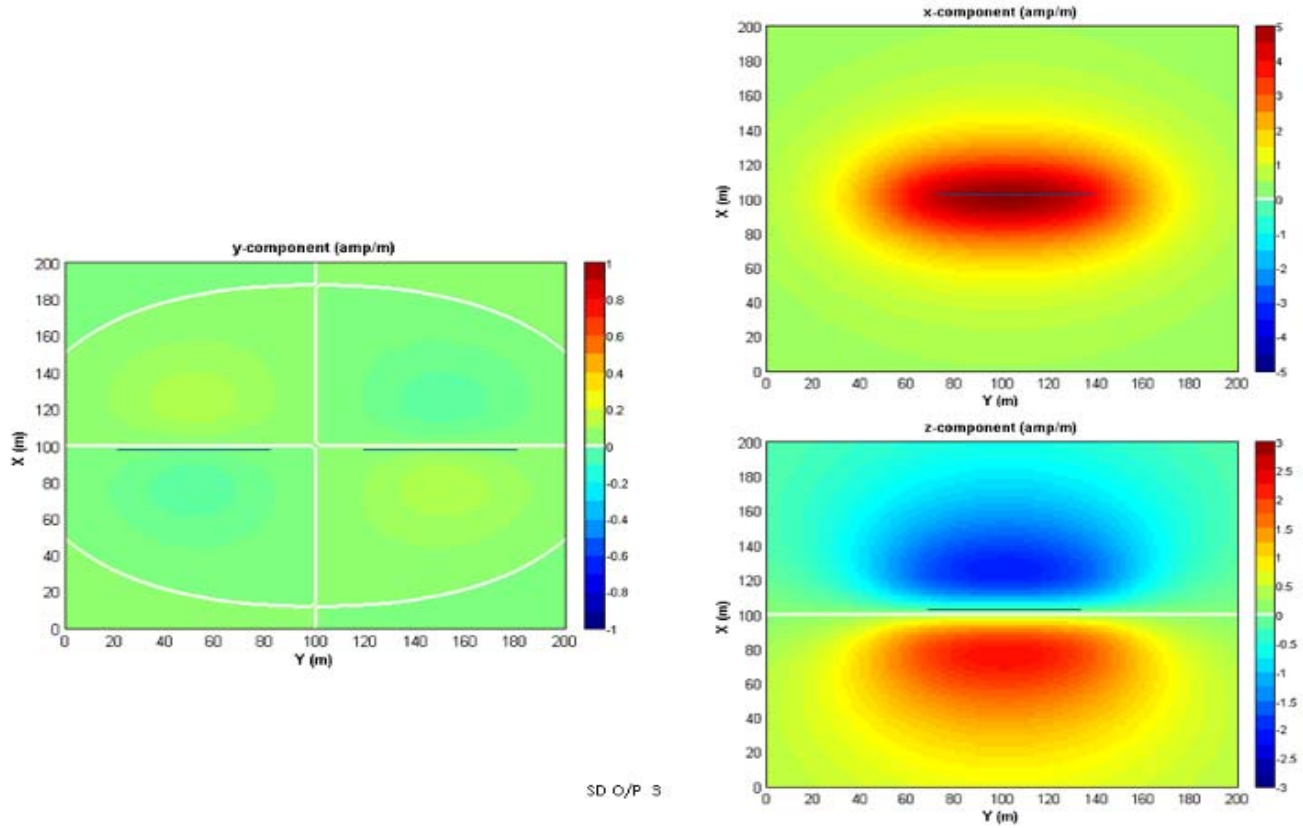
y-component (amp/m)
X (m)
Y (m)
x-component (amp/m)
X (m)
Y (m)
z-component (amp/m)
X (m)
Y (m)
SD O/P S

Figure 54.

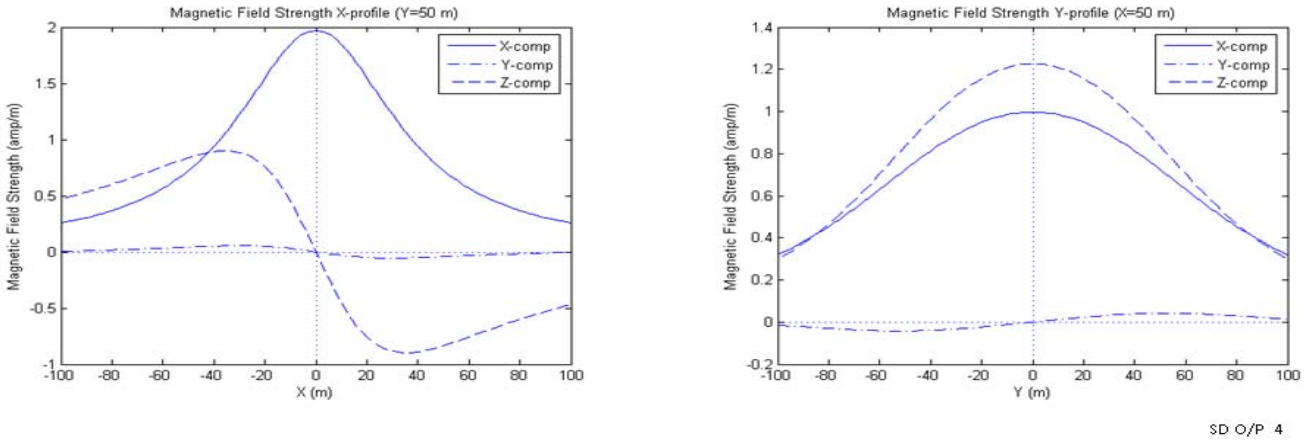

Figure 55. San Diego Type I Case 4 Output

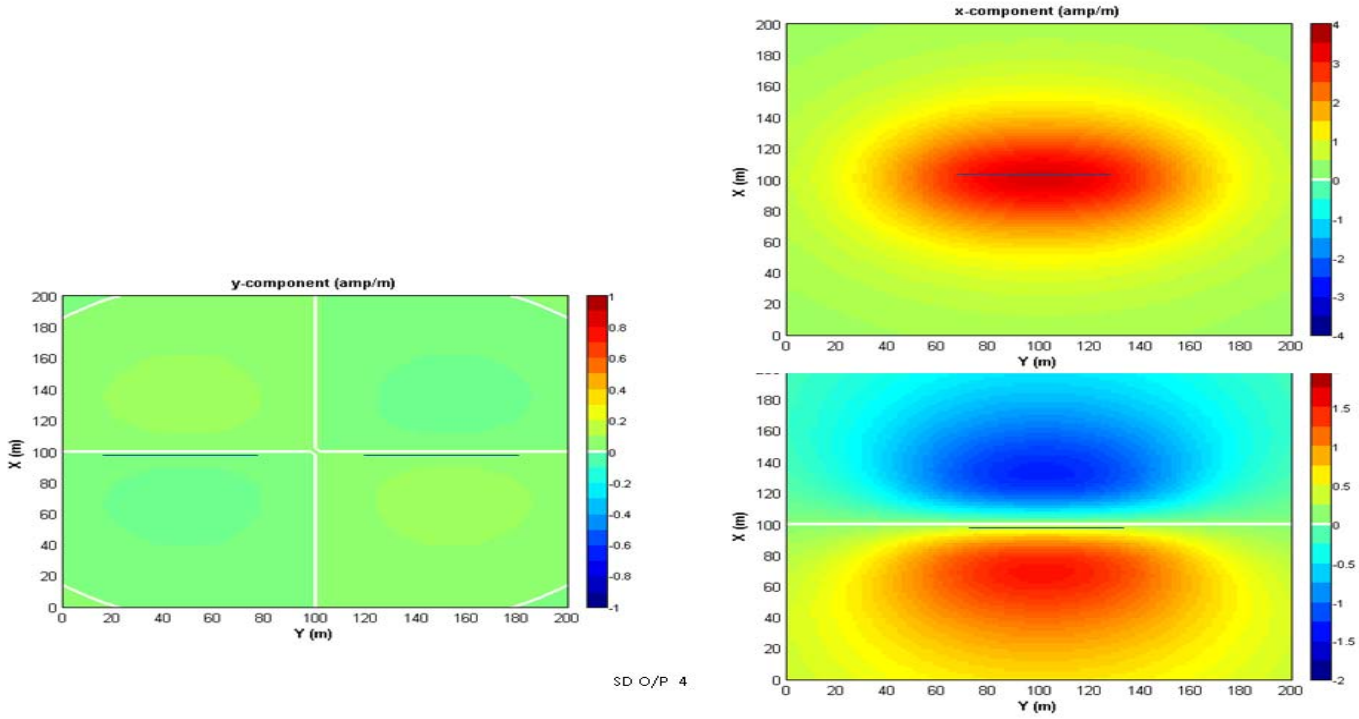

Figure 56. San Diego Type I Case 4

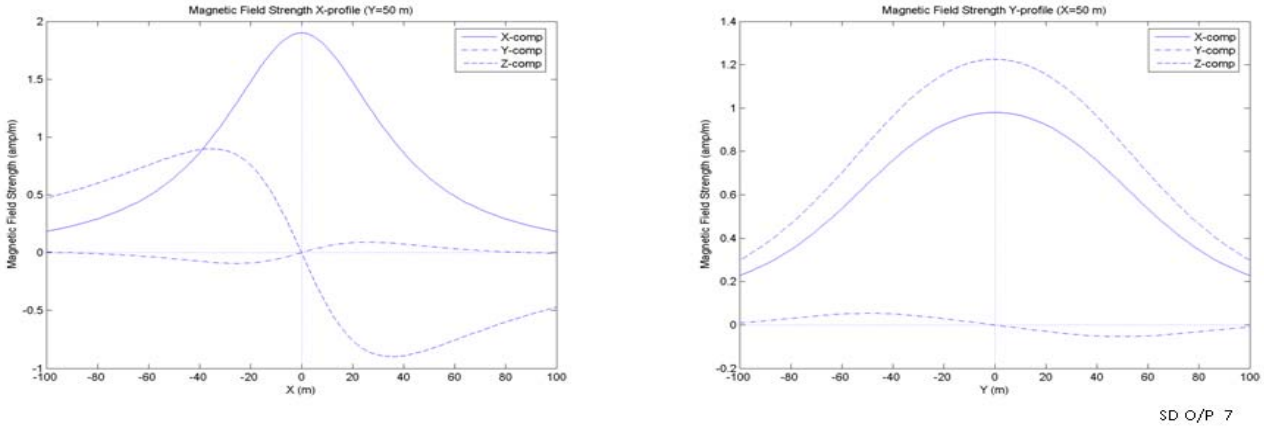

Figure 57. San Diego Type I Case 7 Output

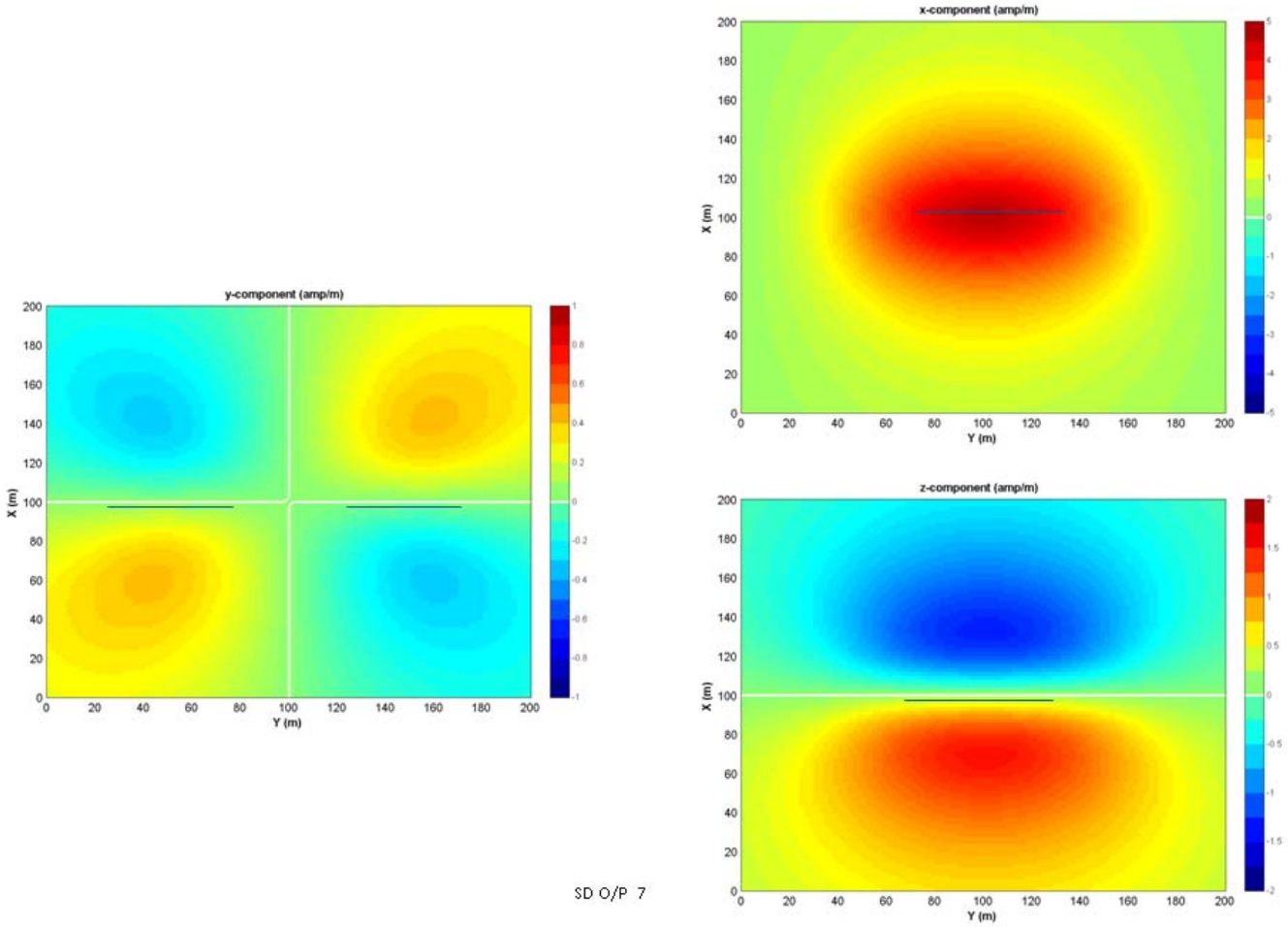

Figure 58. San Diego Type I Case 7 Magnetic Field

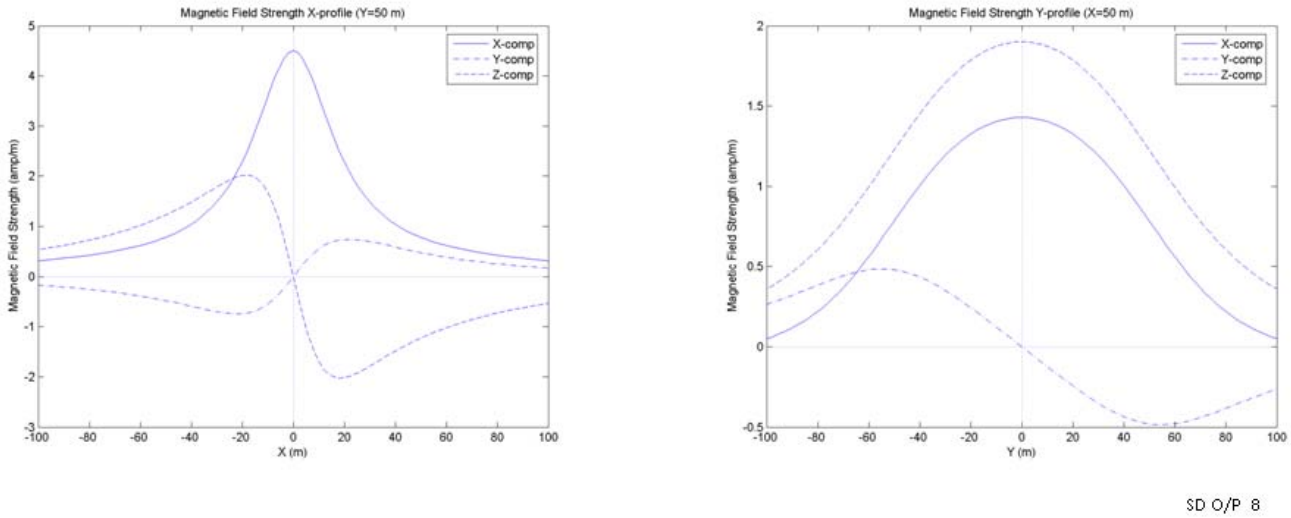

Figure 59. San Diego Type I Case 8 Output

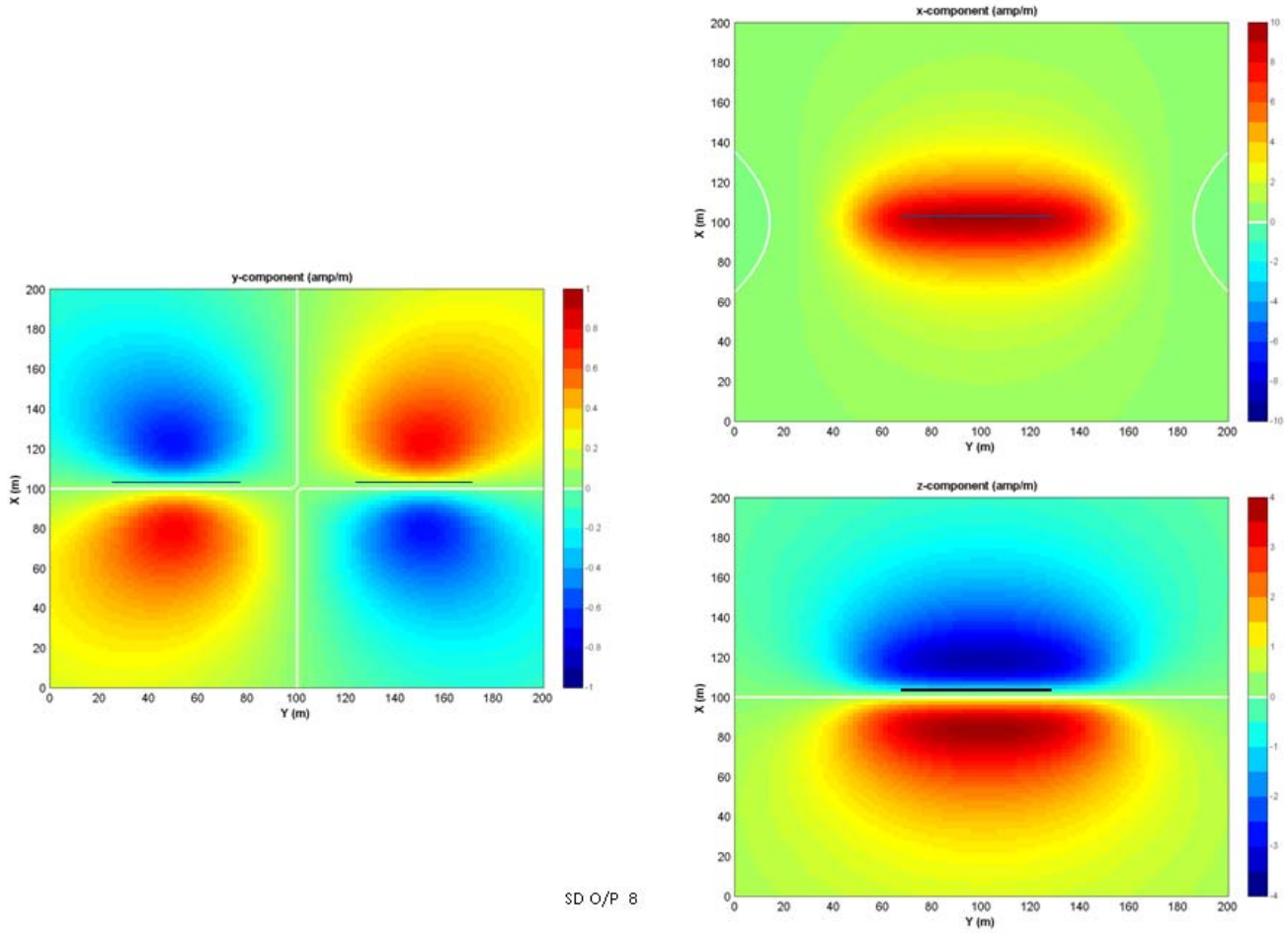

Figure 60. San Diego Type I Case 8 Magnetic Field

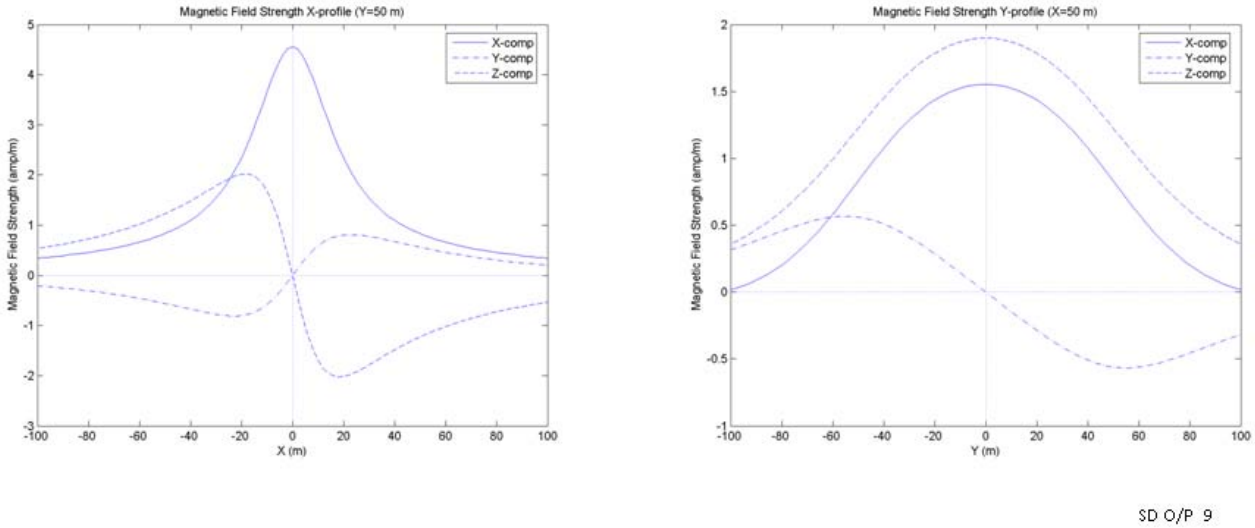

Figure 61. San Diego Type I Case 9 Output

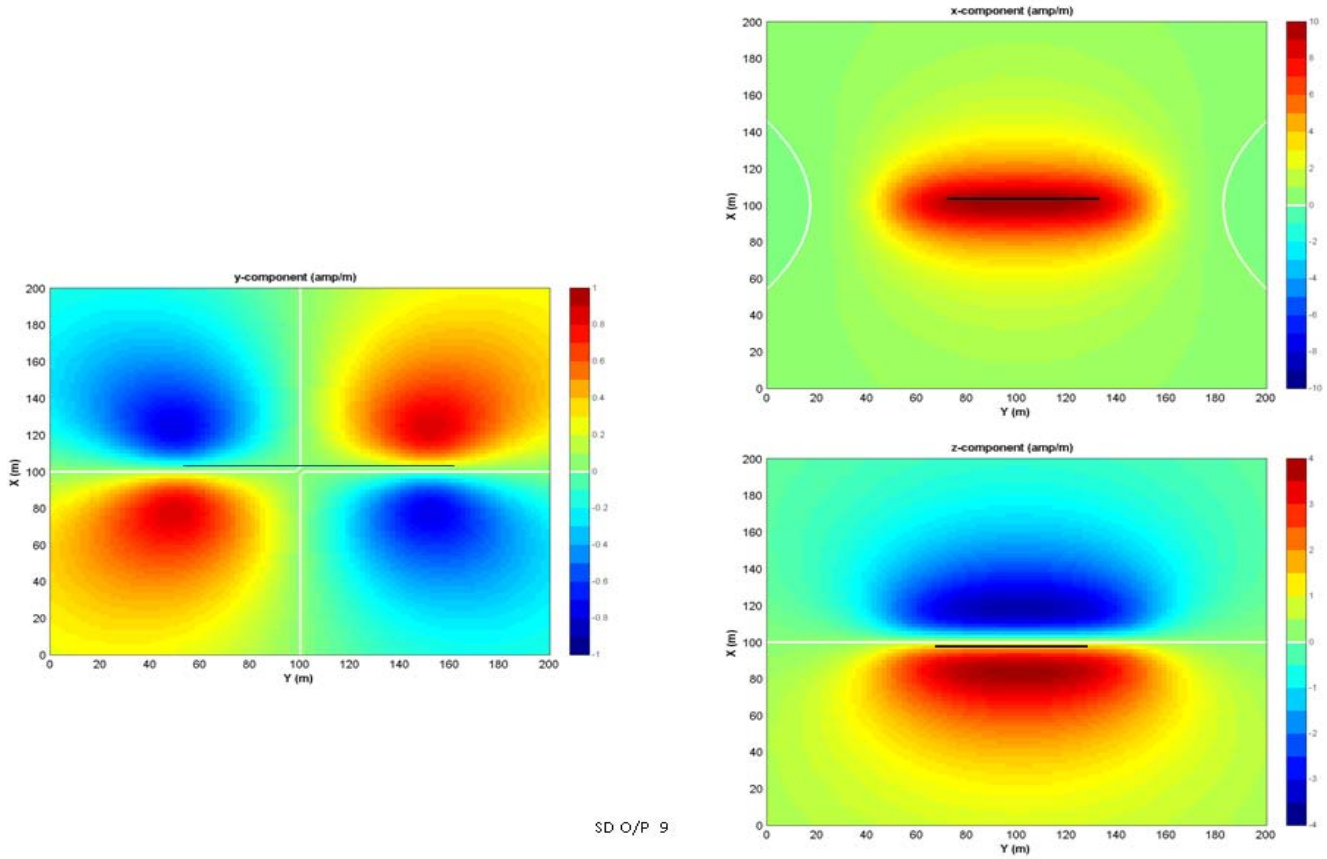

Figure 62. San Diego Type I Case 9 Magnetic Field

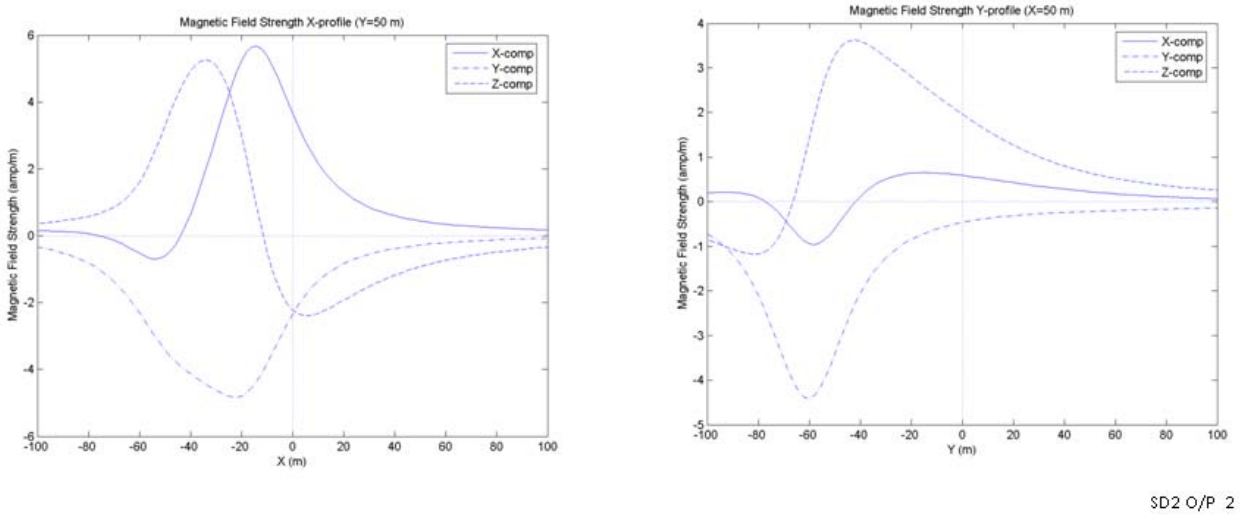

Figure 63. San Diego Type II Case 2 Output

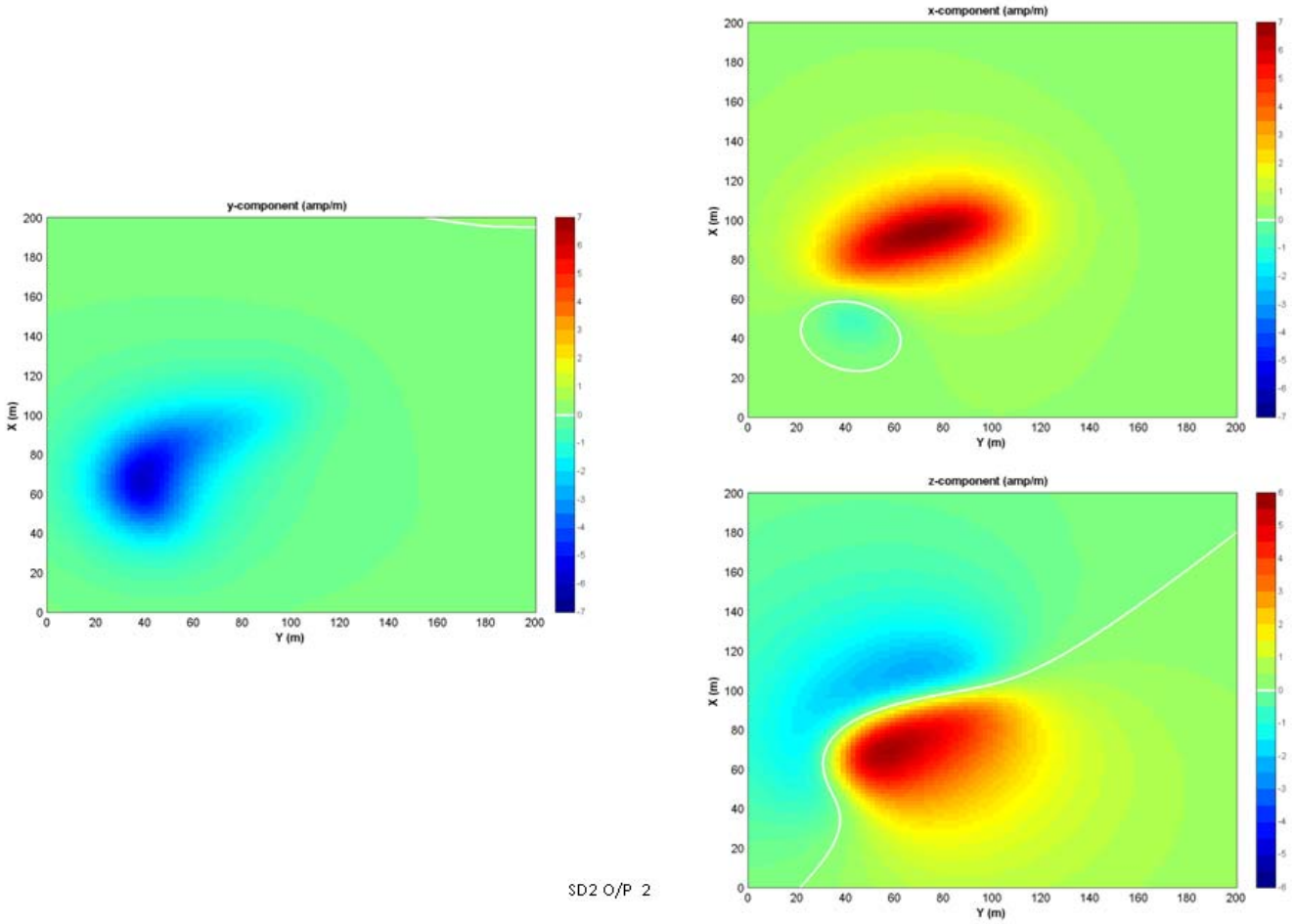

Figure 64. San Diego Type II Case 2 Magnetic Field

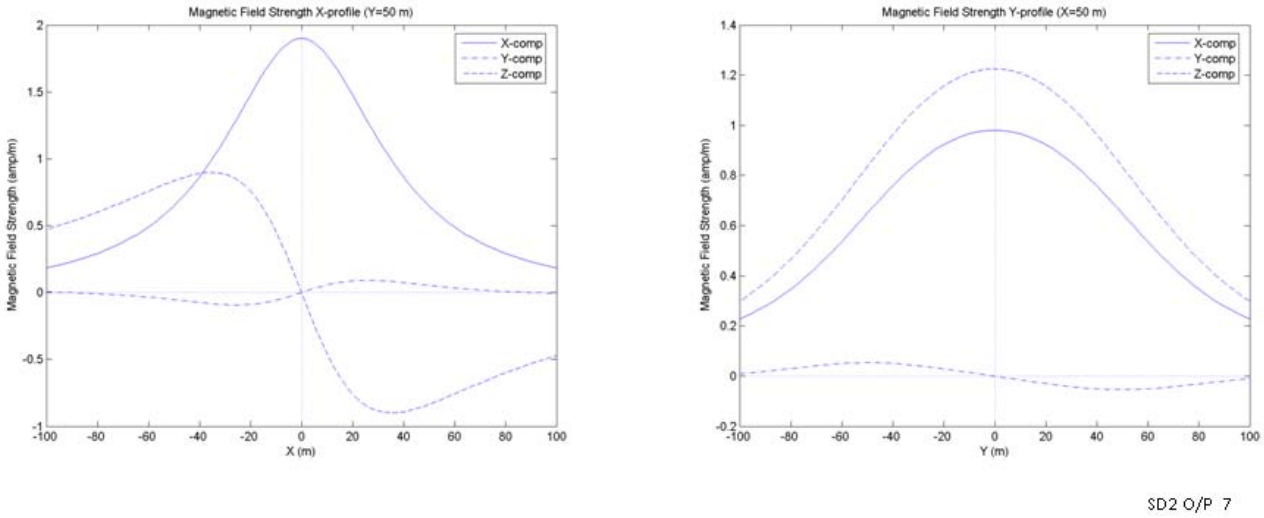

Figure 65. San Diego Type II Case 7 Output

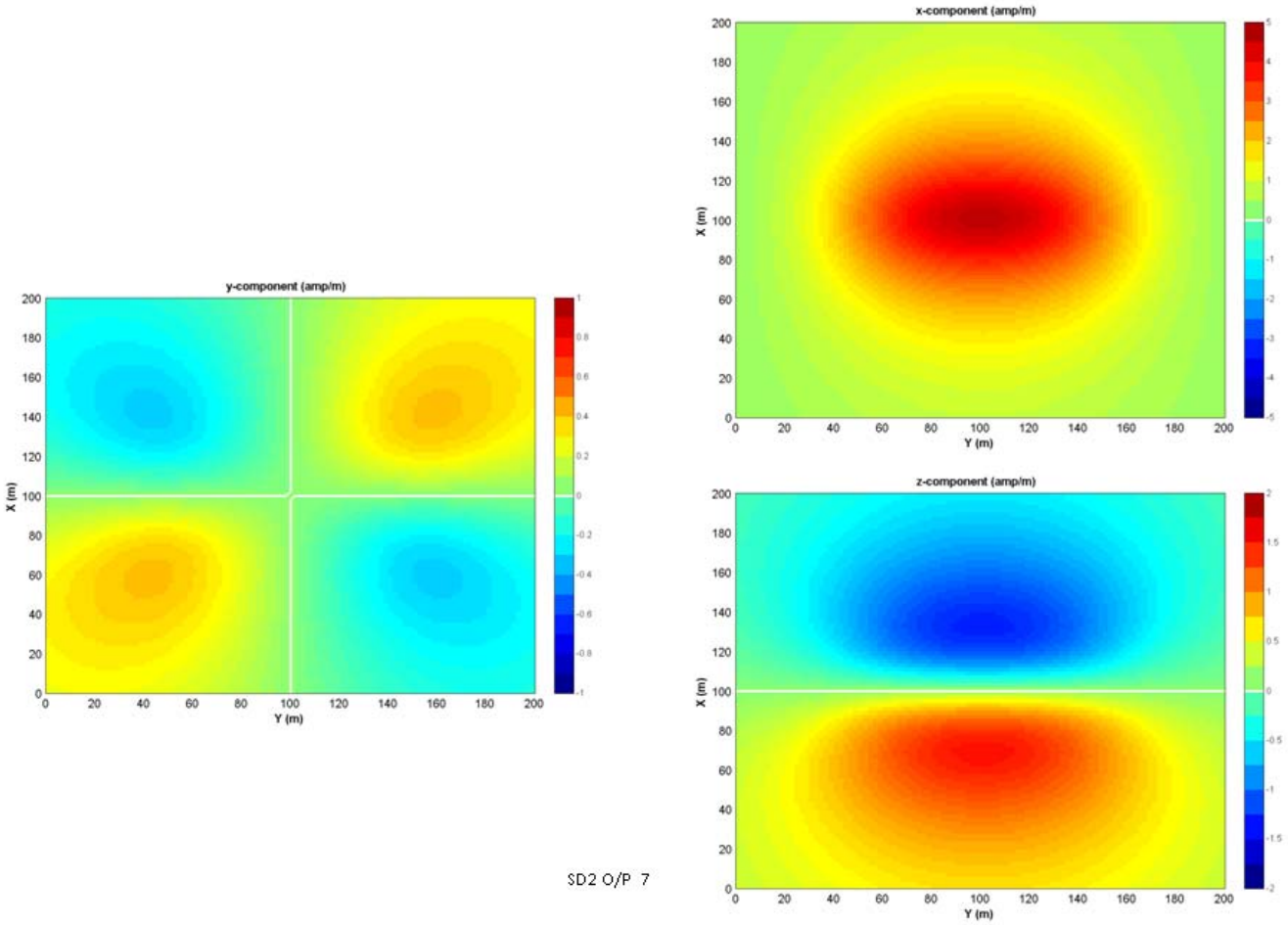

Figure 66. San Diego Type II Case 7 Magnetic Field

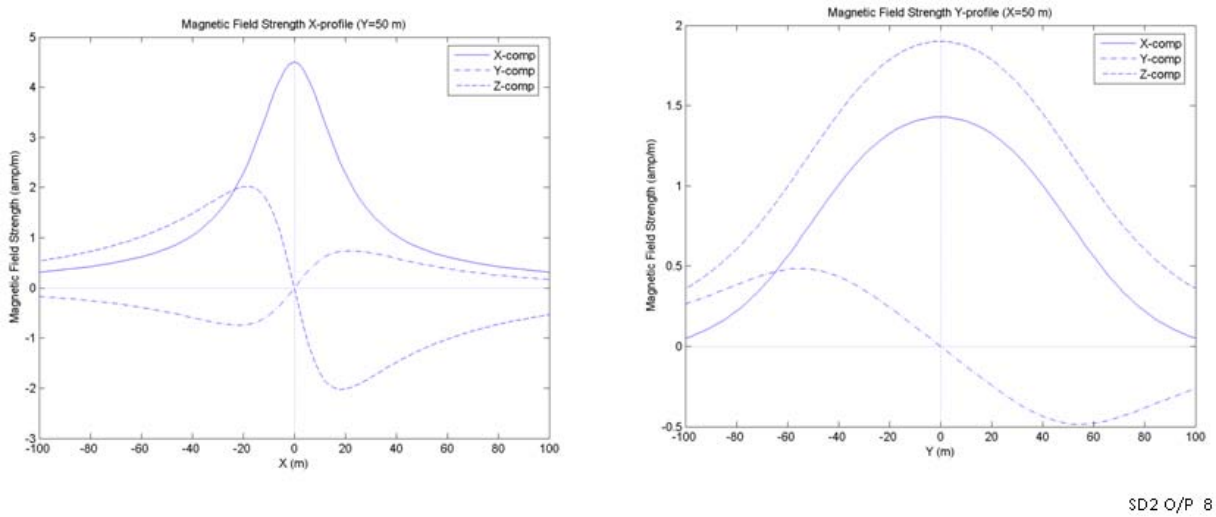

Figure 67. San Diego Type II Case 8 Output

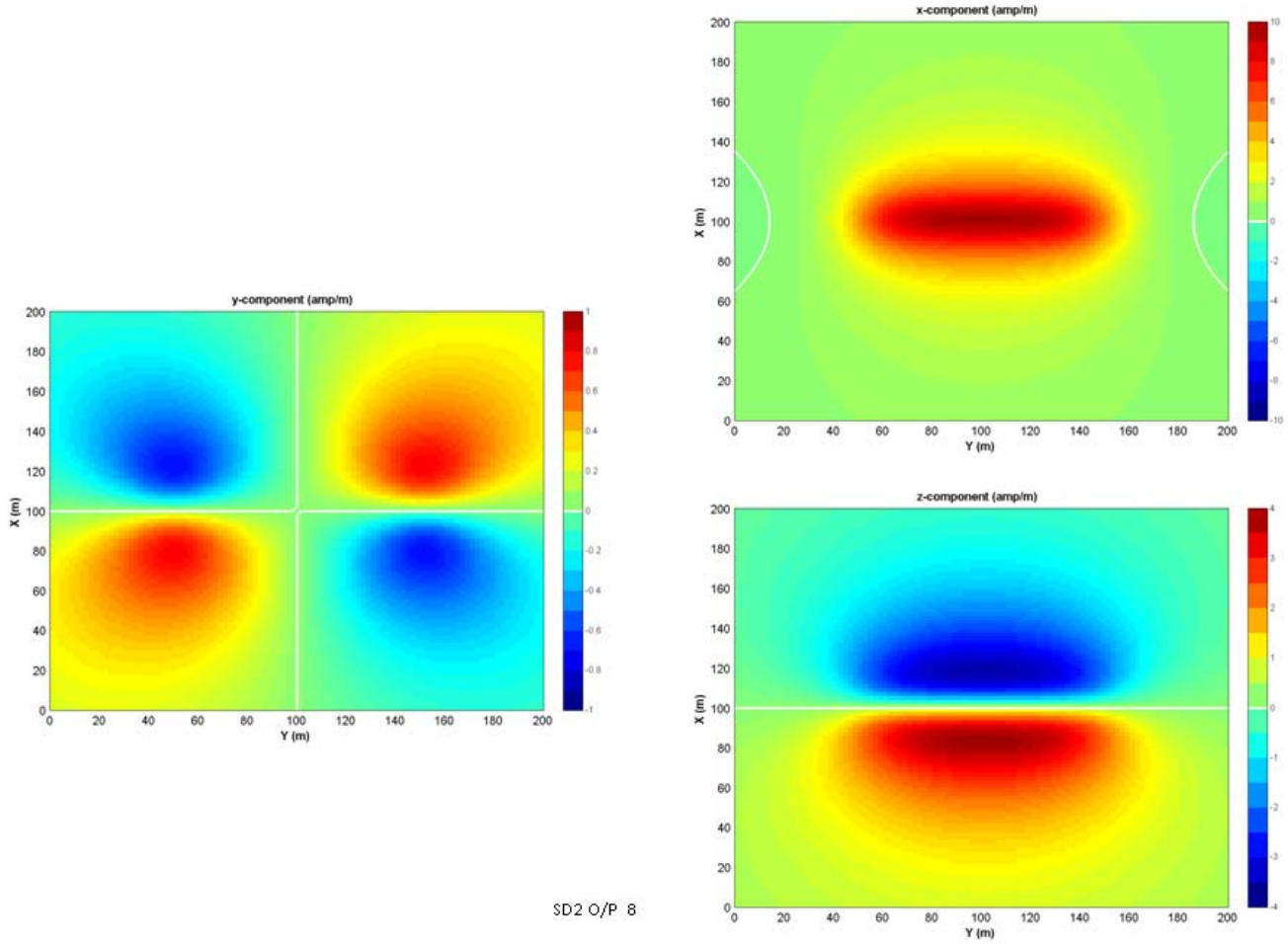

Figure 68. San Diego Type II Case 8 Magnetic Field

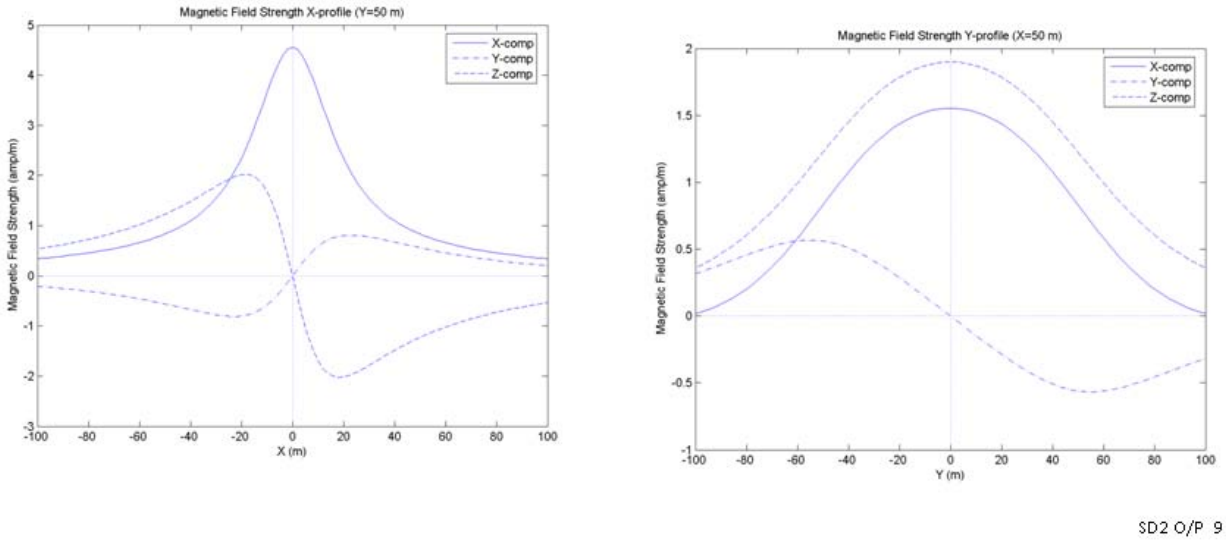

Figure 69. San Diego Type II Case 9 Output

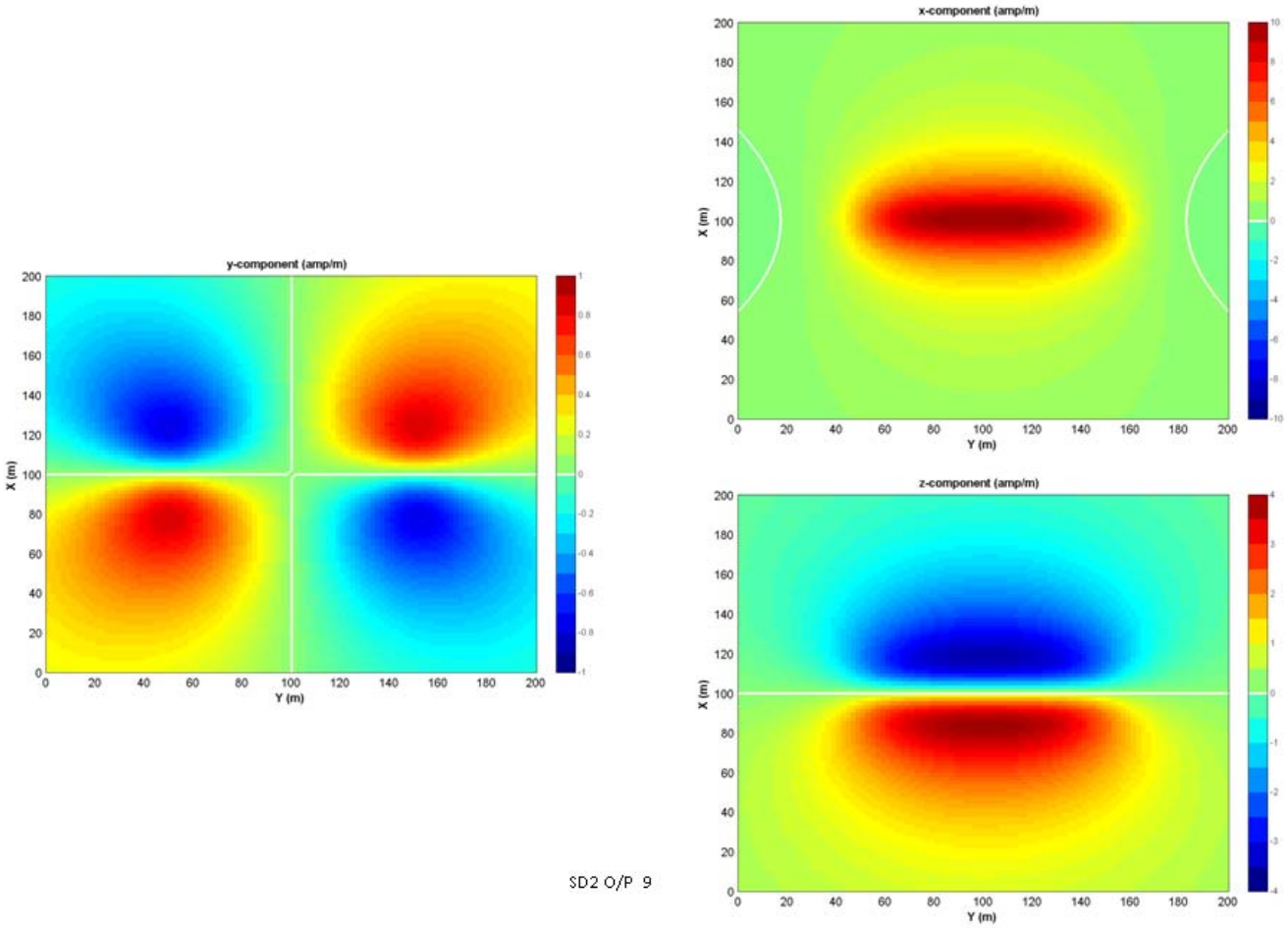

Figure 70. San Diego Type II Case 9 Magnetic Field

THIS PAGE INTENTIONALLY LEFT BLANK

LIST OF REFERENCES

Archie, G.E. (1942). The electrical resistivity log as an aid in determining some reservoir characteristics. J. Pet. Tech., 5:1–8.

Holmes, J J. (2006). Exploitation of a ship's Magnetic Field Signatures Retrieved on August 29, 2010, from www.morganclaypool.com

Armstrong, B, Pentzer, J, Odel, D, Bean, T, Canning, J. Pugsley, D, Frenzel, & J, Anderson, M, Edwards, D (2006) Field measurement of surface ship magnetic signature using multiple AUVs Retrieved June 1, 2010, from GlobalSecurity.org

U.S. Department of Defense. (2007). "Unmanned System Roadmap 2007–2032", December 10, 2007.

Nelson, J. B. Richards, T.C. (2007). "Magnetic source parameters of MR OFFSHORE measured during trial MONGOOS 07", Defense R&D Canada-Atlantic.

Holmes J.J., (2007): Modeling a ship's ferromagnetic signatures. synthesis lectures on computational electromagnetics (editor: C.A. Balanis), Vol 2, No 1, Morgan and Claypool Publishers, 1-75.

Fofonoff, P. & Millard, R.C. Jr, Unesco (1983). Algorithms for computation of fundamental properties of seawater. Unesco Tech.

Fofonoff, P. & Millard, R.C. Jr, UNESCO (1981): Background papers and supporting data on the Practical Salinity Scale 1978. UNESCO technical papers in marine science 37:1-144.

Haeger, S., Horne, R. Chaika, E. Sanford, R. (2001). Technical Review of the N-Layer Magnetic Model (NLMM), A Report by the NLMM CIMREP Panel

Jones, G.O., (2006) Two-layer model for magnetic field for electrode sweep minesweeping

Bradley, M. Bradley, B. Duncan, M., (1997). N-Layered Magnetic Model Software Requirement Specification, Planning Systems Incorporated,

THIS PAGE INTENTIONALLY LEFT BLANK

INITIAL DISTRIBUTION LIST

1. Defense Technical Information Center
   Ft. Belvoir, Virginia

2. Dudley Knox Library
   Naval Postgraduate School
   Monterey, California

3. Rear Admiral David Titley, USN
   Oceanographer and Navigator of the Navy
   Washington, DC

4. Rear Admiral Jonathan White, USN
   Commander, Naval Meteorology and Oceanography Command
   Stennis Space Center, Mississippi

5. Professor Peter Chu
   Naval Postgraduate School
   Monterey, California

6. Roger Meredith
   Naval Oceanographic Office
   Stennis Space Center, Mississippi

7. Ronal Betsch
   Organization of AddresseeMIW Program Manager
   Stennis Space Center, Mississippi

8. Captain Brown
   Naval Oceanographic Office
   Stennis Space Center, Mississippi

9. Captain Ulses
   Director USW
   Stennis Space Center, Mississippi

10. Captain Paul Oosterling
    Chief of Staff
    Commander, Naval Meteorology and Oceanography Command
    Stennis Space Center, Mississippi

11. Dr. James Rigney
Naval Oceanographic Office
Stennis Space Center, Mississippi

12. Mr. Gary Neal
ttjuyt@msn.com

13. LCDR Sam Poteete
EUCOM HQ, Stuttgart, Germany
Samantha.poteete@eucom.navy.mil